Universidade do Minho

Escola de Ciências

Raquel Santos Oliveira

Development of electrochemical-based methods for antioxidant activity evaluation

Doutoramento em Ciências
Especialidade em Química

Sob a orientação de:
Professora Doutora Maria de Fátima Malveiro Bento

October 2013

DECLARAÇÃO

Autora: Raquel Santos Oliveira

E-mail: oliveira.s.raquel@gmail.com

Telf.: (+351) 253604399

Cartão do Cidadão: 12114470

Título: Desenvolvimento de métodos electroquímicos para avaliar a atividade antioxidante

Title: Development of electrochemical-based methods for antioxidant activity evaluation

Orientadora:

Professora Doutora Maria de Fátima Malveiro Bento

Ano de Conclusão: 2013

Doutoramento em Ciências em Especialidade de Química

Universidade do Minho, ____/_____/_____

Assinatura: _____

Acknowledgement

I've always knew these would be a journey but I never thought it would be so important the people I had next to me and those who I've met during this four years.

First of all I want to express my heartfelt gratitude to my supervisor Prof. Dr. Fátima Bento. She was by my side during the whole process with serenity, knowledge and the ability to guide me through every step of this journey.
The work of a researcher can be solitary, so they say, but I never felt alone, she was always there for me, helping me and sometimes just having someone to talk about work or casual daily life stories makes all the difference. For all that I have to say: thank you.

I would also like to acknowledge to all the people in the chemistry department of Universidade do Minho especially to Prof. Dr. Dulce Geraldo and Prof. Dr. Paula Bettencourt for their support and advices.
A special thanks also to Prof. Dr. Paula Margarida and to Prof. Dr. João Carlos Marcos, who were always available to discuss with me in the area of organic and biochemistry respectively. Your technical support was really important.

During my PhD I did an internship in ENS in the group of Prof. Dr. Christian Amatore to whom I am extremely grateful for all the discussions we had. I specially thank to Dr. Laurent Thouin for being my supervisor and for Catherine Sella for being patient with me when she was helping me with the microfluidics. I truly appreciate the opportunity they gave me. It was a great experience and I will never forget the way they received me, I really felt I belonged to the group. Thank you all for showing me the wide world of microfluidics.

Along these four years, most of them spent in the lab, I had the pleasure to divide my work space with excellent partners. I knew people who were truly examples of good partnership. I will not discriminate their names because, thankfully, they were a lot but to all of them I must say it was a pleasure to know you and to work side by side with you.

Lastly, but not least, I would like to thank my parents and my sisters, Sofia and Susana, for all their support. Although most of the times they didn't even understand, they made an effort to read my papers. A special thanks to my mother that was always available to read my work and to correct the English. To them I thank the enthusiastic way they see my work. All my accomplishments are celebrated with them.

Thank you all!

Abstract

In the last decades researchers have been studying the importance of antioxidants and in order to do that they have developed methods to evaluate antioxidants capacity / activity as they are of major importance for health and food industry

The application of electrochemical techniques for the characterization of antioxidants can bring numerous advantages related to the use of less reagents and the miniaturization of the analytical systems.

The present methods for the evaluation of antioxidants capacity / activity are classified according to the type of reaction of the assay, as electron transfer reactions (ET) or hydrogen atom transfer reactions (HAT). In both types of assays, antioxidants are tested in reactions with reactants or radicals that are added or generated in-situ using specific reagents.

The characterisation of antioxidants by voltammetric techniques has attracted a growing number of researchers that have demonstrated that electrochemical data provides similar information to the classical ET methods concerning the antioxidants reducing power. The possibility of developing further approaches for the characterization of antioxidants based on electrochemical methods has driven to the present work.

In what concerns the characterization of antioxidants by ET-based assays two methodologies are proposed based on direct electron transfer reactions with an anode. The first, denominated by RACE (Reducing Antioxidant Capacity Evaluated by Electrolysis), is based on a coulometric assay. The second consists in the chronoamperometric analysis of antioxidants using microchannel band electrodes devices operating under thin-layer regime. Both methods have the advantage of allowing to characterize antioxidants capacity by the amount of charge that species are able to transfer without the need of calibration steps. The second methodology has further advantages related to the use of small sample volumes and to the short time of analysis.

Regarding the characterization of antioxidants by HAT-based assays, it is proposed and demonstrated the suitability of electrogenerated HO radical for this aim. Although the electrogenerated HO radicals by the oxidation of water are well known in the scope of wastewater treatment using anodes as BDD (boron doped diamond), their use in antioxidant assays was not reported. With this purpose it is demonstrated that using a Pt anode it is possible to carry out hydroxylation reactions in galvanostatic electrolysis, as with BDD anodes, although the reactions rates are lower and sensitive to the reactivity of the organics. The possibility of carrying out reactions between electrogenerated HO radicals and

electroactive compounds was analysed and the proportion between the rates of the direct oxidation and the mediated by HO radicals was shown to be controlled by means of the electrolyses charge density. The apparent rate constant of consumption of organics by the HO radicals was shown to be related to the species reactivity despite their electroactive nature.

A kinetic model that allows the evaluation of the rate constants of reactions between organics and electrogenerated HO radicals is proposed and tested in different circumstances, namely for single species and for mixtures of two organic compounds. The possibility of applying the developed methodology in natural samples was also demonstrated using a commercial green tea-based beverage.

Resumo

A importância dos antioxidantes tem vindo a ser estudada nas últimas décadas com a finalidade de desenvolver métodos que avaliem a capacidade / atividade dos antioxidantes devido ao papel fulcral que desempenham na saúde e na indústria alimentar.

A aplicação de técnicas electroquímicas para a caracterização de antioxidantes pode trazer inúmeras vantagens em relação à menor necessidade de utilizar reagentes e à possibilidade de miniaturização dos sistemas analíticos.

Os atuais métodos para a avaliação da capacidade / atividade de antioxidantes são classificados de acordo com o tipo de reação de ensaio , tal como as reações de transferência de electrões (ET) ou reações de transferência de um átomo de hidrogénio (HAT). Em ambos os tipos de ensaios , os antioxidantes são testados em reações com reagentes ou radicais que são adicionados ou gerados *in situ*, utilizando por isso reagentes específicos.

A caracterização de antioxidantes por técnicas voltamétricas tem atraído um número crescente de investigadores que demonstraram que os dados electroquímicos fornecem informações semelhantes aos métodos ET clássicos no que diz respeito à capacidade redutora dos antioxidantes. O presente trabalho surge com a finalidade de criar uma nova abordagem baseada em métodos eletroquímicos para avaliarem e caraterizarem a atividade / capacidade antioxidante.

Relativamente à caraterização de antioxidantes baseada em ensaios ET são propostas duas metodologias que se baseiam na transferência electrónica com o ânodo. A primeira, denominada por RACE (Reducing Antioxidant Capacity Evaluated by Electrolysis), é baseada num ensaio coulométrico. A segunda consiste na análise cronoamperométrica de antioxidantes usando um dispositivo de microcanais de bandas de elétrodos que operam sob um regime de camada fina. Ambos os métodos têm a vantagem de permitir caracterizar a capacidade antioxidantes pela quantidade de carga que a espécie é capaz de transferir, sem a necessidade de recorrer a curvas de calibração. O segundo método proporciona ainda vantagens relacionadas com a utilização de volumes pequenos de amostra e ao tempo curto de análise.

Relativamente à caracterização de antioxidantes baseada em ensaios HAT, propõe-se o uso de radicais hidroxilo gerados electroquimicamente e demonstra-se a sua aplicabilidade. Apesar de os radicais hidroxilo eletrogerados, como produto da oxidação da água, serem utilizados no âmbito do tratamento de águas residuais usando ânodos como o BDD (boron doped diamond), a utilização destes radicais HO eletrogerados em ensaios de avaliação da atividade antioxidante não foi reportada. Com este

objectivo é demonstrado que utilizando um ânodo de Pt é possível realizar reações de hidroxilação em electrólises galvanostáticas, como acontece com os ânodos de BDD, embora as velocidades de consumo serem mais baixas e sensíveis à reatividade dos compostos orgânicos. A possibilidade de levar a cabo reações entre os radicais HO eletrogerados e compostos eletroativos foi analisada e a proporção entre as velocidades de oxidação direta e a mediada por radicais HO foi controlada pela densidade de carga da electrólise. A constante de velocidade aparente relativa ao consumo dos compostos orgânicos por reação com os radicais HO relaciona-se com a reatividade das espécies independentemente da sua natureza eletroativa .

Foi proposto e testado um modelo cinético, que permite avaliar as constantes de velocidade das reações entre os compostos orgânicos e os radicais HO eletrogerados. Este modelo foi testado em compostos orgânicos e em misturas de dois compostos orgânicos. A possibilidade de aplicar a metodologia desenvolvida em amostras naturais também foi demonstrada utilizando uma bebida comercial à base de chá verde.

Table of Contents

Preface

The work presented in this thesis is organized as follows: State of the Art, Results and Discussion and Conclusion.

The *State of the Art* is presented in the form of a review article entitled *Characterization of antioxidants: electrochemical strategies and applications* and provides the reader an overview of the most recent work performed in the scope of the electrochemical methods for antioxidants characterization. This paper has been submitted for publication.

In *Results and Discussion* is presented the outcome of the research conducted in the framework of this PhD thesis. This section comprises six papers, four of which were published in journals in the field of electrochemistry and analytical chemistry. The two other articles were submitted for publication.

Results comprising the direct evaluation of antioxidants by coulometry and chronoamperometry resulted in the development of two analytical methods for the assessment of antioxidants capacity and were published in the two first presented papers:

- Reducing Antioxidant Capacity Evaluated by Means of Controlled Potential Electrolysis

- Direct Electroanalytical Method for Alternative Assessment of Global Antioxidant Capacity Using Microchannel Electrodes.

Studies performed on the electrochemical generation and reactions of HO radicals were published in the following three papers:

- Aromatic hydroxylation reactions by electrogenerated HO radicals: A kinetic study,

- Reactivity of hydroxy-containing aromatic compounds towards electrogenerated hydroxyl radicals

- Electrogenerated HO radical reactions: the role of competing reactions on the degradation kinetics of hydroxy-containing aromatic compounds.

Results concerning the application of electrogenerated HO radicals in the evaluation of the scavenging activity of antioxidants are presented in the last paper:

- Radical scavenging activity of antioxidants evaluated by means of electrogenerated HO radical.

Besides the referred papers, the work carried out for this PhD thesis was presented in scientific meetings as: one invited keynote, three oral communications and seventeen poster communications. Furthermore one patent was published (PT 105103) and another is in process of analysis.

I. State of the art

Characterization of antioxidants: electrochemical strategies and applications

Raquel Oliveira, Fátima Bento*

Department of Chemistry, Universidade do Minho, Campus de Gualtar 4710-057, Portugal

* Corresponding author T: +351 253604399; e-mail: fbento@quimica.uminho.pt

1. Introduction

Compounds that have the ability to prevent or delay the oxidation of other substances are denominated antioxidants (AOs). Besides antioxidant enzymes, low molecular weight molecules, such as vitamin C and vitamin E (endogenous AOs), natural substances such as tocopherols, phenolic compounds, carotenoids (exogenous AOs) and synthetic molecules like propyl gallate (PG), tertiary butylhydroquinone (TBHQ), butylated hydroxyanisole (BHA) and butylated hydroxytoluene (BHT) are also effective on preventing oxidation [1].

Although antioxidants are not a recent topic, it attracts a growing number of researchers as it is demonstrated by the increasing number of publications through the last decade. Under this topic there are listed: 326,361 publications in the last 10 years (32,636 publications per year); 213,865 publications in the last 5 years (42,773 publications per year) and 74,674 publications in the last year (results from ISI web of knowledge until 2013/10/07).

The search for AOs with high activity has attracted chemists of different areas, namely food chemists, natural products chemists and synthetic chemists. The identification of antioxidant rich-foods (goji, berries, propolys, among others) and the synthesis of new compounds with antioxidant activity (chalcones, flavones, among others) are important outcomes that chemists have brought to this multidisciplinary area. The characterization of the antioxidant activity of compounds and antioxidant capacity of samples demand the use of methods that are both reliable and fast. Also in this scope, chemists gave important contributions. An example is the well-known ORAC assay (oxygen radical absorbance capacity) that is currently one of the most used methods, developed by Cutler and Cao in 1993 [2].

This review focuses on the relevancy of electrochemistry for the development of new tools for antioxidants characterization and provides the reader with an overview on the recent work (mostly after 2010) carried out in this scope. Rather than attempting a comprehensive review, we pretend to show the diversity and relevancy of the electrochemical solutions for antioxidants characterization, allowing to detect and characterize individual antioxidants or rather quantify capacity indexes.

2. Indirect characterization of antioxidants

The indirect characterization of antioxidants is the base of a broad range of analytical methods that evaluate antioxidants and global antioxidant capacities by means of reagents or biomolecules. Most of these methods involve the evaluation of: i) the extent of the reduction reaction involving a synthetic oxidant (SOX) and the antioxidant; or ii) the damage degree of a molecular probe (biological or synthetic) in the sequence of a step where it is exposed to a reactive oxygen species (ROS) in the presence of the antioxidants, or iii) the products or mediators of enzymatic reactions involving the antioxidants or reactive species. While chemical assays are mostly centred on the two first strategies, biosensors generally employ the two last approaches.

2.1 Antioxidant capacity assays using electrochemical techniques

The conventional antioxidant capacity assays use spectrophotometric measurements [3,4] to monitor the total antioxidant capacity, despite the electrochemical techniques are becoming more used [5–8]. Electrochemical techniques can introduce important advantages in this scope regarding the possibility of performing experiments in coloured or turbid media and the simplicity of the instrumentation that enable to construct sensors and miniaturized devices of simple operation and of low cost.

The well known assays Ceric Reducing Antioxidant Capacity (CERAC) [9], Trolox Equivalent Antioxidant Capacity (TEAC) [10] and DPPH (2,2-diphenyl-1-picrylhydrazyl) [11] use the SOX Ce(IV), ABTS radical and DPPH radical, respectively. They were conveniently used in the original assays as they can be optically detected. The modification of these original methods by replacing the optical detection of the SOX (either in the oxidized or in the reduced forms) by the electrochemical detection was accomplished by several authors [12–15]. The determination of synthetic antioxidants and polyphenols was reported using chronoamperometric detection of Ce(III) [14]. Similarly the quantification of antioxidants was carried out in beverages following the biamperometric detection of DPPH/DPPH radical [12] and the amperometric detection of DPPH [13,15].

The electrogeneration of the radical cation ABTS is described in different works [16–18] and provides significant improvement to the original TEAC assay [10]. By mean of coulometric titrations with optical end-point detection were analysed wine [16,17], brandy and vinegar [17] samples. The total antioxidant capacity of tea and coffee samples was characterized by a flow injection assay coupled with spectrophotometric detection [18].

The electrogeneration of halogens as oxidants for the determination of antioxidant capacity is proposed and applied by several authors [19–27]. The coulometric titration of antioxidants is reported using biamperometric end-point detection [19–22,24–27]. Samples of teas [25], wines [20,22], extracts of juices and vegetable [21], pharmaceutical formulations [26,27] and human blood [24] were analysed using bromine. Similarly, electrogenerated chlorine was described for the evaluation of the total phenolic content in wines by means of a potentiometric titration [23].

Electrogenerated hexacyanoferrate(III) was also used as a SOX for the coulometric titration of hydroxycinnamic acids in coffee bean with biamperometric detection [28].

2.2 Electrochemical sensors and biosensors

Electrochemical biosensors are devices that use a biological recognition element connected with an electrochemical transducer. The antioxidants determination with this type of sensors is always indirect in the electrochemical point of view as antioxidants are not directly involved in the electron transfer process. In opposition, the response of an electrochemical sensor can be due to the direct or to the indirect participation of the antioxidant on the electrode reaction. In this section only sensors which functioning does not involve the direct electron transfer to antioxidants are reported. The electrochemical sensors that detect antioxidants by means of their heterogeneous electron transfer processed are addressed in section 3.1.

Biosensors devised for antioxidants evaluation can be classified in two main groups. The first group relies on the direct interaction between the biological element (enzyme) and the AO, while the second group involves the quantification of the concentration of reactive oxygen species (ROS), as H_2O_2 or $O_2^{\bullet-}$, (using cytochrome C, superoxide dismutase and peroxidase) or the extent of the damages induced by ROS on biological probes, such as DNA, purine bases and bovine serum albumin (BSA) in the presence of antioxidants.

2.2.1 Enzymatic biosensors

From the selective interaction between the AOs and an enzyme is generated a primary signal that is electrochemically detected at the electrode where the enzyme is immobilized. Antioxidant detection using enzymatic biosensors mostly relies on the measurement of the catalytic current of the enzymatically-oxidized antioxidant. Tyrosinase and laccase are used to detect phenolic antioxidants. The oxidation products are electrochemical detected at low potentials minimizing electrochemical

interferences. The design of this type of sensors, as well as their functioning and performance, is varied according to the enzyme type, the immobilization techniques and the catalytic properties of the electrode.

Since the pioneering work of Wang and co-workers in 1989 [29], more than 400 original papers have been published in this scope. The success of these sensors have been demonstrated by the diversity of the matrixes analysed. Since 2010, there are 123 original papers published under this topic. Concerning the applications in natural matrices, the detection of phenols is described in plants [30,31], alcoholic beverage [32–37], in fruit juices [38], teas [35,36,39,40], pharmaceutical formulations [35,36,41,42] and in propolis extracts [43,44].

Besides the nature and activity of the enzyme, the sensor performance depends strongly on the catalytic properties of the transducer. Several electrode materials and modifications were used to improve the antioxidant sensors performance. The addition of carbon nanotubes and cobalt phthalocyanine to carbon paste electrodes is reported for the analysis of pharmaceutical samples [42].

Several works report the use of graphite screen-printed electrodes (SPE) with charge transfer mediators, such as ferrocene [33], rutenium [45], as well as the modification of SPEs surface using: conducting polymers, such as polyvinyl alcohol photopolymer [39]; nanoparticles, such as platinum nanoparticles [40], tin oxide nanoparticles [43], reduced graphene oxide [40], carbon nanotubes [32] [46]; and bismuth film [47,48].

The use of gold electrodes modified nanoparticles of silver [35], nickel [38] or copper [36] is also reported for enzymatic biosensors of polyphenols.

Due to the free-radical-scavenging properties of uric acid it is considered to have a potential therapeutic role as an antioxidant. Besides, uric acid is used as a marker of oxidative stress [49]. The determination of uric acid by enzymatic biosensors was recently reviewed [50]. Since the first electrochemical biosensor for uric acid proposed by Blanco [51] in 1996, more than 45 original papers have been published, where 28 of these papers date from 2010.

Electrochemical biosensors of uric acid use urate oxidase, also denominated by uricase. For most oxidases the detection strategy is based on the quantification of the concentration decrease of O_2 or on the concentration increase of H_2O_2 associated with the enzyme mediated oxidation of uric acid. These sensors functioning have been validated in biological fluids such as serum [52–56], blood [57] and

urine [56,58]. Different sensor designs were suggested for this sensor by improving the immobilization techniques [54,58–60], the catalytic properties of the electrode [53,55,61] or the nature of the charge transfer mediators [54].

Nanoceria (CeO_2 nanoparticles) is known to be a powerful antioxidant [62]. The assessment of the radical scavenging activity of nanoceria (CeO_2 nanoparticles) was evaluated by means of a *cytochrome c* electrochemical biosensor by monitoring the concentration of extracellular $O_2^{\bullet-}$ released by cells in the hippocampus of brain slices from mice [63]. Also following a similar approach, the antioxidant capacity of commercial blueberry based capsules was characterized using an amperometric biosensor based on superoxide dismutase [64]. Likewise the H_2O_2 detection by an amperometric biosensor based on peroxidases from *Brassica napus* hairy roots was used to determine the antioxidant content of wine and tea samples [65].

2.2.2 DNA and BSA biosensors

Electrochemical DNA biosensors using double strand-DNA (ds-DNA), single strand-DNA (ss-DNA) or the purine bases adenine and guanine are reported for the evaluation of antioxidants capacity. These sensors operation is based on the monitoring of the electrochemical response of adenine and guanine that varies according to the degree of damage of the immobilized biomolecules.

For biosensor using ds-DNA, the purine bases electrochemical response is residual for the undamaged DNA and tend to increase after exposing the sensor to the presence of ROS [66–69]. In opposition, for ss-DNA [70,71] and adenine/guanine [72–75] biosensors the electrochemical signal is maximum in the absence of oxidative damage and tend to decrease by exposing the sensor to the action of ROS. These DNA sensors were used to characterize the antioxidant activity of specific species, such as ascorbic acid and rutin [69] and to evaluate the total antioxidant capacity of fruit juices [68,75], and flavoured waters [70,72,73].

Bovine serum albumin (BSA) biosensors were devised for antioxidant capacity. The operating principal of these sensors are based on the voltammetric response of poly-o-phenylenediamine immobilized on the sensor [76] or of tris(2,2'-bipyridyl)cobalt(III)perchlorate in solution [77] that depends on the extension of the damages induced by HO radicals on BSA.

2.2.3. Chemical sensors

A voltammetric sensor for the evaluation of antioxidant capacity of edible oil samples was proposed based on the measurement of the catalytic current associated to ABTS oxidation in the presence of antioxidant species [78].

The scavenging ability of antioxidants was evaluated from their quenching effect in electrochemiluminescence assays. This approach was described in the characterization of isolated substances as quercetin [79] and phenolic compounds [80] and of food [81] and beverages [82].

The use gold nanoparticles and nanoshells was also reported for the detection of antioxidants following a common strategy based on the evidence that antioxidants induce the growth of these nanostructures. Following the response of $K_3[Fe(CN)_6]$ as a probe, two sensor configurations were proposed, one employ gold electrodes modified with gold nanoparticles [83] and the other uses ITO (tin-doped indium oxide) electrodes modified with gold nanoshells [84].

A sensor that aims to characterize the HO radical scavenging properties of antioxidants was devised using ITO electrodes modified with palladium oxide nanoparticles [85]. The HO scavenging properties of antioxidants is evaluated from the measurement of the catalytic current of the reduction of palladium oxide nanoparticles in the presence of: hydrogen peroxide or dissolved oxygen and of the antioxidant molecules.

The electrogeneration of superoxide radical and its use in voltammetric measurements of O_2^- radical scavenging activity is the base of operation of the sensors used in the characterization of flavonoids [86], 3-hydroxycoumarin, carvacrol, vanillin and gallic acid [87], chrisin [88], polyphenols [89], blood plasma samples [90] and plant extracts [91].

3. Direct characterization of antioxidants

As most of the antioxidants are electroactive, electrochemical techniques can be used to detect these species in a straightforward way [92–96]. Besides the evaluation of antioxidants concentration, the assessment of the antioxidants activity of species and of the antioxidant capacity of samples is widely reported using electrochemical techniques. The electrochemical variables, potential, current and charge, that are obtained directly from voltammograms, are pertinent for characterizing their electron transfer reactivity. Besides the relevance of the electrochemical data, the direct characterization of

antioxidants by electrochemical techniques presents important advantages related to the simplicity, low cost and short time of analysis.

Although electrochemical techniques were not included by IUPAC in the group of the ET-based methods for the characterization of antioxidants [4], there is a growing number of users that employ electrochemical techniques for this purpose. Moreover, results of electrochemical direct assessment of antioxidant activity / capacity are comparable with results from conventional methods, as showed by different authors regarding different methodologies and samples [97–108].

3.1 Electrochemical sensors

There are more than one thousand original papers published on the use of electrochemical sensors (excluding biosensors) for the direct assessment of antioxidants and particularly of polyphenols. The increase of the average number of papers per year, from 82 in the last ten years to about 144 in the last three years, demonstrates that the application of voltammetric or chronoamperometric techniques for antioxidants characterization is quite well established and disseminated.

Voltammetric techniques such as cyclic voltammetry (CV), differential pulse voltammetry (DPV) and square wave voltammetry (SWV) have been used for antioxidants characterization. The analysis of the voltammograms usually focuses on peak or wave position (considering either E_p or $E_{1/2}$) and on current (considering either the peak current, I_p, or a limiting current plateau ,I_l). Alternatively to current, some authors use the area under voltammograms integrated between fixed potentials. The potential where oxidation occurs is taken as a measure of the antioxidants reactivity and is used to establish relative scales of antioxidant activity [106,109–112], whereas current is used to assess the concentration of the antioxidant.

In most of the reported works, carbon electrodes are used, due to their electrocatalytic activity for the oxidation of a variety of organic compounds with antioxidant activity. In addition, carbon electrodes are accessible in different forms (e.g., glassy carbon, carbon fibers, screen printed, carbon pastes) and their cost is low. Besides, for increasing the sensitivity and selectivity of the detection, carbon electrodes can be readily modified by incorporating reagents (including electrocatalysts, surfactants, polymers and carbon or metallic nanoparticles) in graphite pastes and inks or by the immobilization of reagents at the electrode surface (as for other electrodes).

Different types of modifications have been developed for improving the performance of glassy carbon electrodes for the selective determination of antioxidants. The selective determination of rutin is described by coating the electrode with graphene nanosheets [113], or with a lead film [114]. Similarly, for the determination of ascorbic acid carbon supported palladium nanoparticles [115] were used. The determination of catechin was also performed using a GC electrode modified with a film of poly-aspartic acid [116]. The simultaneous quantification of the synthetic antioxidants tert-butylhydroquinone (TBHQ) and butyl hydroxyanisole (BHA) in biodiesel was achieved using a GC electrode modified with gold nanoparticles [117]. Also by modifying the GC electrode surface different authors report the simultaneous detection of ascorbic acid (AA) and other important analytes. For the determination of AA with paracetamol in pharmaceutical formulations, multi-wall carbon nanotubes dispersed in polyhistidine were used [118]. The determination of AA and uric acid was achieved using GC electrodes modified either with gold nanotube arrays [119] or with poly-xanthurenic acid / multi-walled carbon nanotube [120]. The determination of AA and dopamine was performed by modifying the GC electrode with docosyltrimethylammonium chloride [121] or with a poly(caffeic acid) thin film [122]. For the determination of AA, dopamine and uric acid the GC electrode was modified with polymeric films of sulfonazo III [123], poly(4-aminobutyric acid) [124] and poly (3-(3-pyridyl) acrylic acid) [125]. The determination GC modified with electroactive species doped PEDOT (Poly(3,4-ethylenedioxythiophene)) films for the simultaneous determination of vitamins B2, B6 and C in orange juices samples [126]. Using silver nanoparticles-decorated reduced graphene oxide it is reported the simultaneous determination of ascorbic acid, dopamine, uric acid, and tryptophan [127].

A carbon fibber microelectrode modified with nickel oxide and ruthenium hexacyanoferrate was successfully applied for the determination of ascorbic acid in human gastric juice [128].

Carbon paste electrodes (CPE) of graphite powder, carbon nanotubes or carbon microspheres are reported for the detection of a wide variety of antioxidants [111]. The improvement of the performance of carbon paste electrodes is reported by the incorporation of different reagents. The determination of catechin in tea samples is reported using beta-cylcodextrin [129] and copper(II) immobilized in a polyester resin [130]. The use of a CPE modified with poly(vinylpyrrolidone) was used for the determination of rutin [131]. The simultaneous determination of ascorbic acid and dopamine was described using a CPE modified with a thionine-nafion supported on multi-walled carbon nanotube [132].

Carbon screen-printed electrodes (SPE) were used to determine rutin in pharmaceutical formulation [94]. By modifying SPEs with an o-aminophenol film the selective determination of ascorbic acid in juices and vegetables [133] was accomplished. Gold electrodes modified with PEDOT were used for the simultaneously determination of ascorbic acid and uric acid in human blood serum [134].

Besides the selective evaluation of antioxidants, electrochemical sensors are successfully used for the characterization of the antioxidant capacity or for the evaluation of the total poliphenol content of samples. Typically the current or area under voltammograms is quantified and is used to define capacity parameters [135–138], or alternatively, these data are interpolated in calibration curves of a reference antioxidant (typically gallic acid or trolox) and expressed as equivalent concentration units [101,103,107].

Flow injection assay with amperometric detection was used for the evaluation of the total polyphenol content of wine samples [138].

Cyclic voltammetry or linear sweep voltammetry assays have been used for evaluation of the overall antioxidant capacity of different samples, such as cane and palm sugars [139], seaweeds extracts [140], tea infusions [99,108,130,141–143], grape juices [144], wines [107,145–148], pharmaceutical formulations [149], blood and saliva [136]. Besides cyclic voltammetry, differential pulse voltammetry and square wave voltammetry were also employed to increase the sensitivity of the detection. The use of DPV for the evaluation of antioxidant capacity is reported in wines [101,103,107,150], fruit extracts [101,151], grape skin extracts [101,151], tea [151], wild medicinal plants [152] and cotton cultivars [153]. The assessment antioxidant capacity by SWV is described in the characterization of wines [154], teas [155], fruit extracts [156,157], fruit juices [105,156] and blood plasma [158].

Despite antioxidants characterization is mostly performed in aqueous solutions, the use of organic solvents is sometimes needed due to solubility constraints. The determination of lipophilic antioxidants in methanol/hexane [159], flavonoids in acetonitrile [160] and propolis extracts in ethanol [100] have been reported.

Following an alternative concept, it is proposed an innovative sensor-type microfluidic device [137] that provides an absolute measure of the total antioxidant capacity of samples. The chronoamperometric response of samples in a thin-layer regime is independent of the diffusion coefficient of the individual antioxidants. Under this regime current is a direct measure of the total antioxidant capacity, defined as

$Q_{AO}=\sum n_i c_i$, where n_i is the number of electrons and c_i concentration of individual antioxidants in mixtures.

3.2 Antioxidant capacity assays

Only one method is reported regarding the assessment of antioxidant capacity by means of potentiostatic electrolysis assays: RACE (Reducing Antioxidant Capacity Evaluated by Electrolysis) [102]. In these assays the action of a reactive oxygen species (ROS) are simulated by means of the electrolyses potential that is settled at the formal potential of a specific ROS. The antioxidant activities are estimated from the charge that antioxidants can provide to reduce the simulated ROS.

3.3 HPLC and CE coupled with electrochemical detection

The determination of antioxidants using high-performance liquid chromatography with electrochemical detection has been reported for the analysis of olive oils [161], teas [162] and foodstuff [163,164].

Quantification of antioxidants in food by capillary electrophoresis and microchip electrophoresis with electrochemical detection is reported by different authors. Characterization of antioxidants is described in samples of rosemary [165], grapefruit peel and juice [166], pharmaceutical preparations [167], orange and tomatoes [168] and plant extracts [169].

4. Electrogeneration of oxygen radicals relevant for HAT based assays

The concept of antioxidant activity deals with the ability of these species to react with radicals, evaluated from a kinetic point of view [4]. A wide group of methods have been designed to characterize the kinetics of antioxidants reactions. These methods are commonly denominated HAT assays. In HAT assays, antioxidants are characterized following the consumption of a molecular probe exposed to oxygen radicals in the presence of the antioxidants.

The in situ generation of peroxyl radicals is carried out in assays such as Oxygen Radical Absorbance Capacity (ORAC) and Total Radical Trapping Antioxidant Parameter (TRAP). This radical is generated by the thermal decomposition of peroxyl radicals generated through the thermal decomposition of azoinitiators, mostly 2,2′-diazobis(2-amidinopropane) hydrochloride (ABAP) and 2,2′-diazobis(2-amidinopropane) dihydrochloride (AAPH) [170]. Other meaningful radicals that are used in antioxidant

assays are the superoxide radical, usually generated by xanthine/xanthine oxidase system [171] and hydroxyl radical, generally produced by Fenton reaction [172].

The production of oxygen radicals by electrochemical means can bring several advantages, such as the minimization of the used reactants and the increased control of the generation process. Despite the electrochemical processes of generation for superoxide and hydroxyl radicals were created in a different context, their optimization and use for in the assessment of antioxidants is reported by several authors.

The electrochemical generation of superoxide radical is carried out by means of the reduction of oxygen [173] or by the oxidation of hydrogen peroxide [174,175]. These processes were integrated in the design of some electrochemical sensors for the characterization of antioxidants activity [86–91].

Regarding the generation of HO radicals several electrochemical based methods are available, namely electro-Fenton, the electroreduction of H_2O_2 and the electrooxidation of H_2O.

The electro-Fenton is a common designation for different methods that allow to generate HO radicals by electrochemically assisted processes, involving one or more of the following reactions: electrogeneration of H_2O_2 by oxygen reduction [176]; electrogeneration of Fe^{2+} by the oxidation of iron [177]; electrogeneration of Fe^{2+} by the reduction of Fe^{3+} [178]. The use of OH radicals generated by electro-Fenton reactions is described in references [74] and [75] regarding the evaluation of antioxidant activity using adenine/guanine biosensors.

The electroreduction of H_2O_2 or of O_2 at palladium dispersed carbon electrodes was described to produce HO radicals [179]. Following a similar approach, it is described in reference [85] a sensor that generates HO radicals and evaluates its consumption by the catalytic current of hydrogen peroxide or dissolved oxygen reduction on palladium oxide nanoparticles.

The generation of HO radicals during the electrooxidation of water using different anode materials (e.g. Pt, IrO_2, SnO_2 and BDD) have been confirmed using spin traps, as N,N-dimethyl-p-nitrosoaniline [180] or 5,5-dimethyl-1-pyrroline-N-oxide [181] and by the formation of hydroxylated products [182]. The extent and rate of the oxidation reactions of electrogenerated HO radicals depend strongly on the degree of adsorption of these radicals at the anode surface. While quasi-free HO radicals are formed at BDD (boron doped diamond) anodes, strongly adsorbed HO radicals are formed at Pt anodes [183]. The generation of strongly adsorbed HO radicals in galvanostatic electrolysis assays was used to compare the reactivity of different phenolic compounds [184].

5. Conclusion

In this review we have identified a number of innovative methods and applications that employ electrochemical strategies for the characterization and quantification of antioxidants. An important number of works report the application of electrochemical techniques as transducers of sensors and biosensors or in assays where the detection of antioxidants are made in an indirect way. Nevertheless, most of the reported papers explore the ability of electrochemical techniques to detect and characterize antioxidants following their direct electrochemical response in voltammetric or amperometric assays. This approach is gaining popularity for the assessment of antioxidants capacity due to the simplicity, low cost and the short time of the assays. Electrochemical methods are also reported in the in situ generation of synthetic oxidants and oxygen radicals used in ET and HAT based assays. The growing number of electrochemical based methods that are available and the diversity of applications reported demonstrate the relevance of electrochemistry in the scope of antioxidants characterization.

References

[1]   P. Kulawik, F. Özogul, R. Glew, Y. Özogul, Significance of Antioxidants for Seafood Safety and Human Health, J. Agric. Food Chem. 61 (2013) 475–491.

[2]   G. Cao, H.M. Alessio, R.G. Cutler, Oxygen-radical absorbance capacity assay for antioxidants, Free Radic. Biol. Med. 14 (1993) 303–311.

[3]   D. Huang, B. Ou, R.L. Prior, The Chemistry behind Antioxidant Capacity Assays, J. Agric. Food Chem. 53 (2005) 1841–1856.

[4]   R. Apak, S. Gorinstein, V. Böhm, K.M. Schaich, M. Özyürek, K. Güçlü, Methods of measurement and evaluation of natural antioxidant capacity/activity (IUPAC Technical Report), Pure Appl. Chem. 85 (2013) 957–998.

[5]   M. Antolovich, P.D. Prenzler, E. Patsalides, S. McDonald, K. Robards, Methods for testing antioxidant activity, Analyst. 127 (2002) 183–198.

[6]   R.L. Prior, X.L. Wu, K. Schaich, Standardized methods for the determination of antioxidant capacity and phenolics in foods and dietary supplements, J. Agric. Food Chem. 53 (2005) 4290–4302.

[7]   L.M. Magalhães, M.A. Segundo, S. Reis, J.L.F.C. Lima, Methodological aspects about in vitro evaluation of antioxidant properties, Anal. Chim. Acta. 613 (2008) 1–19.

[8]   B. Halliwell, M. Whiteman, Measuring reactive species and oxidative damage in vivo and in cell culture: how should you do it and what do the results mean?, Br. J. Pharmacol. 142 (2004) 231–255.

[9]   D. Ozyurt, B. Demirata, R. Apak, Determination of total antioxidant capacity by a new spectrophotometric method based on Ce(IV) reducing capacity measurement, Talanta. 71 (2007) 1155–1165.

[10]   N. Salah, N.J. Miller, G. Paganga, L. Tijburg, G.P. Bolwell, C. Rice-Evans, Polyphenolic flavanols as scavengers of aqueous phase radicals and as chain-breaking antioxidants, Arch. Biochem. Biophys. 322 (1995) 339–346.

[11]   T. Kurechi, K. Kikugawa, T. Kato, Studies on the Antioxidants. XIII. Hydrogen Donating Capability of Antioxidants to 2, 2-Diphenyl-1-picrylhydrazyl, Chem. Pharm. Bull. (Tokyo). 28 (1980) 2089–2093.

[12]   S. Milardovic, D. Iveković, V. Rumenjak, B.S. Grabarić, Use of DPPH·|DPPH Redox Couple for Biamperometric Determination of Antioxidant Activity, Electroanalysis. 17 (2005) 1847–1853.

[13]   S. Milardović, D. Iveković, B.S. Grabarić, A novel amperometric method for antioxidant activity determination using DPPH free radical, Bioelectrochemistry. 68 (2006) 175–180.

[14]   R. de Q. Ferreira, L.A. Avaca, Electrochemical determination of the antioxidant capacity: The ceric reducing/antioxidant capacity (CRAC) assay, Electroanalysis. 20 (2008) 1323–1329.

[15]   M. Amatatongchai, S. Laosing, O. Chailapakul, D. Nacapricha, Simple flow injection for screening of total antioxidant capacity by amperometric detection of DPPH radical on carbon nanotube modified-glassy carbon electrode, Talanta. 97 (2012) 267–272.

[16] Á.M. Alonso, C. Domínguez, D.A. Guillén, C.G. Barroso, Determination of Antioxidant Power of Red and White Wines by a New Electrochemical Method and Its Correlation with Polyphenolic Content, J. Agric. Food Chem. 50 (2002) 3112–3115.

[17] Á.M. Alonso, D.A. Guillén, C.G. Barroso, Development of an electrochemical method for the determination of antioxidant activity. Application to grape-derived products, Eur. Food Res. Technol. 216 (2003) 445–448.

[18] D. Ivekovic, S. Milardovic, M. Roboz, B.S. Grabaric, Evaluation of the antioxidant activity by flow injection analysis method with electrochemically generated ABTS radical cation, Analyst. 130 (2005) 708–714.

[19] I.F. Abdullin, E.N. Turova, G.K. Budnikov, Coulometric Determination of the Antioxidant Capacity of Tea Extracts Using Electrogenerated Bromine, J. Anal. Chem. 56 (2001) 557–559.

[20] D. Lowinsohn, M. Bertotti, Determination of sulphite in wine by coulometric titration, Food Addit. Contam. 18 (2001) 773–777.

[21] I.F. Abdullin, E.N. Turova, G.K. Ziyatdinova, G.K. Budnikov, Determination of Fat-Soluble Antioxidants by Galvanostatic Coulometry Using Electrogenerated Oxidants, J. Anal. Chem. 57 (2002) 730–732.

[22] V. Castaignède, H. Durliat, M. Comtat, Amperometric and Potentiometric Determination of Catechin as Model of Polyphenols in Wines, Anal. Lett. 36 (2003) 1707–1720.

[23] S. Martinez, L. Valek, J. Piljac, M. Metikoš-Huković, Determination of wine antioxidant capacity by derivative potentiometric titration with electrogenerated chlorine, Eur. Food Res. Technol. 220 (2005) 658–661.

[24] G.K. Ziyatdinova, H.C. Budnikov, V.I. Pogorel'tzev, T.S. Ganeev, The application of coulometry for total antioxidant capacity determination of human blood, Talanta. 68 (2006) 800–805.

[25] A.M. Nizamova, G.K. Ziyatdinova, G.K. Budnikov, Electrogenerated bromine as a coulometric reagent for the estimation of the bioavailability of polyphenols, J. Anal. Chem. 66 (2011) 301–309.

[26] G. Ziyatdinova, E. Ziganshina, H. Budnikov, Surfactant media for constant-current coulometry. Application for the determination of antioxidants in pharmaceuticals, Anal. Chim. Acta. 744 (2012) 23–28.

[27] T. Kanyanee, P. Fuekhad, K. Grudpan, Micro coulometric titration in a liquid drop, Talanta. 115 (2013) 258–262.

[28] G. Ziyatdinova, I. Aytuganova, A. Nizamova, H. Budnikov, Differential Pulse Voltammetric Assay of Coffee Antioxidant Capacity with MWNT-Modified Electrode, Food Anal. Methods. (2013) 1–10.

[29] M.P. Connnor, J. Sanchez, J. Wang, M.R. Smyth, S. Mannino, Silicone-grease-based immobilization method for the preparation of enzyme electrodes, Analyst. 114 (1989) 1427–1429.

[30] M. Diaconu, S.C. Litescu, G.L. Radu, Laccase–MWCNT–chitosan biosensor—A new tool for total polyphenolic content evaluation from in vitro cultivated plants, Sensors Actuators B Chem. 145 (2010) 800–806.

[31] S.A. V Eremia, G.-L. Radu, S.-C. Litescu, Monitoring of Rosmarinic Acid Accumulation in Sage Cell Cultures using Laccase Biosensor, Phytochem. Anal. 24 (2013) 53–58.

[32] M. Di Fusco, C. Tortolini, D. Deriu, F. Mazzei, Laccase-based biosensor for the determination of polyphenol index in wine, Talanta. 81 (2010) 235–240.

[33] M.R. Montereali, L. Della Seta, W. Vastarella, R. Pilloton, A disposable Laccase–Tyrosinase based biosensor for amperometric detection of phenolic compounds in must and wine, J. Mol. Catal. B Enzym. 64 (2010) 189–194.

[34] E. Martinez-Periñan, M.P. Hernández-Artiga, J.M. Palacios-Santander, M. ElKaoutit, I. Naranjo-Rodriguez, D. Bellido-Milla, Estimation of beer stability by sulphur dioxide and polyphenol determination. Evaluation of a Laccase-Sonogel-Carbon biosensor, Food Chem. 127 (2011) 234–239.

[35] R. Rawal, S. Chawla, C.S. Pundir, Polyphenol biosensor based on laccase immobilized onto silver nanoparticles/multiwalled carbon nanotube/polyaniline gold electrode, Anal. Biochem. 419 (2011) 196–204.

[36] S. Chawla, R. Rawal, C.S. Pundir, Fabrication of polyphenol biosensor based on laccase immobilized on copper nanoparticles/chitosan/multiwalled carbon nanotubes/polyaniline-modified gold electrode, J. Biotechnol. 156 (2011) 39–45.

[37] M. Sys, B. Pekec, K. Kalcher, K. Vytras, Amperometric Enzyme Carbon Paste-Based Biosensor for Quantification of Hydroquinone and Polyphenolic Antioxidant Capacity, Int. J. Electrochem. Sci. 8 (2013) 9030–9040.

[38] S. Chawla, R. Rawal, S. Sharma, C.S. Pundir, An amperometric biosensor based on laccase immobilized onto nickel nanoparticles/carboxylated multiwalled carbon nanotubes/polyaniline modified gold electrode for determination of phenolic content in fruit juices, Biochem. Eng. J. 68 (2012) 76–84.

[39] P. Ibarra-Escutia, J.J. Gómez, C. Calas-Blanchard, J.L. Marty, M.T. Ramírez-Silva, Amperometric biosensor based on a high resolution photopolymer deposited onto a screen-printed electrode for phenolic compounds monitoring in tea infusions, Talanta. 81 (2010) 1636–1642.

[40] S.A. V Eremia, I. Vasilescu, A. Radoi, S.-C. Litescu, G.-L. Radu, Disposable biosensor based on platinum nanoparticles-reduced graphene oxide-laccase biocomposite for the determination of total polyphenolic content, Talanta. 110 (2013) 164–170.

[41] E. Zapp, D. Brondani, I.C. Vieira, J. Dupont, C.W. Scheeren, Bioelectroanalytical Determination of Rutin Based on bi-Enzymatic Sensor Containing Iridium Nanoparticles in Ionic Liquid Phase Supported in Clay, Electroanalysis. 23 (2011) 764–776.

[42] I.M. Apetrei, M.L. Rodriguez-Mendez, C. Apetrei, J.A. de Saja, Enzyme sensor based on carbon nanotubes/cobalt(II) phthalocyanine and tyrosinase used in pharmaceutical analysis, Sensors Actuators B Chem. 177 (2013) 138–144.

[43] R. Penu, I. Vasilescu, S.A. V Eremia, F. Gatea, G.-L. Radu, S.-C. Litescu, Development of a nanocomposite system and its application in biosensors construction, Cent. Eur. J. Chem. 11 (2013) 968–978.

[44] A.C. Moţ, C. Coman, C. Miron, G. Damian, C. Sarbu, R. Silaghi-Dumitrescu, An assay for pro-oxidant reactivity based on phenoxyl radicals generated by laccase, Food Chem. 143 (2014) 214–222.

[45] E. Akyilmaz, O. Kozgus, H. Türkmen, B. Çetinkaya, A mediated polyphenol oxidase biosensor immobilized by electropolymerization of 1,2-diamino benzene, Bioelectrochemistry. 78 (2010) 135–140.

[46] I.M. Apetrei, G. Bahrim, M. Luz Rodriguez-Mendez, Electrochemical study of polyphenols with amperometric tyrosinase based biosensors, Rom. Biotechnol. Lett. 17 (2012) 7684–7693.

[47] A. Merkoçi, U. Anik, S. Çevik, M. Çubukçu, M. Guix, Bismuth Film Combined with Screen-Printed Electrode as Biosensing Platform for Phenol Detection, Electroanalysis. 22 (2010) 1429–1436.

[48] C.C. Mayorga-Martinez, M. Cadevall, M. Guix, J. Ros, A. Merkoçi, Bismuth nanoparticles for phenolic compounds biosensing application, Biosens. Bioelectron. 40 (2013) 57–62.

[49] G.K. Glantzounis, E.C. Tsimoyiannis, A.M. Kappas, D.A. Galaris, Uric acid and oxidative stress, Curr. Pharm. Des. 11 (2005) 4145–4151.

[50] P.E. Erden, E. Kılıç, A review of enzymatic uric acid biosensors based on amperometric detection, Talanta. 107 (2013) 312–323.

[51] E. Miland, A.J. Miranda Ordieres, P. Tuñón Blanco, M.R. Smyth, C.Ó. Fágáin, Poly(o-aminophenol)-modified bienzyme carbon paste electrode for the detection of uric acid, Talanta. 43 (1996) 785–796.

[52] M. Bhambi, G. Sumana, B.D. Malhotra, C.S. Pundir, An Amperomertic Uric Acid Biosensor Based on Immobilization of Uricase onto Polyaniline-multiwalled Carbon Nanotube Composite Film, Artif. Cells, Blood Substitutes Biotechnol. 38 (2010) 178–185.

[53] N. Chauhan, C.S. Pundir, An amperometric uric acid biosensor based on multiwalled carbon nanotube–gold nanoparticle composite, Anal. Biochem. 413 (2011) 97–103.

[54] P.E. Erden, S. Pekyardimci, E. Kilic, Amperometric carbon paste enzyme electrodes for uric acid determination with different mediators, Collect. Czechoslov. Chem. Commun. 76 (2011) 1055–1073.

[55] R. Rawal, S. Chawla, N. Chauhan, T. Dahiya, C.S. Pundir, Construction of amperometric uric acid biosensor based on uricase immobilized on PBNPs/cMWCNT/PANI/Au composite, Int. J. Biol. Macromol. 50 (2012) 112–118.

[56] Y. Wang, Y. Hasebe, Uricase-adsorbed carbon-felt reactor coupled with a peroxidase-modified carbon-felt-based H2O2 detector for highly sensitive amperometric flow determination of uric acid, J. Pharm. Biomed. Anal. 57 (2012) 125–132.

[57] B. Thakur, S.N. Sawant, Polyaniline/Prussian-Blue-Based Amperometric Biosensor for Detection of Uric Acid, Chempluschem. 78 (2013) 166–174.

[58] P. Kanyong, R.M. Pemberton, S.K. Jackson, J.P. Hart, Development of a sandwich format, amperometric screen-printed uric acid biosensor for urine analysis, Anal. Biochem. 428 (2012) 39–43.

[59] T. Ahuja, Rajeshb, D. Kumar, V.K. Tanwar, V. Sharma, N. Singh, et al., An amperometric uric acid biosensor based on Bis[sulfosuccinimidyl] suberate crosslinker/3-aminopropyltriethoxysilane surface modified ITO glass electrode, Thin Solid Films. 519 (2010) 1128–1134.

[60] S. Kurşun, B.Z. Ekinci, A. Paşahan, E. Ekinci, Preparation and properties of amperometric uric acid sensor based on poly(2-aminophenol), J. Appl. Polym. Sci. 120 (2011) 406–410.

[61] Y. Liu, M. Yuan, L. Liu, R. Guo, A facile electrochemical uricase biosensor designed from gold/amino acid nanocomposites, Sensors Actuators B Chem. 176 (2013) 592–597.

20

[62]   A.S. Karakoti, N.A. Monteiro-Riviere, R. Aggarwal, J.P. Davis, R.J. Narayan, W.T. Self, et al., Nanoceria as antioxidant: Synthesis and biomedical applications, JOM. 60 (2008) 33–37.

[63]   M. Ganesana, J.S. Erlichman, S. Andreescu, Real-time monitoring of superoxide accumulation and antioxidant activity in a brain slice model using an electrochemical cytochrome c biosensor, Free Radic. Biol. Med. 53 (2012) 2240–2249.

[64]   L.. Campanella, R.. Gabbianelli, T.. Gatta, E.. Mazzone, M.. Tomassetti, A superoxide dismutase biosensor for measuring the antioxidant capacity of blueberry based integrators, Curr. Pharm. Anal. 9 (2013) 208–216.

[65]   A.M. Granero, H. Fernández, E. Agostini, M.A. Zón, An amperometric biosensor based on peroxidases from Brassica napus for the determination of the total polyphenolic content in wine and tea samples, Talanta. 83 (2010) 249–255.

[66]   Y. Chen, H. Xiong, X. Zhang, S. Wang, Electrochemical detection of in situ DNA damage induced by enzyme-catalyzed Fenton reaction. Part II in hydrophobic room temperature ionic liquid, Microchim. Acta. 178 (2012) 45–51.

[67]   H. Xiong, Y. Chen, X. Zhang, H. Gu, S. Wang, An electrochemical biosensor for the rapid detection of DNA damage induced by xanthine oxidase-catalyzed Fenton reaction, Sensors Actuators, B Chem. 181 (2013) 85–91.

[68]   M. Mazloum-Ardakani, E. Salehpour, M.M. Heidari, A. Zomorodipour, The effect of pomegranate juice as a natural antioxidant to prevent DNA damages is detectable by application of electrochemical methods, Sci. Iran. (2013).

[69]   M. Chen, H. Xiong, X. Zhang, H. Gu, S. Wang, Electrochemical biosensors for the monitoring of DNA damage induced by ferric ions mediated oxidation of dopamine, Electrochem. Commun. 28 (2013) 91–94.

[70]   M.F. Barroso, N. De-los-Santos-Álvarez, M.J. Lobo-Castañón, A.J. Miranda-Ordieres, C. Delerue-Matos, M.B.P.P. Oliveira, et al., DNA-based biosensor for the electrocatalytic determination of antioxidant capacity in beverages, Biosens. Bioelectron. 26 (2011) 2396–2401.

[71]   M.F. Barroso, N. De-Los-Santos-Álvarez, M.J. Lobo-Castañón, A.J. Miranda-Ordieres, C. Delerue-Matos, M.B.P.P. Oliveira, et al., Electrocatalytic evaluation of DNA damage by superoxide radical for antioxidant capacity assessment, J. Electroanal. Chem. 659 (2011) 43–49.

[72]   M.F. Barroso, C. Delerue-Matos, M.B.P.P. Oliveira, Electrochemical DNA-sensor for evaluation of total antioxidant capacity of flavours and flavoured waters using superoxide radical damage, Biosens. Bioelectron. 26 (2011) 3748–3754.

[73]   M.F. Barroso, C. Delerue-Matos, M.B.P.P. Oliveira, Evaluation of the total antioxidant capacity of flavored water and electrochemical purine damage by sulfate radicals using a purine-based sensor, Electrochim. Acta. 56 (2011) 8954–8961.

[74]   M.F. Barroso, C. Delerue-Matos, M.B.P.P. Oliveira, Electrochemical evaluation of total antioxidant capacity of beverages using a purine-biosensor, Food Chem. 132 (2012) 1055–1062.

[75]   Y. Yang, J. Zhou, H. Zhang, P. Gai, X. Zhang, J. Chen, Electrochemical evaluation of total antioxidant capacities in fruit juice based on the guanine/graphene nanoribbon/glassy carbon electrode, Talanta. 106 (2013) 206–211.

[76] C. Bian, H. Xiong, X. Zhang, W. Wen, S. Wang, An electrochemical biosensor for analysis of Fenton-mediated oxidative damage to BSA using poly-o-phenylenediamine as electroactive probe, Biosens. Bioelectron. 28 (2011) 216–220.

[77] Y. Wang, H. Xiong, X. Zhang, H. Gu, S. Wang, An electrochemical biosensor for rapid detection of bovine serum albumin damage induced by hydroxyl radicals in room temperature ionic liquid, Sensors Actuators B Chem. 188 (2013) 741–746.

[78] R. Gulaboski, V. Mirčeski, S. Mitrev, Development of a rapid and simple voltammetric method to determine total antioxidative capacity of edible oils, Food Chem. 138 (2013) 116–121.

[79] A. Wu, J. Sun, Y. Fang, R. Zheng, G. Chen, Hot electron induced cathodic electrochemiluminescence at disposable screen printed carbon electrodes, Electroanalysis. 22 (2010) 2702–2707.

[80] D. Yuan, S. Chen, J. Zhang, H. Wang, R. Yuan, W. Zhang, An electrochemiluminescent sensor for phenolic compounds based on the inhibition of peroxydisulfate electrochemiluminescence, Sensors Actuators B Chem. 185 (2013) 417–423.

[81] W. Xiuhua, L. Chao, T. Yifeng, Microemulsion-enhanced electrochemiluminescence of luminol-H 2 O 2 for sensitive flow injection analysis of antioxidant compounds, Talanta. 94 (2012) 289–294.

[82] C. Liu, X. Wei, Y. Tu, Development of a reagentless electrochemiluminescent electrode for flow injection analysis using copolymerised luminol/aniline on nano-TiO2 functionalised indium-tin oxide glass, Talanta. 111 (2013) 156–162.

[83] J. Wang, N. Zhou, Z. Zhu, J. Huang, G. Li, Detection of flavonoids and assay for their antioxidant activity based on enlargement of gold nanoparticles, Anal. Bioanal. Chem. 388 (2007) 1199–1205.

[84] X. Ma, W. Qian, Phenolic acid induced growth of gold nanoshells precursor composites and their application in antioxidant capacity assay, Biosens. Bioelectron. 26 (2010) 1049–1055.

[85] J. Liu, G. Lagger, P. Tacchini, H.H. Girault, Generation of OH radicals at palladium oxide nanoparticle modified electrodes, and scavenging by fluorescent probes and antioxidants, J. Electroanal. Chem. 619–620 (2008) 131–136.

[86] C. Le Bourvellec, D. Hauchard, A. Darchen, J.-L. Burgot, M.-L. Abasq, Validation of a new method using the reactivity of electrogenerated superoxide radical in the antioxidant capacity determination of flavonoids, Talanta. 75 (2008) 1098–1103.

[87] A. Palma, M. Ruiz Montoya, J.E. Arteaga, J.M. Rodriguez Mellado, Analysis of the Interaction of Radical Scavengers with ROS Electrogenerated from Hydrogen Peroxide, J. Electrochem. Soc. 160 (2013) H213–H218.

[88] Z. Jian-Bin, Z. Hong-Fang, G. Hong, Investigation on Electrochemical Behavior and Scavenging Superoxide Anion Ability of Chrysin at Mercury Electrode, Chinese J. Chem. 23 (2005) 1042–1046.

[89] A. René, M.-L. Abasq, D. Hauchard, P. Hapiot, How Do Phenolic Compounds React toward Superoxide Ion? A Simple Electrochemical Method for Evaluating Antioxidant Capacity, Anal. Chem. 82 (2010) 8703–8710.

[90] G.K. Ziyatdinova, H.C. Budnikov, V.I. Pogorel'tzev, Electrochemical determination of the total antioxidant capacity of human plasma, Anal. Bioanal. Chem. 381 (2005) 1546–1551.

[91] S. Ahmed, F. Shakeel, Voltammetric determination of antioxidant character in Berberis lycium Royel, Zanthoxylum armatum and Morus nigra Linn plants, Pak. J. Pharm. Sci. 25 (2012) 501–507.

[92] S. Chevion, E.M. Berry, N. Kitrossky, R. Kohen, Evaluation of Plasma Low Molecular Weight Antioxidant Capacity by Cyclic Voltammetry, Free Radic. Biol. Med. 22 (1997) 411–421.

[93] P.A. Kilmartin, Electrochemical Detection of Natural Antioxidants: Principles and Protocols, Antioxid. Redox Signal. 3 (2001) 941–955.

[94] A. de Oliveira-Roberth, D.I. V Santos, D.D. Cordeiro, F.M. de A. Lino, M.T.F. Bara, E. de S. Gil, Voltammetric determination of Rutin at Screen-Printed carbon disposable electrodes, Cent. Eur. J. Chem. 10 (2012) 1609–1616.

[95] R.P. Caramit, A.G. de Freitas Andrade, J.B. Gomes de Souza, T.A. de Araujo, L.H. Viana, M.A.G. Trindade, et al., A new voltammetric method for the simultaneous determination of the antioxidants TBHQ and BHA in biodiesel using multi-walled carbon nanotube screen-printed electrodes, Fuel. 105 (2013) 306–313.

[96] S.N. Robledo, V.G.L. Zachetti, M.A. Zon, H. Fernández, Quantitative determination of tocopherols in edible vegetable oils using electrochemical ultra-microsensors combined with chemometric tools, Talanta. 116 (2013) 964–971.

[97] A. Rodrigues, A.C. Silva Ferreira, P. de Pinho, F. Bento, D. Geraldo, Resistance to Oxidation of White Wines Assessed by Voltammetric Means, J. Agric. Food Chem. 55 (2007) 10557–10562.

[98] R.C. Martins, R. Oliveira, F. Bento, D. Geraldo, V. V Lopes, P. Guedes de Pinho, et al., Oxidation Management of White Wines Using Cyclic Voltammetry and Multivariate Process Monitoring, J. Agric. Food Chem. 56 (2008) 12092–12098.

[99] J. Piljac-Žegarac, L. Valek, T. Stipčević, S. Martinez, Electrochemical determination of antioxidant capacity of fruit tea infusions, Food Chem. 121 (2010) 820–825.

[100] R.A. Laskar, I. Sk, N. Roy, N.A. Begum, Antioxidant activity of Indian propolis and its chemical constituents, Food Chem. 122 (2010) 233–237.

[101] M.J. Aguirre, Y.Y. Chen, M. Isaacs, B. Matsuhiro, L. Mendoza, S. Torres, Electrochemical behaviour and antioxidant capacity of anthocyanins from Chilean red wine, grape and raspberry, Food Chem. 121 (2010) 44–48.

[102] R. Oliveira, J. Marques, F. Bento, D. Geraldo, P. Bettencourt, Reducing Antioxidant Capacity Evaluated by Means of Controlled Potential Electrolysis, Electroanalysis. 23 (2011) 692–700.

[103] M. Seruga, I. Novak, L. Jakobek, Determination of polyphenols content and antioxidant activity of some red wines by differential pulse voltammetry, HPLC and spectrophotometric methods, Food Chem. 124 (2011) 1208–1216.

[104] H. Zieliński, D. Zielińska, H. Kostyra, Antioxidant capacity of a new crispy type food products determined by updated analytical strategies, Food Chem. 130 (2012) 1098–1104.

[105] J. Giné Bordonaba, L.A. Terry, Electrochemical behaviour of polyphenol rich fruit juices using disposable screen-printed carbon electrodes: Towards a rapid sensor for antioxidant capacity and individual antioxidants, Talanta. 90 (2012) 38–45.

[106] J.F. Arteaga, M. Ruiz-Montoya, A. Palma, G. Alonso-Garrido, S. Pintado, J.M. Rodríguez-Mellad, Comparison of the simple cyclic voltammetry (CV) and DPPH assays for the determination of antioxidant capacity of active principles, Molecules. 17 (2012) 5126–5138.

[107] M.J. Rebelo, R. Rego, M. Ferreira, M.C. Oliveira, Comparative study of the antioxidant capacity and polyphenol content of Douro wines by chemical and electrochemical methods, Food Chem. 141 (2013) 566–573.

[108] J.N. Veljković, A.N. Pavlović, S.S. Mitić, S.B. Tošić, G.S. Stojanović, B.M. Kaličanin, et al., Evaluation of individual phenolic compounds and antioxidant properties of black, green, herbal and fruit tea infusions consumed in Serbia: Spectrophotometrical and electrochemical approaches, J. Food Nutr. Res. 52 (2013) 12–24.

[109] D. Zielińska, H. Zieliński, Antioxidant activity of flavone C-glucosides determined by updated analytical strategies, Food Chem. 124 (2011) 672–678.

[110] M.S. Estevão, L.C. Carvalho, L.M. Ferreira, E. Fernandes, M.M.B. Marques, Analysis of the antioxidant activity of an indole library: cyclic voltammetry versus ROS scavenging activity, Tetrahedron Lett. 52 (2011) 101–106.

[111] C. Apetrei, I.M. Apetrei, J.A. De Saja, M.L. Rodriguez-Mendez, Carbon Paste Electrodes Made from Different Carbonaceous Materials: Application in the Study of Antioxidants, Sensors. 11 (2011) 1328–1344.

[112] J. Teixeira, A. Gaspar, E.M. Garrido, J. Garrido, F. Borges, Hydroxycinnamic acid antioxidants: An electrochemical overview, Biomed Res. Int. 2013 (2013).

[113] H. Du, J. Ye, J. Zhang, X. Huang, C. Yu, Graphene Nanosheets Modified Glassy Carbon Electrode as a Highly Sensitive and Selective Voltammetric Sensor for Rutin, Electroanalysis. 22 (2010) 2399–2406.

[114] K. Tyszczuk, Sensitive voltammetric determination of rutin at an in situ plated lead film electrode, J. Pharm. Biomed. Anal. 49 (2009) 558–561.

[115] X. Zhang, Y. Cao, S. Yu, F. Yang, P. Xi, An electrochemical biosensor for ascorbic acid based on carbon-supported PdNinanoparticles, Biosens. Bioelectron. 44 (2013) 183–190.

[116] X.-G. Wang, J. Li, Y.-J. Fan, Fast detection of catechin in tea beverage using a poly-aspartic acid film based sensor, Microchim. Acta. 169 (2010) 173–179.

[117] X. Lin, Y. Ni, S. Kokot, Glassy carbon electrodes modified with gold nanoparticles for the simultaneous determination of three food antioxidants, Anal. Chim. Acta. 765 (2013) 54–62.

[118] P.R. Dalmasso, M.L. Pedano, G.A. Rivas, Electrochemical determination of ascorbic acid and paracetamol in pharmaceutical formulations using a glassy carbon electrode modified with multi-wall carbon nanotubes dispersed in polyhistidine, Sensors Actuators B Chem. 173 (2012) 732–736.

[119] G. Yang, L. Li, J. Jiang, Y. Yang, Direct electrodeposition of gold nanotube arrays of rough and porous wall by cyclic voltammetry and its applications of simultaneous determination of ascorbic acid and uric acid, Mater. Sci. Eng. C. 32 (2012) 1323–1330.

[120] F.A.S. Silva, C.B. Lopes, L.T. Kubota, P.R. Lima, M.O.F. Goulart, Poly-xanthurenic acid modified electrodes: An amperometric sensor for the simultaneous determination of ascorbic and uric acids, Sensors Actuators B Chem. 168 (2012) 289–296.

[121] L.-Q. Luo, Q.-X. Li, Y.-P. Ding, Y. Zhang, X. Shen, Docosyltrimethylammonium chloride modified glassy carbon electrode for simultaneous determination of dopamine and ascorbic acid, J. Solid State Electrochem. 14 (2010) 1311–1316.

[122] N. Li, W. Ren, H. Luo, Simultaneous voltammetric measurement of ascorbic acid and dopamine on poly(caffeic acid)-modified glassy carbon electrode, J. Solid State Electrochem. 12 (2008) 693–699.

[123] A.A. Ensafi, M. Taei, T. Khayamian, A. Arabzadeh, Highly selective determination of ascorbic acid, dopamine, and uric acid by differential pulse voltammetry using poly(sulfonazo III) modified glassy carbon electrode, Sensors Actuators B Chem. 147 (2010) 213–221.

[124] X. Zheng, X. Zhou, X. Ji, R. Lin, W. Lin, Simultaneous determination of ascorbic acid, dopamine and uric acid using poly(4-aminobutyric acid) modified glassy carbon electrode, Sensors Actuators B Chem. 178 (2013) 359–365.

[125] Y. Zhang, S. Su, Y. Pan, L. Zhang, Y. Cai, Poly (3-(3-Pyridyl) Acrylic Acid) Modified Glassy Carbon Electrode for Simultaneous Determination of Dopamine, Ascorbic Acid and Uric Acid, Ann. Chim. 97 (2007) 665–674.

[126] T. Nie, J.-K. Xu, L.-M. Lu, K.-X. Zhang, L. Bai, Y.-P. Wen, Electroactive species-doped poly(3,4-ethylenedioxythiophene) films: Enhanced sensitivity for electrochemical simultaneous determination of vitamins B2, B6 and C, Biosens. Bioelectron. 50 (2013) 244–250.

[127] B. Kaur, T. Pandiyan, B. Satpati, R. Srivastava, Simultaneous and sensitive determination of ascorbic acid, dopamine, uric acid, and tryptophan with silver nanoparticles-decorated reduced graphene oxide modified electrode, Colloids Surfaces B Biointerfaces. 111 (2013) 97–106.

[128] E.A. Hutton, R. Pauliukaitè, S.B. Hocevar, B. Ogorevc, M.R. Smyth, Amperometric microsensor for direct probing of ascorbic acid in human gastric juice, Anal. Chim. Acta. 678 (2010) 176–182.

[129] D. El-Hady, N. El-Maali, Selective square wave voltammetric determination of (+)-catechin in commercial tea samples using beta-cyclodextrin modified carbon paste electrode, Microchim. Acta. 161 (2008) 225–231.

[130] K.H.G. Freitas, O. Fatibello-Filho, Carbon Composite Electrode Modified with Copper(II) Phosphate Immobilized in a Polyester Resin for Voltammetric Determination of Catechin in Teas, Anal. Lett. 43 (2010) 2091–2104.

[131] A.C. Franzoi, A. Spinelli, I.C. Vieira, Rutin determination in pharmaceutical formulations using a carbon paste electrode modified with poly(vinylpyrrolidone), J. Pharm. Biomed. Anal. 47 (2008) 973–977.

[132] S. Shahrokhian, H.R. Zare-Mehrjardi, Application of thionine-nafion supported on multi-walled carbon nanotube for preparation of a modified electrode in simultaneous voltammetric detection of dopamine and ascorbic acid, Electrochim. Acta. 52 (2007) 6310–6317.

[133] L. Civit, H.M. Nassef, A. Fragoso, C.K. O'Sullivan, Amperometric Determination of Ascorbic Acid in Real Samples Using a Disposable Screen-Printed Electrode Modified with Electrografted o-Aminophenol Film, J. Agric. Food Chem. 56 (2008) 10452–10455.

[134] F. Sekli-Belaidi, P. Temple-Boyer, P. Gros, Voltammetric microsensor using PEDOT-modified gold electrode for the simultaneous assay of ascorbic and uric acids, J. Electroanal. Chem. 647 (2010) 159–168.

[135] E.I. Korotkova, Y.A. Karbainov, A. V Shevchuk, Study of antioxidant properties by voltammetry, J. Electroanal. Chem. 518 (2002) 56–60.

[136] P. Tacchini, A. Lesch, A. Neequaye, G. Lagger, J. Liu, F. Cortés-Salazar, et al., Electrochemical pseudo-titration of water-soluble antioxidants, Electroanalysis. 25 (2013) 922–930.

[137] R. Oliveira, F. Bento, C. Sella, L. Thouin, C. Amatore, Direct Electroanalytical Method for Alternative Assessment of Global Antioxidant Capacity Using Microchannel Electrodes, Anal. Chem. 85 (2013) 9057–9063.

[138] A. Sánchez Arribas, M. Martínez-Fernández, M. Moreno, E. Bermejo, A. Zapardiel, M. Chicharro, Analysis of total polyphenols in wines by FIA with highly stable amperometric detection using carbon nanotube-modified electrodes, Food Chem. 136 (2013) 1183–1192.

[139] J. Sia, H.-B. Yee, J.H. Santos, M.K.-A. Abdurrahman, Cyclic voltammetric analysis of antioxidant activity in cane sugars and palm sugars from Southeast Asia, Food Chem. 118 (2010) 840–846.

[140] R. Keyrouz, M.L. Abasq, C. Le Bourvellec, N. Blanc, L. Audibert, E. ArGall, et al., Total phenolic contents, radical scavenging and cyclic voltammetry of seaweeds from Brittany, Food Chem. 126 (2011) 831–836.

[141] P.A. Kilmartin, C.F. Hsu, Characterisation of polyphenols in green, oolong, and black teas, and in coffee, using cyclic voltammetry, Food Chem. 82 (2003) 501–512.

[142] S. Dubeau, G. Samson, H.-A. Tajmir-Riahi, Dual effect of milk on the antioxidant capacity of green, Darjeeling, and English breakfast teas, Food Chem. 122 (2010) 539–545.

[143] E. Rozoy, M. Araya-Farias, S. Simard, D. Kitts, J. Lessard, L. Bazinet, Redox properties of catechins and enriched green tea extracts effectively preserve l-5-methyltetrahydrofolate: Assessment using cyclic voltammetry analysis, Food Chem. 138 (2013) 1982–1991.

[144] O. Makhotkina, P.A. Kilmartin, The phenolic composition of Sauvignon blanc juice profiled by cyclic voltammetry, Electrochim. Acta. 83 (2012) 188–195.

[145] P.A. Kilmartin, H. Zou, A.L. Waterhouse, A Cyclic Voltammetry Method Suitable for Characterizing Antioxidant Properties of Wine and Wine Phenolics, J. Agric. Food Chem. 49 (2001) 1957–1965.

[146] P.A. Kilmartin, H. Zou, A.L. Waterhouse, Correlation of Wine Phenolic Composition versus Cyclic Voltammetry Response, Am. J. Enol. Vitic. 53 (2002) 294–302.

[147] O. Makhotkina, P.A. Kilmartin, The use of cyclic voltammetry for wine analysis: Determination of polyphenols and free sulfur dioxide, Anal. Chim. Acta. 668 (2010) 155–165.

[148] A. Dhroso, S. Laschi, G. Marrazza, M. Mascini, A Fast Electrochemical Technique for Characterization of Phenolic Content in Wine, Anal. Lett. 43 (2010) 1190–1198.

[149] P. Deng, Z. Xu, J. Li, Simultaneous determination of ascorbic acid and rutin in pharmaceutical preparations with electrochemical method based on multi-walled carbon nanotubes-chitosan composite film modified electrode, J. Pharm. Biomed. Anal. 76 (2013) 234–242.

[150] M.J. Aguirre, M. Isaacs, B. Matsuhiro, L. Mendoza, L.S. Santos, S. Torres, Anthocyanin composition in aged Chilean Cabernet Sauvignon red wines, Food Chem. 129 (2011) 514–519.

[151] A. Romani, M. Minunni, N. Mulinacci, P. Pinelli, F.F. Vincieri, M. Del Carlo, et al., Comparison among Differential Pulse Voltammetry, Amperometric Biosensor, and HPLC/DAD Analysis for Polyphenol Determination, J. Agric. Food Chem. 48 (2000) 1197–1203.

[152] L. Barros, L. Cabrita, M. V Boas, A.M. Carvalho, I.C.F.R. Ferreira, Chemical, biochemical and electrochemical assays to evaluate phytochemicals and antioxidant activity of wild plants, Food Chem. 127 (2011) 1600–1608.

[153] G. Magarelli, J.G. da Silva, I.A. de Sousa Filho, I.S.D. Lopes, J.R. SouzaDe, L.V. Hoffmann, et al., Development and validation of a voltammetric method for determination of total phenolic acids in cotton cultivars, Microchem. J. 109 (2013) 23–28.

[154] H. Filik, G. Çetintaş, A.A. Avan, S. Aydar, S.N. Koç, İ. Boz, Square-wave stripping voltammetric determination of caffeic acid on electrochemically reduced graphene oxide–Nafion composite film, Talanta. 116 (2013) 245–250.

[155] I. Novak, M. Šeruga, Š. Komorsky-Lovrić, Characterisation of catechins in green and black teas using square-wave voltammetry and RP-HPLC-ECD, Food Chem. 122 (2010) 1283–1289.

[156] M. Cuartero, J.A. Ortuño, P. Truchado, M.S. García, F.A. Tomás-Barberán, M.I. Albero, Voltammetric behaviour and square-wave voltammetric determination of the potent antioxidant and anticarcinogenic agent ellagic acid in foodstuffs, Food Chem. 128 (2011) 549–554.

[157] F.J.N. Maia, C. da S. Clemente, T.M.B.F. Oliveira, D. Lomonaco, T.I.S. Oliveira, M.O. Almeida, et al., Electrochemical and computational studies of phenolic antioxidants from cashew nut shell liquid, Electrochim. Acta. 79 (2012) 67–73.

[158] M. Pohanka, H. Bandouchova, J. Sobotka, J. Sedlackova, I. Soukupova, J. Pikula, Ferric Reducing Antioxidant Power and Square Wave Voltammetry for Assay of Low Molecular Weight Antioxidants in Blood Plasma: Performance and Comparison of Methods, Sensors. 9 (2009) 9094–9103.

[159] T. Kondo, K. Sakai, T. Watanabe, Y. Einaga, M. Yuasa, Electrochemical detection of lipophilic antioxidants with high sensitivity at boron-doped diamond electrode, Electrochim. Acta. 95 (2013) 205–211.

[160] A. Masek, M. Zaborski, E. Chrzescijanska, Electrooxidation of flavonoids at platinum electrode studied by cyclic voltammetry, Food Chem. 127 (2011) 699–704.

[161] B. Bayram, B. Ozcelik, G. Schultheiss, J. Frank, G. Rimbach, A validated method for the determination of selected phenolics in olive oil using high-performance liquid chromatography with coulometric electrochemical detection and a fused-core column, Food Chem. 138 (2013) 1663–1669.

[162] W. Andlauer, J. Héritier, Rapid electrochemical screening of antioxidant capacity (RESAC) of selected tea samples, Food Chem. 125 (2011) 1517–1520.

[163] C. André, I. Castanheira, J.M. Cruz, P. Paseiro, A. Sanches-Silva, Analytical strategies to evaluate antioxidants in food: a review, Trends Food Sci. Technol. 21 (2010) 229–246.

[164] L.L. Okumura, L.O. Regasini, D.C. Fernandes, D.H.S. Da Silva, M.V.B. Zanoni, V. Da Silva Bolzan, Fast screening for antioxidant properties of flavonoids from pterogyne nitens using electrochemical methods, J. AOAC Int. 95 (2012) 773–777.

[165] Y. Peng, J. Yuan, F. Liu, J. Ye, Determination of active components in rosemary by capillary electrophoresis with electrochemical detection, J. Pharm. Biomed. Anal. 39 (2005) 431–437.

[166] T. Wu, Y. Guan, J. Ye, Determination of flavonoids and ascorbic acid in grapefruit peel and juice by capillary electrophoresis with electrochemical detection, Food Chem. 100 (2007) 1573–1579.

[167]   L. Zhang, S. Dong, Z. Yang, Q. Wang, P. He, Y. Fang, Determination of four polyphenolic active ingredients from a pharmaceutical preparation by capillary zone electrophoresis with amperometric detection, J. Pharm. Biomed. Anal. 48 (2008) 198–200.

[168]   S. Dong, L. Chi, P. He, Q. Wang, Y. Fang, Simultaneous determination of antioxidants at a chemically modified electrode with vitamin B12 by capillary zone electrophoresis coupled with amperometric detection, Talanta. 80 (2009) 809–814.

[169]   R. Castañeda, D. Vilela, M.C. González, S. Mendoza, A. Escarpa, SU-8/Pyrex microchip electrophoresis with integrated electrochemical detection for class-selective electrochemical index determination of phenolic compounds in complex samples, Electrophoresis. 34 (2013) 2129–2135.

[170]   L.R.C. Barclay, S.J. Locke, J.M. MacNeil, J. VanKessel, G.W. Burton, K.U. Ingold, Autoxidation of micelles and model membranes. Quantitative kinetic measurements can be made by using either water-soluble or lipid-soluble initiators with water-soluble or lipid-soluble chain-breaking antioxidants, J. Am. Chem. Soc. 106 (1984) 2479–2481.

[171]   P.F. Knowles, J.F. Gibson, F.M. Pick, R.C. Bray, Electron-spin-resonance evidence for enzymic reduction of oxygen to a free radical, the superoxide ion, Biochem. J. 111 (1969) 53–58.

[172]   H.B. Dunford, Oxidations of iron(II)/(III) by hydrogen peroxide: from aquo to enzyme, Coord. Chem. Rev. 233–234 (2002) 311–318.

[173]   J. Chevalet, F. Rouelle, L. Gierst, J.P. Lambert, Electrogeneration and some properties of the superoxide ion in aqueous solutions, J. Electroanal. Chem. Interfacial Electrochem. 39 (1972) 201–216.

[174]   M. Březina, M. Wedell, Oxidation of hydrogen peroxide at the dropping mercury electrode, Collect. Czechoslov. Chem. Commun. 49 (1984) 2320–2331.

[175]   K. Aoki, M. Ishida, K. Tokuda, K. Hasebe, Electrode kinetics of the oxidation of hydrogen peroxide at pretreated glassy carbon and carbon fiber electrodes, J. Electroanal. Chem. Interfacial Electrochem. 251 (1988) 63–71.

[176]   M. Sudoh, T. Kodera, K. Sakai, J.Q. Zhang, K. Koide, Oxidative degradation of aqueous phenol effluent with electrogenerated fenton's reagent, J. Chem. Eng. Japan. 19 (1986) 513–518.

[177]   K. Pratap, A.T. Lemley, Electrochemical peroxide treatment of aqueous herbicide solutions, J. Agric. Food Chem. 42 (1994) 209–215.

[178]   M. Gnann, C.-H. Gregor, S. Schelle, Chemical oxidative process for purifying highly contaminated wastewater., 1993.

[179]   X. Cai, K. Kalcher, G. Kölbl, C. Neuhold, W. Diewald, B. Ogorevc, Electrocatalytic reduction of hydrogen peroxide on a palladium-modified carbon paste electrode, Electroanalysis. 7 (1995) 340–345.

[180]   C. Comninellis, Electrocatalysis in the electrochemical conversion/combustion of organic pollutants for waste water treatment, Electrochim. Acta. 39 (1994) 1857–1862.

[181]   B. Marselli, J. Garcia-Gomez, P.-A. Michaud, M.A. Rodrigo, C. Comninellis, Electrogeneration of Hydroxyl Radicals on Boron-Doped Diamond Electrodes, J. Electrochem. Soc. . 150 (2003) D79–D83.

[182]   R. Oliveira, F. Bento, D. Geraldo, Aromatic hydroxylation reactions by electrogenerated HO radicals: A kinetic study, J. Electroanal. Chem. 682 (2012) 7–13.

[183] A. Kapałka, H. Baltruschat, C. Comninellis, Electrochemical Oxidation of Organic Compounds Induced by Electro-Generated Free Hydroxyl Radicals on BDD Electrodes, in: Synth. Diam. Film., John Wiley & Sons, Inc., 2011: pp. 237–260.

[184] R. Oliveira, N. Pereira, D. Geraldo, F. Bento, Reactivity of hydroxy-containing aromatic compounds towards electrogenerated hydroxyl radicals, Electrochim. Acta. 105 (2013) 371–377.

II. Results and Discussion

1 Reducing Antioxidant Capacity Evaluated by means of a Controlled Potential Electrolysis

Raquel Oliveira, Juliana Marques, Fátima Bento*, Dulce Geraldo, Paula Bettencourt

Department of Chemistry, Universidade do Minho, Campus de Gualtar 4710-057, Portugal

* Corresponding author T: +351 253604399; e-mail: fbento@quimica.uminho.pt

Abstract

An analytical method suitable for an antioxidant sensor is presented following the response of these substances to an extensive oxidation imposed by electrochemical means. The electrochemical assay simulates the action of a reactive oxygen species (ROS) by means of electrolyses carried out at a potential which is settled at the formal potential of the ROS.

The antioxidant activities of trolox and ascorbic, gallic and caffeic acids and of mixtures of these antioxidants were estimated from the charge required for the complete oxidation of the antioxidants from assays where the oxidative attack by O_2 and by $O_2^{\bullet-}$ were simulated.

Keywords

1. Introduction

The characterization of the reactivity of substances usually denominated antioxidants (AOs) has attracted the attention of many researchers. The importance of these substances is closely related to their potential action in the prevention of oxidative stress [1-3]. Many studies are carried out with the aim to establish correlations between the intake of AOs (in food or food supplements) and health maintenance [4-6]. Other works deal with the possibility of detecting early stages of diseases or the propensity for diseases associated with oxidative stress, from measurements of antioxidant capacity in physiological fluids such as blood serum, saliva or urine [7,8]. Besides the importance of AOs in health, their action in preventing the oxidative deterioration of food has also been widely studied, with special focus on white wines, given the costs involved when its early deterioration occurs [9].

Several analytical methods have been proposed to characterize the action of AOs and quantify their activity in preventing or delaying the oxidation of other species [10-15]. Most of the available methods are based on the analysis of the response of AOs to an oxidative attack by reactive species that can be either added or generated during the assay. Results of these assays often lead to the definition of a scale of reactivity inherent to each method, enabling to compare different AOs. As these parameters represent in most cases relative values of reactivity, the information that they contain is not easily transposed in terms of the protection degree provided by AOs against an attack by a specific reactive oxygen species (ROS). In recent years several reviews were published in this scope, where the available methods for the evaluation of antioxidant activity are discussed [11, 12, 14, 16-19]. In these papers it is possible to obtain information about the meaning of the parameters estimated from the different methods, as well as the processes/reactions involved in the assays. Thus, there is a consensual difficulty in establishing a relation among results from different methods even when the reactions involved are identical, due to the use of different reactive species, different experimental conditions, or because different parameters (e.g. time, absorbance) are monitored.

Usually the assays used to evaluate antioxidant activity are divided into two categories based on the chemical reactions involved, namely assays based on hydrogen atom transfer reactions (HAT) and on electron transfer reactions (ET) [13, 17, 19]. HAT assays monitor the kinetics of competitive reactions, while ET assays involve a redox reaction with a synthetic oxidant (SOX). The Oxygen Radical Absorbance Capacity (ORAC) and the Total Radical Trapping Antioxidant Parameter (TRAP) assays are well-known examples of methods based on HAT reactions in which the antioxidant activity is evaluated from the delay in the reaction between the peroxyl radical and an optical probe in the presence of an

AO. Among the most widespread ET based assays are: Trolox Equivalent Antioxidant Capacity (TEAC), the Ferric Reducing Antioxidant Power (FRAP) and the DPPH (2,2-diphenyl-1-picrylhydrazyl) Radical Scavenging Capacity. These assays are based on the spectrophotometric quantification of the extent of redox reactions between AOs and a SOX whose optical characteristics change during the reaction.

In recent years a rising number of methods has been proposed for the evaluation of antioxidant activity based on electrochemical assays, given the relevance of electrochemistry in the context of the production and monitoring of species with redox activity [19-26]. Beyond the simplicity that electrochemical techniques can grant, there are recognized additional advantages related to the ability of performing measurements in media with colour or turbidity. Examples are potentiometric titrations [27, 28] and amperometric titrations using galvanostatic generated species such as the radical cation ABTS, Ce(IV), Cl_2, Br_2 and I_2 [7, 26, 29-35].

In a different approach from the above-mentioned the activity of AOs has been characterized by voltammetric methods. In this context the popularity of cyclic voltammetry is growing and several papers report the voltammetric characterization of a wide range of compounds with recognized antioxidant activity [20, 22, 36-39]. The wide use of this technique is related not only with the relevance of the information provided but also with the simplicity of the assay. Voltammetric techniques such as cyclic voltammetry and differential pulse voltammetry have also been used for the characterization of AOs mixtures [8, 39-41] Besides the identification of peak potentials or of wave potentials, the estimation of antioxidant capacity was performed based on measurements of peak current or of the area under voltammograms at fixed potential ranges. The use of voltammetry in complex media like blood plasma [42] or skin and cosmetics [43] are recent examples that enabled the characterization of the antioxidant properties of these natural matrixes. Voltammetric methods constitute one of the most effective means to control and monitor electron-transfer reactions, although quantitative information is not straight obtained from voltammograms of AOs mixtures. Recently it was demonstrated that cyclic voltammetry is adequate for establishing robust multivariate control charts for monitoring and diagnostic of the oxidation of white wines [44].

Based on voltammetric approaches two different antioxidant sensors were purposed based on the electrogeneration of $HO^{\bullet -}$ [45] or of H_2O_2 [46] and on the monitoring of the elimination of these ROS by AOs.

This paper presents an analytical method suitable for the development of an AO sensor, providing a mode to discriminate antioxidants molecules by means of a selective interaction according to their

reducing capacity based on the extensive oxidation of AOs. The AO detection is accomplished by a coulometric analysis.

2. Experimental

2.1. Chemicals

All reagents employed were of analytical grade. Caffeic acid, 2,2'-azino-bis(3-ethylbenzthiazoline-6-sulphonic acid) diammonium salt (ABTS), potassium persulphate, potassium chloride, were purchased from Fluka. Gallic acid, L- ascorbic acid, 6-hydroxy-2,5,7,8-tetramethylchroman-2-carboxylic acid (trolox), 2,2-diphenyl-1-picrylhydrazyl (DPPH), sulfuric acid were provided by Sigma-Aldrich. Phosphoric acid, potassium dihydrogen phosphate and dipotassium hydrogenphosphate were obtained from ACROS Organics. Other chemicals included hydroquinone (May & Baker Ltd), fructose (Vaz Pereira), sucrose (HiMedia), methanol (Fisher Scientific), potassium ferricyanide (José Gomes Santos) and ethanol (Panreac).

The concentration of buffer solution was 0.1 M. Buffer solution of pH 7.0, was prepared mixing adequate amounts of dipotassium hydrogen phosphate and of potassium dihydrogen phosphate, whereas buffer solution of pH 3.5, was prepared using potassium dihydrogen phosphate and phosphoric acid.

2.2. Electrochemical measurements

Voltammetric measurements and controlled potential electrolysis were performed using a potentiostat (Autolab type PGSTAT30, Ecochemie) controlled by GPES 4.9 software provided by Ecochemie.

2.2.1. Cyclic voltammetry

Cyclic voltammetric experiments were carried out from 0 to 1.4 V at a scan rate of 100 mV/s in an undivided three-electrode cell. The working electrode was a 3 mm glassy carbon disk electrode (CHI104, CH Instruments, Inc.), an Ag/AgCl/3 M KCl (CHI111, CH Instruments, Inc.), was used as reference electrode and a platinum wire as counter electrode. The electrode surface of the working electrode was cleaned between scans by polishing with polycrystalline diamond suspension (3F μm) for 1 min.

2.2.2. RACE (Reducing Antioxidant Capacity Evaluated by Electrolysis) assays

Potentiostatic electrolyses were carried out at 0.81 V and 0.99 V in a divided three-electrode cell where the two compartments are separated by a glass frit membrane. The volume of the anodic compartment was 9.0 ml and the solution was mechanically stirred with a magnetic stir bar. The oxygen concentration of the sample solutions did not affect results as similar coulometric data were obtained from deaerated and non-deaerated solutions. The reference electrode was an Ag/AgCl/3 M KCl (CHI111, CH Instruments, Inc.) electrode. The working and counter electrodes were made of a piece (20 mm x 10 mm) of platinum gauze (52 mesh woven from 0.1 mm diameter wire, 99.9%, from Alfa Aesar). Pt was selected as electrode material for electrolysis as in the course of bulk electrolysis no significant passivation was noticed, in opposition to glassy carbon that suffered from severe inactivation. The area of the working electrode, 5.6 cm^2, was determined using a 1.00 mM of $K_3Fe(CN)_6$ in 0.1 M KCl, in a cronoamperometry experiment. The diffusion coefficient was 7.63×10^{-6} $cm^2 s^{-1}$ [47]. Before each experiment the anode was electrochemically cleaned at 2 V in a 1 M H_2SO_4 solution during 300 s to 1200 s.

2.3. Antioxidant capacity assays based on SOX

The antioxidant capacity assays of samples were carried out following procedures described by Rivero-Pérez [48]. Absorbance measurements were transformed in antioxidant activity using a calibration curve obtained with trolox.

2.3.1. TEAC assay

In this assay, radical cation $ABTS^{\bullet+}$ generated by reaction of a 7 mM ABTS with 2.45 mM $K_2O_8S_2$ (1:1). The mixture was held in darkness at room temperature for 20 h, to obtain stable absorbance values at 734 nm. The $ABTS^{\bullet+}$ working solution was obtained by the dilution of the stock solution with 0.01 M phosphate buffer (pH 7.4) to give an absorbance value of circa 0.70 at 734 nm. In this assay 100 μL of each samples was mixed with 4900 μL of $ABTS^{\bullet+}$ and absorbance was measured after 15 min of reaction time. Solutions of 0.50 mM of single AOs and mixture of AOs were directly measured, except for gallic acid containing solutions which were half-diluted before the mixture.

2.3.2. DPPH assay

The assay consist in mixing 4900 μL of a freshly prepared 60 μM DPPH$^\bullet$ in methanol with 100 μL of sample solutions. The absorbance was measured at 517 nm after 2 h of reaction.

3. Results and discussion

3.1. Description of the method RACE (Reducing Antioxidant Capacity Evaluated by Electrolysis)

This paper proposes an analytical method to evaluate the antioxidant capacity of small molecules given their reducing power. The reducing power of an antioxidant (AO) is assessed by an electron transfer (ET) reaction at an anode and does not rely on synthetic oxidants (SOX) as the available ET methods. The oxidation of AOs occurs in large scale during a controlled potential electrolysis and its consumption is directly monitored at the anode by the current decrease. The potential of the anode determines the selectivity of the method in the same way that the reducing power of a SOX determines the selectivity of a conventional ET assay. Thus, applying higher potentials, larger number of AOs will be quantified, including AOs of smaller reducing power, like when a high oxidant power SOX is used, e.g. ABTS ($E^{0\prime}$= 0.90 V vs Ag/AgCl/3 M KCl). On the other hand, applying lower potentials only the AOs with higher reducing power will be detected, as when a less reactive SOX, like DPPH ($E^{0\prime}$= 0.227 V vs Ag/AgCl/3 M KCl) is employed. The selection of the anode potential is one of the key variables, which determines the method performance, namely the analytical selectivity and the trueness. For potential selection the analytical context must be taken in account, considering both the nature of the relevant ROS and the pH of the sample. Figure 1 shows the formal electrode potentials of major ROS as a function of pH, for their reduction to water.

In the most widespread ET methods, like TEAC and DPPH, the extent of the reaction depends on multiple variables such as the SOX concentration, the assay time and the difference $E^{o\prime}_{AO}$-$E^{o\prime}_{SOX}$, making it difficult to control this variable. In opposition, in the RACE method the oxidative attack extension can be easily controlled by the experimental variables that determine the conversion degree of an electrolysis. These variables are the anode area (A), the sample volume (V), the mass transport efficiency and the electrolysis time [49]. The possibility to control the extent of oxidation by means of the electrolysis duration is an important advantage of the RACE method, allowing the characterization of the antioxidant reducing capacity at different degrees of conversion without eliminating it from the

sample. Thus, a moderate oxidative attack can be simulated by short electrolyses in order to achieve a low degree of conversion of the AO into its oxidized forms. In contrast, a large oxidation degree of the AO can be forced through long electrolysis enabling to estimate the antioxidant activity in the presence of high concentrations of the AO oxidation products. Experiments carried out in these two extreme situations may be important to detect pro-oxidant or synergistic effects.
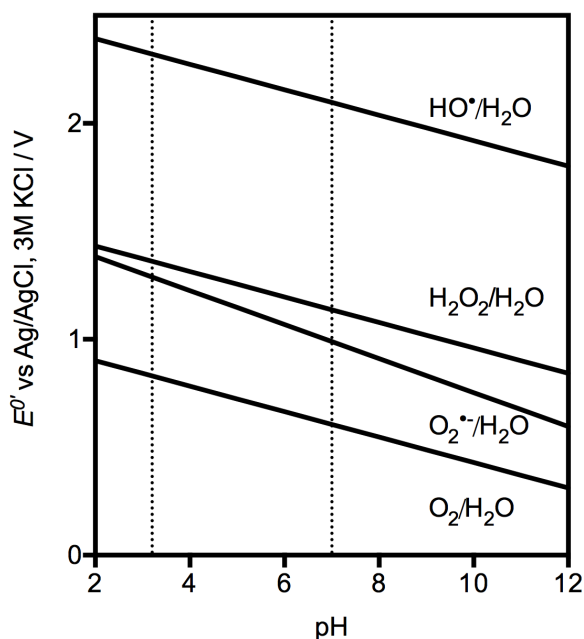
Figure 1 – Formal electrode potentials of some significant reactive oxygen species (ROS) as a function of pH. The dashed vertical lines indicate pH 3.5 and 7.0 which are typical values for drinks and physiological media, respectively.

When the oxidation is conducted in an extensive way, the steady consumption of AO can be monitored through the decrease of current that is a measure of the rate of charge transfer between the AO and the anode. The current decrease along time can be described by a first order kinetics and the charge Q_∞ can be estimated from the integral of the exponential function given by a curve fit of experimental data to t_∞. This parameter corresponds to the charge needed for the complete oxidation of the active AOs. In terms of the antioxidant activity this quantity measures the charge that the AOs are capable of transfer to eliminate the ROS simulated. Q_∞ is an absolute measure whose determination does not require any prior calibration and has a precise and unequivocal meaning. Q_∞ can be easily converted into the amount of ROS that the AOs present in the sample can eliminate.

3.2. Characterization of electrolysis cell

Hydroquinone (HQ) ($E^{0\,'}$ = 0.263 V (vs Ag/AgCl/3 M KCl), pH 3.5) was used to characterize the electrochemical cell and optimize its operating conditions as it is one of the simplest polyphenols whose oxidation involves the hydroxyl groups conversion into the quinone form, which is a typical reaction of antioxidants from different classes. Constant potential electrolyses of 0.50 mM HQ solutions were carried out, at pH 3.5 and 7.0 during 1500 s, at potentials between 0.50 and 1.0 V. The charge obtained in blank assays, from electrolyses conducted in buffer solutions during 500 s at E = 0.81 and 0.99 V, are less than 1.6% of the charge from electrolyses of 0.50 mM HQ solutions. The current decrease during electrolyses of HQ follows an exponential decay, $I = I_0 \exp(-pt)$. In Figure 2, data from an electrolysis of HQ at pH 3.5 is displayed with the curve obtained by an exponential fitting, which has a correlation coefficient of 0.997. The average value of p calculated from three replicates is p = (2.12± 0.01) x 10^{-3} s^{-1}. This value was identical for the two solutions pH and for the two electrolyses potentials. However, it was found that the p value was sensitive to the anode pre-treatment, namely the duration of the electrochemical cleaning at constant current. For electrochemical cleaning times lower than 500 s, smaller p values were obtained, circa 30% of those obtained following electrochemical cleanings conducted for 1000 s. For longer electrochemical cleaning there was no significant variations of p values. A similar effect was observed for current. The variation of p and I with the electrochemical cleaning time can be due to the variation of the anode active area that increases with the efficiency of cleaning. Despite the variation of I and p, Q_∞ values estimated from the ratio I_0 / p (where I_0 is the current extrapolated to t = 0 s) showed variations less than 14 %. This experimental observation is consistent with the expected independence of the coulometric data from the working electrode area [49].

Taking into account the average value of p, 2.12 x 10^{-3} s^{-1}, the time required to convert 50% of HQ to its oxidized form is easily estimated, $t_{1/2}$ = 327 s. Thus, to perform analysis simulating an extensive oxidative attack, electrolysis times larger than $t_{1/2}$ should be considered. On the other hand, if it is intended to characterize the AO behaviour in the absence of its reaction products, the electrolysis should be carried out for times where low conversion degrees are attained. However, it should be noticed that for a good definition of the exponential fitting, the conversion degree must enable to define a curvature.
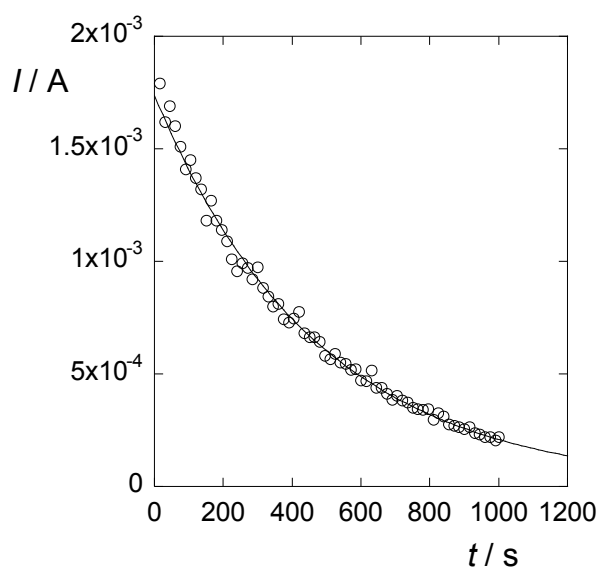
Figure 2 – I - t curve for the electrolysis of hydroquinone (HQ) carried out at $E = 0.81$ V, [HQ] = 0.50 mM in a 0.1 M buffer solution containing potassium dihydrogen phosphate and phosphoric acid (pH 3.5), anode area = 5.6 cm^2 and $V = 9.0$ ml. The line corresponds to the exponential curve fit: $I = 1.74 \times 10^{-3} \exp(-2.12 \times 10^{-3} \, t)$ and $r = 0.997$.

3.3. Application of RACE to the characterization of antioxidants

The antioxidant activity estimation by the RACE method was performed with recognized AOs of different classes, e.g., a sugar acid (ascorbic acid, AA), a tocopherol derivative (trolox, T), a hydroxycinnamic acid (caffeic acid, CA) and a hydroxybenzoic acid (gallic acid, GA) in dilute AO solutions (0.50 mM) at pH 3.5 and pH 7.0. The potentials used for electrolyses were selected so that the antioxidant activities of these AOs could be estimated according to two relevant situations, namely in the prevention of oxidative degradation of beverages (pH 3.5) by eliminating O_2 and in the prevention of oxidative stress by the elimination of $O_2^{\bullet-}$ from physiological media. Considering data presented in Figure 1, the potentials 0.81 V and 0.99 V were selected. The I - t curves presented in Figure 3 were acquired from solutions of the different AOs when the applied potential (0.81 V) simulated the oxidative attack of O_2. The antioxidant activities estimated from electrolyses carried out for 500s, whose current-time curves are illustrated in Figure 3, are expressed as Q_∞ (Figure 4). Q_∞ values were obtained directly from the I vs. t curves. As charge is an absolute quantity, its meaning is unequivocal in the context of the appraisal of the reducing power of a sample. Besides, this value can be easily converted to the equivalent amount of a specific ROS.
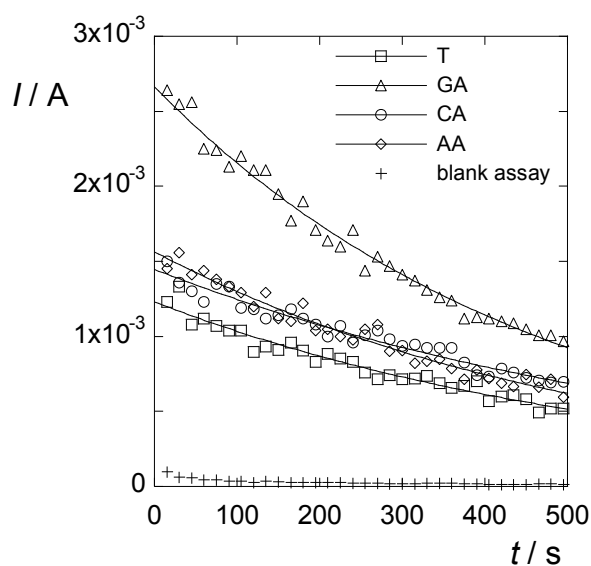
Figure 3 – I - t curves acquired from 0.50 mM solutions of the different AOs in a 0.1 M buffer solution containing potassium dihydrogen phosphate and phosphoric acid (pH 3.5), when the applied potential (E = 0.81 V) simulated the oxidative attack of O_2. Curves displayed are fitted to experimental data by exponential type functions. T: I = 1.23 x 10^{-3} exp(-1.74 x 10^{-3} t), r = 0.98; GA: I = 2.66 x 10^{-3} exp(-2.11 x 10^{-3} t), r = 0.992; CA: I = 1.45 x 10^{-3} exp(-1.49 x 10^{-3} t), r = 0.98 and AA: I = 1.56 x 10^{-3} exp(-1.85 x 10^{-3} t), r = 0.98.
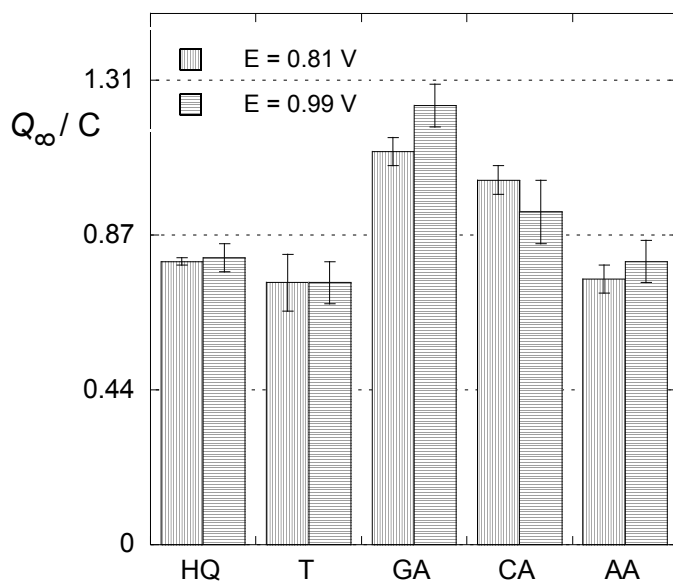
Figure 4 - Antioxidant activities of the 0.50 mM solution of single AOs estimated by RACE method, expressed in units of charge (Q_∞), from assays simulating the oxidative attack by O_2 (E = 0.81 V, in a 0.1 M buffer solution containing potassium dihydrogen phosphate and phosphoric acid, pH 3.5) and by $O_2^{\bullet-}$ (E = 0.99 V, in a 0.1 M buffer solution containing dipotassium hydrogen phosphate and of potassium dihydrogen phosphate, pH 7.0). The assigned values of 0.44 C, 0.87 C and 1.31 C correspond to the charge involved in the exhaustive oxidation of an AO given by Faraday's law for 1, 2 or 3 electrons for the experimental conditions of the assay: [AO] = 0.50 mM and V = 9.0 ml.

From Figure 4 it can be concluded that the estimated antioxidant activity of each AO is similar regarding the two electrolyses potentials, meaning that they are equally able to reduce O_2 and $O_2^{\bullet-}$. The charge obtained for the oxidation of HQ, T, CA and AA is close to the calculated value assuming the involvement of two electrons (0.87 C). On the other hand, the charge obtained for GA is closer to the calculated value for three electrons (1.31 C). The estimated antioxidant activities, presented in Table 1, are expressed in equivalent concentration of the ROS whose attack was simulated by electrolysis. Results expressed in equivalents of ROS indicate the maximum concentration of ROS that the AO in the sample is able to eliminate by reduction.

3.4. Application of RACE to the characterization of antioxidants mixtures

Figure 5 presents antioxidant capacity data from mixtures containing two, three or four AOs obtained by the RACE method regarding the simulation of the oxidative attack by O_2 at pH 3.5 (Figure 5A) and by $O_2^{\bullet-}$ at pH 7.0 (Figure 5B). Mixtures are composed by equimolar concentrations of each AO and the total concentration of AOs was kept constant in all mixtures (0.50 mM). The striped bars correspond to the experimental values of Q_∞ whereas the grey bars represent the predicted values of charge, Q_{pred}, calculated from Q_∞ values of single AOs presented in Table 1 and attending to the AO concentration in the mixture. The estimated antioxidant activity data expressed in units of charge and in equivalent concentration of the simulated ROS are presented in Table 2. Data presented in Figure 4, show that Q_∞ do not differ significantly from Q_{pred} attending to the uncertainties of these variables. Moreover, it can be concluded that the antioxidant activities estimated by electrolyses conducted at the two selected potentials are similar for all mixtures.

Table 1. Characterization of AOs by cyclic voltammetry and by RACE, DPPH and TEAC methods. E_n^a is the anodic peak potential. Q_∞ is the charge estimated for the complete oxidation of AOs. $[O_2]$ and $[O_2^{\bullet-}]$ are the concentrations of the simulated ROS that the AO can eliminate, calculated from Q_∞. Antioxidant activities by DPPH and TEAC assays are expressed as the trolox equivalent concentration. [AO] = 0.50 mM and V = 9.0 ml. Uncertainties were estimated based on standard deviation from 2 to 3 measurements.

	E = 0.81 V, pH 3.5			E = 0.99 V, pH 7.0			DPPH (mM T)	TEAC (mM T)
	Q_∞ (C)	$[O_2]$ (mM)	E_p^a (V)	Q_∞ (C)	$[O_2^{\bullet-}]$ (mM)	E_p^a (V)		
T	0.74±0.08	0.21±0.02	0.327±0.005	0.74±0.06	0.28±0.02	0.213±0.003	0.49±0.02	0.452±0.006
GA	1.11±0.04	0.319±0.008	0.517±0.004	1.24±0.06	0.475±0.02	0.442±0.005	0.99±0.01	1.8±0.2
CA	1.03±0.04	0.295±0.007	0.461±0.001	0.94±0.09	0.36±0.04	0.317±0.002	0.66±0.02	0.726±0.003
AA	0.75±0.04	0.216±0.008	0.421±0.005	0.80±0.06	0.31±0.02	0.384±0.006	0.489±0.006	0.340±0.001

3.5. Comparison with other ET methods

Results obtained by RACE assays from solutions of single AO and of mixtures of AOs were compared with those given by other assays based on ET reactions. The methods used are well described in the literature [48] and employ the ABTS radical cation (TEAC assay) and the DPPH radical as SOX. The antioxidant activities estimated by these methods are presented in Table 1 as trolox equivalent concentration and were obtained by interpolating the absorbance variation in calibration curves for trolox, according to the description of the experimental part. The voltammetric characterization of the antioxidant activities is based on the analysis of recorded voltammograms from 0 to 1.4 V as illustrated in Figure 6.

As presented in Table 1, the antioxidant activities estimated by RACE are in agreement with results from assays based on $ABTS^{\bullet+}$ and on $DPPH^{\bullet}$, displaying higher activity values for GA, followed by CA. In opposition, the relative antioxidant activity of AA and T depends on the method. AA has higher activity then T by RACE, using $DPPH^{\bullet}$ the activity of these two AOs is similar, whereas T is identified as being more active than AA using $ABTS^{\bullet+}$. In terms of the voltammetric analysis, the peak potentials of all AOs are lower than the formal potentials of O_2 and of $O_2^{\bullet-}$ as it can be inferred by means of the voltammograms in Figure 6A and data from Table 1. As all AOs are able to reduce either O_2 or $O_2^{\bullet-}$ they should be efficient on the elimination of these ROS. The absolute values of activity estimated on the basis of both SOX are not comparable, though expressed in the same base. When $ABTS^{\bullet+}$ is used the antioxidant activities estimated for GA and CA are higher than those estimated with $DPPH^{\bullet}$. The opposite is found for AA and T, where the estimated antioxidant activities are higher for the $DPPH^{\bullet}$ assay.

As results from RACE assays are expressed as a function of the concentration of simulated ROS, the absolute values of the antioxidant activities cannot be compared with those obtained by the other assays. Nevertheless, the relative magnitude of these values can be compared using a common reference. Therefore, the activities ratio GA/T estimated by the different assays are: 1.5 for the RACE simulation of the oxidative attack by O_2 (pH 3.5), 2.3 for the RACE simulation of the oxidative attack by $O_2^{\bullet-}$ (pH 7.0), 2.0 for the $DPPH^{\bullet}$ assay and 4.1 for the TEAC assay.

Antioxidant activity data estimated for the mixtures of AOs presented in Table 2 were acquired from RACE, DPPH and TEAC assays, as well as by voltammetric analysis through the integrated area of the anodic scan of voltammograms from mixtures of AOs. Figure 6B presents a voltammogram recorded from the mixture containing 0.125 mM of the four AOs (AA, GA, CA and T) which illustrates a typical response obtained from mixtures of these AOs. In Table 2, the higher values of antioxidant activities are

highlighted. The mixtures identified with higher antioxidant activity by RACE assays simulating the O_2 oxidative attack do not match those identified by means of voltammetric analysis, with exception of AA + GA + CA mixture, which is identified as having increased activity by both methods. The RACE assays assigned higher antioxidant activities to three of the four mixtures containing GA. The antioxidant activities estimated by the RACE simulation of $O_2^{\bullet-}$ oxidative attack were higher for mixtures containing GA. A similar result was obtained from voltammetric analysis and from DPPH and TEAC assays.
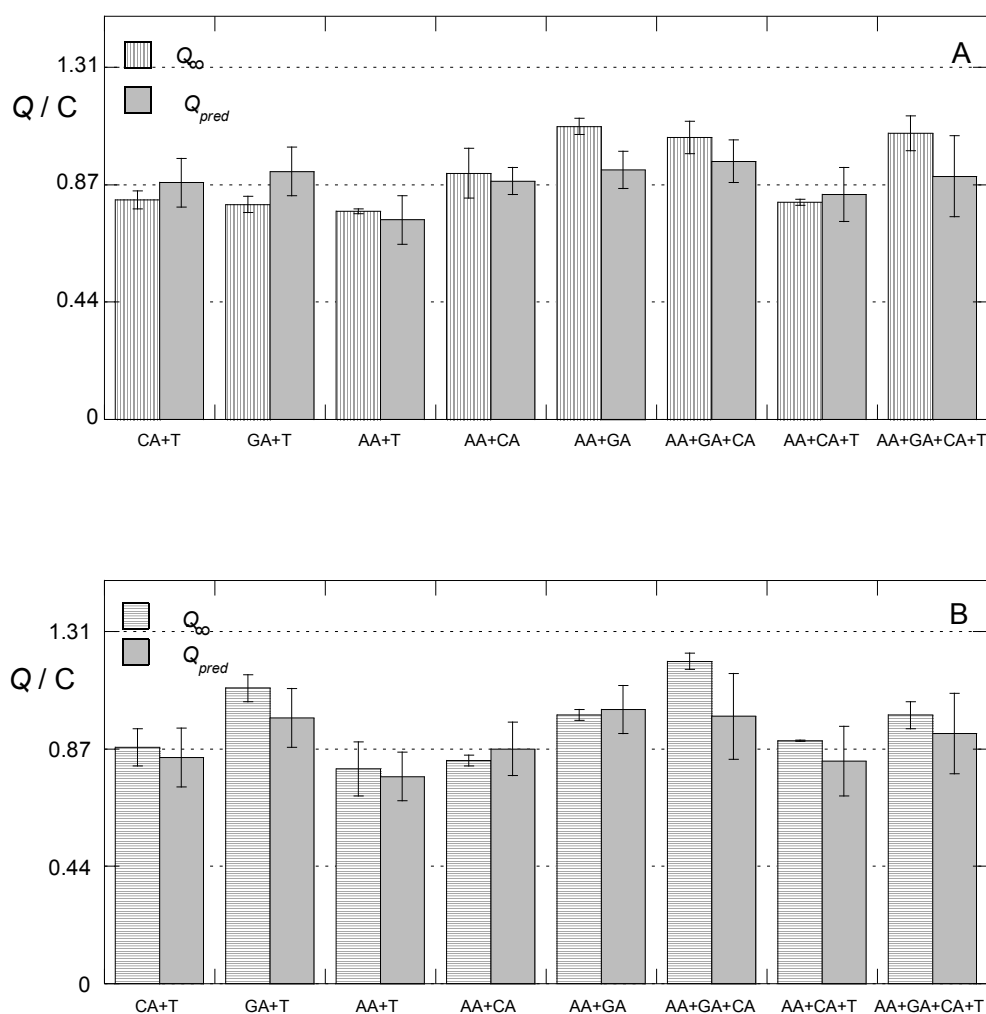
Figure 5 – Antioxidant activities of mixtures of AOs estimated by RACE method expressed in units of charge (Q_∞). All mixtures were composed by equimolar concentrations of each AO to fulfill a total concentration of 0.50 mM and $V = 9.0$ ml. Q_{pred} corresponds to the predicted charge considering the contribution of each AO presented in Table 1, evaluated by RACE method and attending to the AO concentration in each mixture. Results were obtained for the simulation of the oxidative attack by: (A) O_2 ($E = 0.81$ V, in a 0.1 M buffer solution containing potassium dihydrogen phosphate and phosphoric acid, pH 3.5) and (B) $O_2^{\bullet-}$ ($E = 0.99$ V, in a 0.1 M buffer solution containing dipotassium hydrogen phosphate and of potassium dihydrogen phosphate, pH 7.0).

Table 2. Characterization of AOs by cyclic voltammetry and by RACE, DPPH and TEAC methods. $A_{(0\text{-}0.81V)}$ and $A_{(0\text{-}0.99V)}$ are the areas under the voltammograms integrated in the anodic scan between 0 to 0.81 V or between 0 to 0.99 V, respectively. Q_∞ is the charge estimated for the complete oxidation of AOs in mixtures. $[O_2]$ and $[O_2^{\bullet-}]$ are the concentrations of the simulated ROS that the AOs in the mixture can eliminate, calculated from Q_∞. Antioxidant activities by DPPH and TEAC assays are expressed as the trolox equivalent concentration. The total concentration of AOs in each mixtures is 0.50 mM and V = 9.0 ml. Uncertainties were estimated based on standard deviation from 2 to 3 measurements.

	E = 0.81 V, pH 3.5			E = 0.99 V, pH 7.0			DPPH (mM T)	TEAC (mM T)
	Q_∞ (C)	$[O_2]$ (mM)	$A_{(0\text{-}0.81V)}$ (µC)	Q_∞ (C)	$[O_2^{\bullet-}]$ (mM)	$A_{(0\text{-}0.99V)}$ (µC)		
0.25 mM CA + 0.25 mM T	0.82 ±0.03	0.235 ±0.007	42.6 ±0.5	0.88 ±0.07	0.34 ±0.03	43.9 ±0.1	0.572 ±0.008	0.77 ±0.04
0.25 mMGA + 0.25 mM T	0.80 ±0.03	0.230 ±0.006	39.65 ±0.03	1.14 ±0.05	0.42 ±0.02	64.8 ±0.2	0.9 ±0.1	1.33 ±0.02
0.25 mM AA +0.25 mM T	0.78 ±0.01	0.223 ±0.002	33.2 ±0.5	0.8 ±0.1	0.31 ±0.04	27.2 ±0.2	0.486 ±0.001	0.641 ±0.004
0.25 mM AA + 0.25 mM CA	0.92 ±0.09	0.26 ±0.02	39.2 ±0.2	0.83 ±0.02	0.319 ±0.006	28.9 ±0.9	0.59 ±0.02	0.78 ±0.09
0.25 mM AA + 0.25 mM GA	1.09 ±0.03	0.314 ±0.006	38 ±1	1.00 ±0.02	0.384 ±0.007	52.2 ±0.2	0.84 ±0.04	1.39 ±0.03
0.167 mM AA + 0.167 mM GA + 0.167 mM CA	1.05 ±0.06	0.30 ±0.01	44.4 ±0.3	1.22 ±0.01	0.46 ±0.01	61.7 ±0.3	0.849 ±0.004	1.08 ±0.01
0.167 mM AA + 0.167 mM CA + 0.167 mM T	0.81 ±0.01	0.232 ±0.002	38.0 ±0.4	0.904 ±0.002	0.347 ±0.001	33.5 ±0.2	0.563 ±0.009	0.61 ±0.01
0.125 mM AA + 0.125 mM GA + 0.125 mM CA+ 0.125 mM T	1.07 ±0.06	0.307 ±0.004	37.9 ±0.4	1.00 ±0.05	0.39 ±0.02	43.8 ±0.4	0.741 ±0.002	0.86 ±0.01
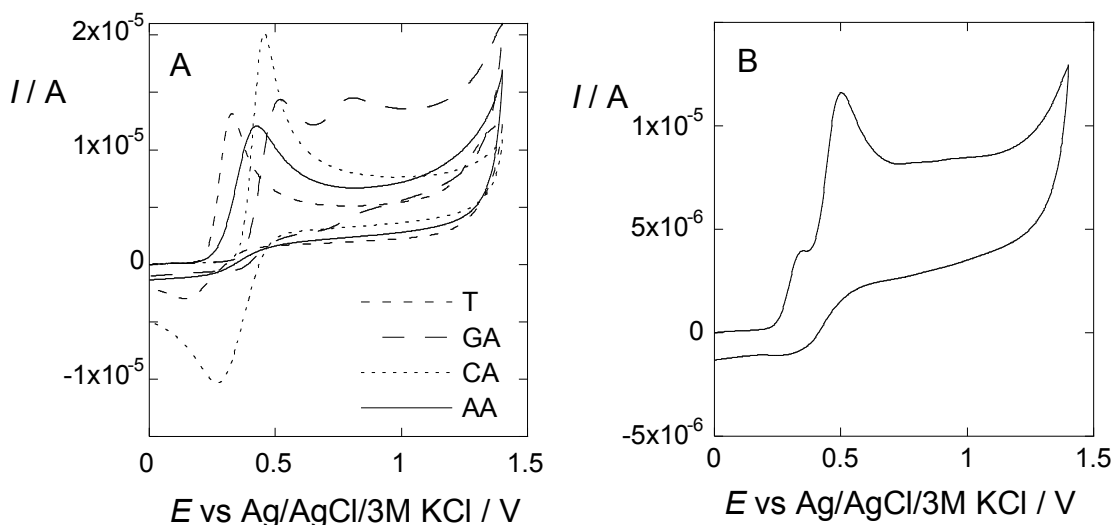
Figure 6 – Cyclic voltammograms recorded at a 3 mm glassy carbon electrode, v = 100 mV/s, 0.1 M buffer solutions (potassium dihydrogen phosphate and phosphoric acid) from: (A) 0.50 mM solutions of single AO and (B) a mixture containing 0.125 mM of each AO (AA, GA, CA and T).

3.6. Limit of quantification, linearity and sensitivity

The quantification limit estimated for the RACE method, based on standard deviation of the charge from electrolyses carried out in 10 blank assays, is 7 μM for both potentials. The linearity was tested using a set of solutions containing an equimolar mixture of AOs (AA + GA + CA + T) at pH 3.5 and E = 0.81 V, varying the total concentration of AO between 10 μM and 2.0 mM. The straight line was characterized by: Q_∞ (C) = 1.1 x 10^{-3} + 1.78 [AO] (mM), r = 0.99995 and n = 8. This correlation suggests that the method responds linearly to the concentration variation in this concentration range, being sensitive to small changes in concentration in the order of 0.18 C by 0.1 mM of AO. This value corresponds to an average value of sensitivity for the set of AOs used in this study and may vary with the nature of the AO, namely with the number of electrons involved in the reduction.

3.7. Selectivity tests

The method selectivity was tested for ethanol, fructose and sucrose as these substances are hydroxyl containing molecules that can be present in the natural matrixes where AOs occur. It is also known that these sugars may interfere with methods for quantification of polyphenols, namely the Folin-Ciocalteu method. Q_∞ obtained for 0.50 mM and 5.0 mM solutions of these species in electrolyses carried out at

0.81 V and 0.99 V, according to the solutions pH, were similar to those of blank assays, with deviations not exceeding 6%.

4. Conclusions

In this work, it is proposed an electrochemical-based method for the characterization of AOs by means of assays that simulate the oxidative attack of specific ROS. The method was characterized by means of the following performance parameters: linearity (10 μM – 2.0 mM, $r = 0.99995$), sensitivity (0.18 C / 0.1 mM), quantification limit (7 μM) and selectivity (against ethanol, fructose and sucrose). Antioxidant activities estimated for mixtures of AOs were identical to the calculated values assuming the additivity of the Q_∞ values from single AOs.

The absolute values of antioxidant activity from single AOs and AOs mixtures estimated by TEAC and by DPPH assays are different, despite expressed using a common reference AO. The antioxidant activities estimated by RACE cannot be comparable to those from the other two methods once results are expressed in different scales. While the antioxidant activity estimated by RACE assays account for the amount of charge that the AO can transfer regarding a meaningful oxidative attack, data from DPPH or TEAC assays are relative values that depend strongly on the reactivity of each used SOX.

Acknowledgments

References

[1]   M. Valko, C.J. Rhodes, J. Moncol, M. Izakovic, M. Mazur, Free radicals, metals and antioxidants in oxidative stress-induced cancer, Chemico-Biological Interactions. 160 (2006) 1–40.

[2]   R. Kohen, A. Nyska, Invited Review: Oxidation of Biological Systems: Oxidative Stress Phenomena, Antioxidants, Redox Reactions, and Methods for Their Quantification, Toxicologic Pathology. 30 (2002) 620–650.

[3]   K. Hensley, K.A. Robinson, S.P. Gabbita, S. Salsman, R.A. Floyd, Reactive oxygen species, cell signaling, and cell injury, Free Radical Biology and Medicine. 28 (2000) 1456–1462.

[4]   H.E. Seifried, D.E. Anderson, E.I. Fisher, J.A. Milner, A review of the interaction among dietary antioxidants and reactive oxygen species, The Journal of Nutritional Biochemistry. 18 (2007) 567–579.

[5]   M. Singh, M. Arseneault, T. Sanderson, V. Murthy, C. Ramassamy, Challenges for Research on Polyphenols from Foods in Alzheimer's Disease: Bioavailability, Metabolism, and Cellular and Molecular Mechanisms, Journal of Agricultural and Food Chemistry. 56 (2008) 4855–4873.

[6]   M. Steele, G. Stuchbury, G. Münch, The molecular basis of the prevention of Alzheimer's disease through healthy nutrition, Experimental Gerontology. 42 (2007) 28–36.

[7]   G.K. Ziyatdinova, H.C. Budnikov, V.I. Pogorel'tzev, Electrochemical determination of the total antioxidant capacity of human plasma, Analytical and Bioanalytical Chemistry. 381 (2005) 1546–1551.

[8]   S. Martinez, L. Valek, J. Rešetić, D.F. Ružić, Cyclic voltammetry study of plasma antioxidant capacity – Comparison with the DPPH and TAS spectrophotometric methods, Journal of Electroanalytical Chemistry. 588 (2006) 68–73.

[9]   R.S. Jackson, Wine science: principles, practice, perception., Second Edi, Academic Press, San Diego, 2000.

[10]   A. Ghiselli, M. Serafini, F. Natella, C. Scaccini, Total antioxidant capacity as a tool to assess redox status: critical view and experimental data, Free Radical Biology and Medicine. 29 (2000) 1106–1114.

[11]   M. Antolovich, P.D. Prenzler, E. Patsalides, S. McDonald, K. Robards, Methods for testing antioxidant activity, Analyst. 127 (2002) 183–198.

[12]   R.L. Prior, X.L. Wu, K. Schaich, Standardized methods for the determination of antioxidant capacity and phenolics in foods and dietary supplements, Journal of Agricultural and Food Chemistry. 53 (2005) 4290–4302.

[13]   D. Huang, B. Ou, R.L. Prior, The Chemistry behind Antioxidant Capacity Assays, Journal of Agricultural and Food Chemistry. 53 (2005) 1841–1856.

[14]   L.M. Magalhães, M.A. Segundo, S. Reis, J.L.F.C. Lima, Methodological aspects about in vitro evaluation of antioxidant properties, Analytica Chimica Acta. 613 (2008) 1–19.

[15]   R.L. Prior, G. Cao, In vivo total antioxidant capacity: comparison of different analytical methods1, Free Radical Biology and Medicine. 27 (1999) 1173–1181.

[16]   B. Halliwell, M. Whiteman, Measuring reactive species and oxidative damage in vivo and in cell culture: how should you do it and what do the results mean?, British Journal of Pharmacology. 142 (2004) 231–255.

[17]   A. Karadag, B. Ozcelik, S. Saner, Review of Methods to Determine Antioxidant Capacities, Food Analytical Methods. 2 (2009) 41–60.

[18]   L.M. Magalhães, M. Santos, M.A. Segundo, S. Reis, J.L.F.C. Lima, Flow injection based methods for fast screening of antioxidant capacity, Talanta. 77 (2009) 1559–1566.

[19]   A.J. Blasco, A. González Crevillén, M.C. González, A. Escarpa, Direct Electrochemical Sensing and Detection of Natural Antioxidants and Antioxidant Capacity in Vitro Systems, Electroanalysis. 19 (2007) 2275–2286.

[20]   P.A. Kilmartin, H. Zou, A.L. Waterhouse, A Cyclic Voltammetry Method Suitable for Characterizing Antioxidant Properties of Wine and Wine Phenolics, Journal of Agricultural and Food Chemistry. 49 (2001) 1957–1965.

[21]   N. Ragubeer, D.R. Beukes, J.L. Limson, Critical assessment of voltammetry for rapid screening of antioxidants in marine algae, Food Chemistry. 121 (2010) 227–232.

[22]   S. Chevion, M.A. Roberts, M. Chevion, The use of cyclic voltammetry for the evaluation of antioxidant capacity, Free Radical Biology and Medicine. 28 (2000) 860–870.

[23]   M.N. Peyrat-Maillard, S. Bonnely, C. Berset, Determination of the antioxidant activity of phenolic compounds by coulometric detection, Talanta. 51 (2000) 709–716.

[24]   M. Hilgemann, F. Scholz, H. Kahlert, L.M. de Carvalho, M.B. da Rosa, U. Lindequist, et al., Electrochemical Assay to Quantify the Hydroxyl Radical Scavenging Activity of Medicinal Plant Extracts, Electroanalysis. 22 (2010) 406–412.

[25]   K.Z. Brainina, L. V Alyoshina, E.L. Gerasimova, Y.E. Kazakov, A. V Ivanova, Y.B. Beykin, et al., New Electrochemical Method of Determining Blood and Blood Fractions Antioxidant Activity, Electroanalysis. 21 (2009) 618–624.

[26]   Á.M. Alonso, C. Domínguez, D.A. Guillén, C.G. Barroso, Determination of Antioxidant Power of Red and White Wines by a New Electrochemical Method and Its Correlation with Polyphenolic Content, Journal of Agricultural and Food Chemistry. 50 (2002) 3112–3115.

[27]   C.M. Oliveira, A.C. Silva Ferreira, P. Guedes de Pinho, T.A. Hogg, Development of a Potentiometric Method To Measure the Resistance to Oxidation of White Wines and the Antioxidant Power of Their Constituents, Journal of Agricultural and Food Chemistry. 50 (2002) 2121–2124.

[28]   A.C. Silva Ferreira, C. Oliveira, T. Hogg, P. Guedes de Pinho, Relationship between Potentiometric Measurements, Sensorial Analysis, and Some Substances Responsible for Aroma Degradation of White Wines, Journal of Agricultural and Food Chemistry. 51 (2003) 4668–4672.

[29]   Á.M. Alonso, D.A. Guillén, C.G. Barroso, B. Puertas, A. García, Determination of Antioxidant Activity of Wine Byproducts and Its Correlation with Polyphenolic Content, Journal of Agricultural and Food Chemistry. 50 (2002) 5832–5836.

[30]   R. de Queiroz Ferreira, L.A. Avaca, Electrochemical Determination of the Antioxidant Capacity: The Ceric Reducing/Antioxidant Capacity (CRAC) Assay, Electroanalysis. 20 (2008) 1323–1329.

[31]   S. Martinez, L. Valek, J. Piljac, M. Metikoš-Huković, Determination of wine antioxidant capacity by derivative potentiometric titration with electrogenerated chlorine, European Food Research and Technology. 220 (2005) 658–661.

[32]   J. Piljac, S. Martinez, L. Valek, A Comparison of Methods Used to Define the Phenolic Content and Antioxidant Activity of Croatian Wines, 43 (2005) 271–276.

[33]   I.F. Abdullin, E.N. Turova, G.K. Ziyatdinova, G.K. Budnikov, Determination of Fat-Soluble Antioxidants by Galvanostatic Coulometry Using Electrogenerated Oxidants, Journal of Analytical Chemistry. 57 (2002) 730–732.

[34]   I.F. Abdullin, E.N. Turova, G.K. Budnikov, Coulometric Determination of the Antioxidant Capacity of Tea Extracts Using Electrogenerated Bromine, Journal of Analytical Chemistry. 56 (2001) 557–559.

[35]   G.K. Ziyatdinova, H.C. Budnikov, V.I. Pogorel'tzev, T.S. Ganeev, The application of coulometry for total antioxidant capacity determination of human blood, Talanta. 68 (2006) 800–805.

[36]   P.A. Kilmartin, Electrochemical Detection of Natural Antioxidants: Principles and Protocols, Antioxidants & Redox Signaling. 3 (2001) 941–955.

[37]   P.A. Kilmartin, H. Zou, A.L. Waterhouse, Correlation of Wine Phenolic Composition versus Cyclic Voltammetry Response, Am. J. Enol. Vitic. 53 (2002) 294–302.

[38]   D. De Beer, J.F. Harbertson, P.A. Kilmartin, V. Roginsky, T. Barsukova, D.O. Adams, et al., Phenolics: A Comparison of Diverse Analytical Methods, Am. J. Enol. Vitic. 55 (2004) 389–400.

[39]   H. Tiehua, G. Ping, H. Michael, Rapid Screening of Antioxidants in Pharmaceutical Formulation Development Using Cyclic Voltammetry - Potential And Limitations, Current Drug Discovery Technologies. 1 (2004) 173–179.

[40]   A. Rodrigues, A.C. Silva Ferreira, P. de Pinho, F. Bento, D. Geraldo, Resistance to Oxidation of White Wines Assessed by Voltammetric Means, Journal of Agricultural and Food Chemistry. 55 (2007) 10557–10562.

[41]   P.A. Kilmartin, C.F. Hsu, Characterisation of polyphenols in green, oolong, and black teas, and in coffee, using cyclic voltammetry, Food Chemistry. 82 (2003) 501–512.

[42]   M. Pohanka, H. Bandouchova, J. Sobotka, J. Sedlackova, I. Soukupova, J. Pikula, Ferric Reducing Antioxidant Power and Square Wave Voltammetry for Assay of Low Molecular Weight Antioxidants in Blood Plasma: Performance and Comparison of Methods, Sensors. 9 (2009) 9094–9103.

[43]   C. Guitton, A. Ruffien-Ciszak, P. Gros, M. Comtat, Chapter 8 Voltammetric sensors for the determination of antioxidant properties in dermatology and cosmetics, in: S. Alegret, A. Merkoçi (Eds.), Electrochemical Sensor Analysis, Elsevier, 2007: pp. 163–180.

[44]   R.C. Martins, R. Oliveira, F. Bento, D. Geraldo, V. V Lopes, P. Guedes de Pinho, et al., Oxidation Management of White Wines Using Cyclic Voltammetry and Multivariate Process Monitoring, Journal of Agricultural and Food Chemistry. 56 (2008) 12092–12098.

[45]   J. Liu, G. Lagger, P. Tacchini, H.H. Girault, Generation of OH radicals at palladium oxide nanoparticle modified electrodes, and scavenging by fluorescent probes and antioxidants, Journal of Electroanalytical Chemistry. 619–620 (2008) 131–136.

[46]   Q. Guo, S. Ji, Q. Yue, L. Wang, J. Liu, J. Jia, Antioxidant Sensors Based on Iron Diethylenetriaminepentaacetic Acid, Hematin, and Hemoglobin Modified TiO2 Nanoparticle Printed Electrodes, Analytical Chemistry. 81 (2009) 5381–5389.

[47]   J.E. Baur, 19 - Diffusion Coefficients, in: C.G.Z.B.T.-H. of Electrochemistry (Ed.), Elsevier, Amsterdam, 2007: pp. 829–848.

[48]   M.D. Rivero-Pérez, P. Muñiz, M.L. González-Sanjosé, Antioxidant Profile of Red Wines Evaluated by Total Antioxidant Capacity, Scavenger Activity, and Biomarkers of Oxidative Stress Methodologies, Journal of Agricultural and Food Chemistry. 55 (2007) 5476–5483.

[49]   A.J. Bard, L.R. Faulkner, Electrochemical Methods: Fundamentals and Applications, 2nd ed., Wiley, New York, 2001.

2 Direct Electroanalytical Method for Alternative Assessment of Global Antioxidant Capacity Using Microchannel Electrodes

Raquel Oliveira[a], Fátima Bento[a]*, Catherine Sella,[b] Laurent Thouin[b]* and Christian Amatore[b]

[a] Centro de Química, Universidade do Minho, Campus de Gualtar 4710-057 Braga, Portugal

[b] Ecole Normale Supérieure, Département de Chimie, UMR CNRS-ENS-UPMC 8640 PASTEUR, 24 rue Lhomond, 75231 Paris Cedex 05, France

* Corresponding authors T: +351 253604399; e-mail: fbento@quimica.uminho.pt

T: +33 144323404; e-mail: laurent.thouin@ens.fr

Abstract

A new electroanalytical method for the characterization of global antioxidant capacities is proposed based on chronoamperometric responses monitored at microchannel band electrodes. This approach does not require any titrating species, biological elements or pre-calibration curves. A thin-layer regime is established at the working electrode according to the geometry of the device and hydrodynamic flow rate. Under these conditions, the currents are directly proportional to the total concentration of antioxidants and do not depend on their respective diffusion coefficients. Measurements were performed with synthetic solutions and mixtures of four antioxidants used as sample tests: trolox, ascorbic acid, gallic acid and caffeic acid. Operating potentials were selected at the formal potentials of some reactive oxygen species to simulate their oxidative attacks. The very good agreement obtained between simulations and experimental data validated this new electroanalytical procedure. These results pave the way for the concept of innovative sensor-type microfluidic devices for an alternative determination of antioxidant capacity.

Keywords

1. Introduction

The use of microfluidic devices for analytical purposes has been widely investigated during the past few years. Advantages like low cost, portability, low volumes, short-time analysis but also the ability to perform separations and detections with high resolution and high sensitivity have been commonly demonstrated [1]. Important efforts are now carried out for developing microfluidic devices for health, [2,3] food [4] and environmental analysis [5]. In this context, microfluidic devices are currently under development for the assessment of food safety and quality. The detection of food contaminants and residues at low concentrations, such as (bio)toxins [6,7], chemical residues and pathogens [8,9] are described either in synthetic or natural samples. Regarding food quality, the evaluation of organoleptic properties [10–12] resulting from the presence of additives or compounds associated to food degradation, as well as proteins [13,14] and antioxidants (AOs) [15–17] have been also reported. AOs are currently added to foodstuff not only to prevent deterioration but also to increase their nutritive value due to their recognized action on oxidative stress prevention. The determination of AOs is also carried out in health industry, in pharmaceuticals screening [18] and in human biological fluids for diagnostic of oxidative stress [19,20]. Most of the AOs analysis are performed through the evaluation of their concentration after separation by capillary electrophoresis [21] or by chromatography [22]. The detection is usually achieved by optical methods, such as chemiluminescence [19,23,24] and fluorescence [25], by mass spectroscopy [26] or by electrochemical methods [15–17,27–29]. Instead of quantifying antioxidant concentrations, activity and capacity of AOs are also evaluated through their reactivity versus prooxidants or oxidant probes. These parameters are related to reactions involving electron transfer (ET) or hydrogen atom transfer (HAT) [30]. In ET-based assays, the antioxidant action is usually simulated via the reduction of an oxidizing agent. In HAT-based assays, it is evaluated through its ability to quench generated oxygen radicals by H-atom donation. Depending on the nature of the antioxidant and reactive species, one or both of these reactions can take place.

To our best of knowledge, there are only three examples in literature of microfluidic devices designed to evaluate AO capacity. They are all based on HAT reactions. In two of them, the capacity was estimated through the amount of reactive oxygen species (ROS), H_2O_2 or radical $O_2^{\bullet-}$, reacting with AOs. H_2O_2 was detected either by chemiluminescence [31] or by the combination of fluorescence and amperometry using horseradish peroxidase immobilized on gold electrode [32]. A third application was reported where H_2O_2 and $O_2^{\bullet-}$ were produced by an hypoxanthine/xanthine oxidase assay [33]. In this last example, the AO capacity was determined using two amperometric systems operating at different

potentials with cytochrome C modified electrodes. For ET-based assays, no attempts have been reported to adapt a procedure with microfluidic devices. The antioxidant capacity is mainly estimated under classical conditions by means of the color change of a redox probe simulating the action of ROS [30]. Voltammetry has also been successfully used to characterize single antioxidants, antioxidant mixtures or natural samples such as fruits [27], beverages [34], pharmaceutical formulations [35] and biological fluids [36] but using standard-sized electrochemical cells.

Due to the great interest of methods based on direct evaluation of ET reactions, a novel electrochemical procedure will be proposed to analyse AOs based on their direct amperometric responses at microchannel electrodes. According to the hydrodynamic flow rate and geometry of the devices, optimal conditions will be set to establish a method available for assessing the total AO capacity of complex samples without any calibration steps. This approach will be based on specific hydrodynamic regimes observed at microchannel electrodes in which quantitative electrolysis of AOs is achieved during the detection process [37,38]. On the one hand, selected potentials will simulate the redox potential of some ROS. On the other hand, the AOs oxidation will allow the evaluation of the global charge that they are expected to transfer against some ROS [29]. This charge is an absolute measure whose determination does not require any prior calibration. Although it is not directly related to the radical scavenging capability, it is recognized to be a very important parameter for characterization of antioxidants [30]. In order to demonstrate the validity of this innovative procedure, chronoamperometric experiments will be carried out using synthetic solutions and mixtures of four AOs belonging to two classes of compounds: phenolic compounds (gallic acid and caffeic acid) and non-phenolic compounds (ascorbic acid and trolox). Experimental measurements of AO capacities will be systematically compared to simulated data according to key parameters.

2. Experimental

2.1 Chemicals

All reagents employed were of analytical grade. The AOs were caffeic acid (CA, Fluka), gallic acid (GA, Acros Organics), ascorbic acid (AA, Sigma Aldrich) and 6-hydroxy-2,5,7,8-tetramethylchroman-2-carboxylic acid (trolox T, Acros Organics). Phosphoric acid, potassium dihydrogen phosphate and ferrocene methanol were purchased from Acros Organics. 0.5 mM of AO solutions were prepared in 0.1 M buffer containing potassium dihydrogen phosphate and phosphoric acid at pH 3.2.

The number of electron exchanged during the oxidation of each AO and their diffusion coefficient used for calculations were respectively: $n = 2$ and $D = 2.3 \times 10^{-5}$ cm^2 s^{-1} for CA [39], $n = 3$ and $D = 2.3 \times 10^{-5}$ cm^2 s^{-1} for GA [40], $n = 2$ and $D = 2.4 \times 10^{-5}$ cm^2 s^{-1} for AA [41], and $n = 2$ and $D = 5 \times 10^{-6}$ cm^2 s^{-1} for T [42,43]. The diffusion coefficient of ferrocene methanol was estimated to $D = 7.6 \times 10^{-6}$ cm^2 s^{-1}.

2.2 Microfluidic devices

A schematic view of microfluidic devices used in this study is presented in Figure 1A. The microfluidic device is based on two parts that are assembled together. The device fabrication has been already described in some previous works [37,44,45]. One part is a polydimethylsiloxane (PDMS) block, comprising a linear channel and reservoir elements, which were engraved on its surface and connected to the inlet and outlet tubes across the PDMS matrix. The second part comprises a glass substrate on which microband electrodes (Ti/Pt with 8 nm / 25 nm thickness) were patterned by optical lithography and liftoff techniques. The dimensions of the working electrodes (WE, width $w = 197$ μm and length $l = 500$ μm) and of the microchannel (height $h = 20$ μm and width $l = 500$ μm) were checked optically before use. The counter electrode (CE) consisted of a larger microband electrode (width $w = 600$ μm) located downstream the working electrodes. The reference electrode (Ref) was fabricated by sputtering a 50 nm Ag layer onto an underlying Pt surface and oxidizing it by 5 mM FeCl$_3$ (Sigma). This electrode was located at the entrance of the microchannel. In our experimental conditions, it was cheeked that this reference electrode delivered a constant difference of 0.17 V versus an Ag / AgCl (3.0 M) reference electrode, whatever the nature of the flowing solution.

During the experiments, only one microchannel was filled with solution, the others remaining empty. The liquid flow in the microchannel was pressure driven using a syringe pump (Harvard Apparatus, type 11 Pico Plus) employing an advanced microstepping techniques to eliminate flow pulsation and

control low hydrodynamic flows. The average flow velocities were monitored in situ following a procedure previously described [44] using a two-working-electrodes configuration.
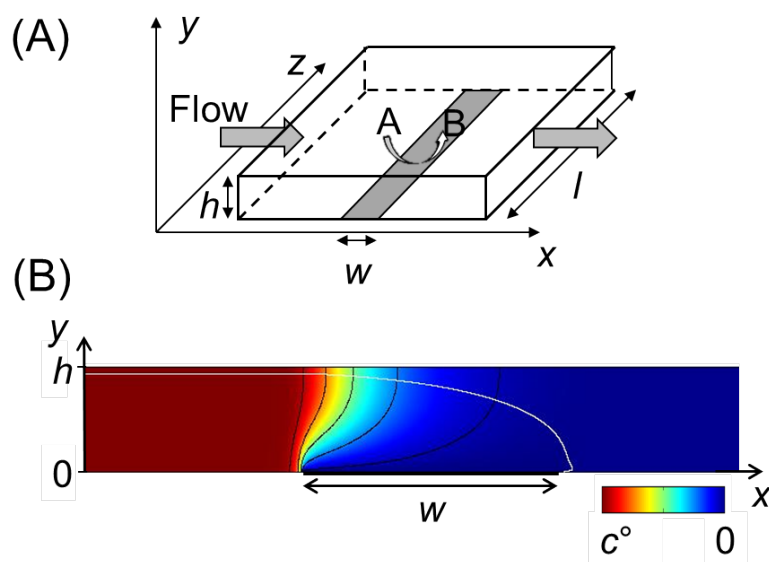
Figure 1: (A) 3D scheme of a microband electrode integrated in a microfluidic channel with geometrical parameters (w, h, l). (B) 2D steady-state concentration profile across the microchannel at $F = 0.1$ µL min^{-1} in the vicinity of a microband electrode ($w = 200$ µm, $l = 500$ µm). In this representation the y scale was expanded four times. The electrode operates amperometrically on the plateau of the detected species having a concentration $c°$ and a diffusion coefficient $D = 6\ 10^{-6}$ cm^2 s^{-1}. The white curve linking the microchannel entrance to the downstream edge of the electrode describes the diffusion-convection layer probed by the electrode. All points located below this line hit the electrode while those located above are carried away by the flow without reaching the electrode. The black curves represent 5 isoconcentration lines corresponding to 0.05, 0.25, 0.5, 0.75 and 0.95$c°$.

2.3 Electrochemical measurements

 All electrochemical experiments (cyclic voltammetry and chronoamperometry) were performed at room temperature using a potentiostat (Autolab type PGSTAT30, Ecochemie) equipped with the Bipot module and controlled by the GPES 4.9 software. Pt working electrodes were electrochemically activated before each measurement by applying 12 times a potential step from 0 V (1 s) to -0.5 V/Ref (1 s) in the solution of interest.

2.4 Numerical simulations

 Numerical simulations were performed as described in some previous works [37,38,46]. Under laminar flow conditions the flow velocity profile is assumed to be parabolic across the microchannel.

Since the length of the microband electrodes *l* is much larger than their width *w*, the formulation of problem reduces to a two dimensional problem. The mass transport equation is then solved numerically in a 2D space as shown in Figure 1B. Time-dependent concentration profiles are established above microchannel electrodes before evaluating their chronoamperometric responses. All computations were carried out using COMSOL Multiphysics 4.2 software.

3. Results and discussion

As most of AOs are electroactive, their electrochemical properties give informations about their chemical reactivity. In this context, voltammetry is the method of choice since it can provide insights about the thermodynamic of electron transfer and amount of AOs that can be oxidized under specific potentials. Antioxidant activity in samples is then related to oxidation potentials whereas antioxidant capacity is linked to current magnitude or charge measured at a given potential. Therefore, an electroanalytical procedure for assessing antioxidant activity - capacity requires suitable potentials to monitor the oxidation of AOs. Furthermore, its implementation in a microfluidic device necessitates optimal flow rates to make it available for analysing complex compositions of samples.

3.1 Operating potentials

In Figure 2 are reported voltammograms monitored at a microchannel electrode for each of the four AOs considered: ascorbic acid (AA), caffeic acid (CA), trolox (T) and gallic acid (GA). In order to distinguish faradic currents from residual and capacitive currents, each response was systematically compared with a voltammogram recorded in buffer solution. It can be observed that the oxidation processes take place at potentials ranging from 0.2 to 1 V/Ref depending on the nature of the AO. T and CA are oxidized at potentials below 0.7 V/Ref in contrast to GA and AA. As expected under these experimental conditions, current plateaus can be monitored due to the limitation of mass transport by a mixed convective-diffusive regime (*see* below) [37]. In each case, this regime is achieved at potentials lower than 1.1 V/Ref before the oxidation of the medium. The selection of the potential is one of the key parameter which determines the method performance, namely the analytical selectivity. To perform the evaluation of antioxidant capacity, the operating potentials were then chosen to simulate to simulate the action of ROS, respectively the oxidation power of O_2, $O_2^{\bullet-}$ and H_2O_2 into H_2O. According to the reference electrode and values of potentials reported in the literature, they correspond successively

to 0.66, 1.12 and 1.19 V/Ref at pH = 3.2. For the ease of comparison, these values were reported in Figure 2 by some vertical dashed lines. It can be deduced from this figure that oxidation of the four AOs are not fully achieved at 0.66 V/Ref since currents do not reach their limiting values. At 1.12 and 1.19 V/Ref, the convective-diffusive regime is established with a slight oxidation of the medium. It can be underlined that at such potentials, additional species from complex mixtures or natural samples other than AOs will be also oxidized. These potentials are probably the highest values that can be selected for the application of this procedure.
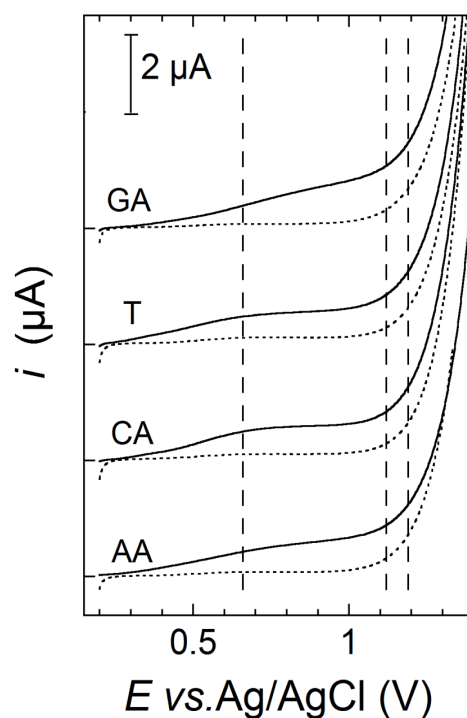
Figure 2: Linear voltammograms recorded at a Pt band electrode (w = 197 μm) in a microfluidic channel (h = 20 μm, l = 500 μm) filled with 0.5 mM AO solutions (solid lines) and 0.1 M buffer solution (dotted lines). v = 0.2 V s^{-1} and F = 2.1 μL min^{-1}. The vertical dashed lines correspond to the applied potentials E = 0.66, 1.12 and 1.19 V/Ref.

3.2 Optimal convective-diffusion regime

The prerequisite for an optimal evaluation of antioxidant capacity is then to perform a complete electrolysis of the solution passing over the working electrode at each potential. This is the easiest way to implement in microfluidics a procedure according to the local hydrodynamic regimes. This condition is comparable to the one required for the anodic abatement of pollutants in microfluidic reactors [47].

Nevertheless, the objective in this context is quite different. If conditions leading to full electrolysis are needed for the implementation of high efficiency abatement, they are envisaged in this case for analytical purposes only. Indeed, we demonstrated previously that under these conditions a thin-layer regime [37] was achieved with current responses independent on the diffusion coefficient of the analysed species. Actually, this is the property on which this novel procedure will be based for the analysis of samples of unknown compositions. At steady state, the mass transport at microchannel electrodes depends on the confining effect and hydrodynamic conditions according to two dimensionless parameters:

$$W = \frac{w}{h}$$
(1)

and:

$$Pe = \frac{u_{av}h}{D}$$
(2)

where w is the electrode width, h the microchannel height, Pe the Peclet number, u_{av} the average linear flow velocity over the section of the microchannel and D the diffusion coefficient of the electroactive species. As a limiting behavior, the thin-layer regime is reached within 5 % error when the following conditions are met [37]:

W/Pe > 1.2   and   W > 4.2
(3)

It corresponds to the situation where the convective-diffusion layer becomes restricted by the channel height as depicted in Figure 1B. The steady-state current i_s tends thus to a limiting current $i_{thin\ layer}$ given by [48]:

$$i_{thin\ layer} = nFc°u_{av}hL$$
(4)

where n is the electron number involved in the electrochemical reaction, F the Faraday's constant and $c°$ the concentration of the electroactive species. In this regime, i_s becomes independent of the diffusion coefficient of the species. As a consequence, the antioxidant capacity Q_{AO} which is equal in this case to:

$$Q_{AO} = nc°$$
(5)

can be evaluated directly from i_s and the flow velocity. Since the average linear flow velocity u_{av} is related to the volumic flow rate Φ by:

$$\Phi = u_{av}hL$$
(6)

the antioxidant capacity Q_{AO} is given by:

$$Q_{AO} = \frac{i_s}{Fu_{av}hL} \quad\quad (7)$$

or:

$$Q_{AO} = \frac{i_s}{F\Phi} \quad\quad (8)$$

According to W and Pe, u_{av} or Φ have to be low enough to fulfil the requirements of a thin-layer regime (Eq.(3)). Besides, values of Q_{AO} can be easily converted to the equivalent amount of ROS. Note here that Q_{AO} is expressed in unit of concentration.

To investigate the influence of flow rate prior to the evaluation of antioxidant capacity, chronoamperometric experiments were then performed at 1.12 V/Ref for different concentrations of trolox and various flow rates (Figure 3). They were compared to corresponding theoretical values issued from numerical simulations. Taking into account the geometric dimensions of the microchannel electrode ($w = 197$ μm, $l = 500$ μm and $h = 20$ μm) and diffusion coefficient of trolox ($D = 5 \times 10^{-6}$ cm^2 s^{-1}), the optimal flow velocities estimated for a thin-layer regime (Eq.(3)) were found under these conditions lower than 0.12 μL min^{-1}. Note that this range of flow velocities applies also for the other AOs considered in this study since these latter have higher diffusion coefficients than trolox. Experimental chronoamperometric responses reported in Figure 3A show that steady-state currents i_s can be measured after a few seconds. However, residual currents are still observed for responses monitored in buffer solution due to the slight oxidation of the medium at such a potential and possible formation of platinum oxides [49] (*see* Figure 2). Values of i_s were thus corrected from the residual currents before being compared to simulated ones. A good fit was observed between data whatever the range of concentration and flow rate investigated (Figures 3B and 3C). Knowing the concentrations c^o of trolox, values of Q_{AO}/c^0 estimated from Eq.(8) were very close to the predicted ones (*i.e.*, $Q_{AO}/c^0 = n = 2$) but only at a flow rate of 0.1 μL min^{-1}. One must point out that lower values of flow rate were not investigated experimentally since they could not be controlled precisely with the experimental setup used in this work. Within the accuracy of the measurements, these results were fully consistent with the optimal flow rates evaluated above.

3.3 Control of thin layer regime

As the flow rate is a critical parameter to ensure a thin layer regime, its magnitude was measured in situ using two microchannel electrodes WE$_1$ and WE$_2$ operating in generator-generator mode (Figure 4A). Ferrocene methanol was introduced in the flowing solution as the redox mediator. The two

working electrodes were biased independently and simultaneously at a constant potential of 0.3 V/Ref corresponding to the oxidation plateau of ferrocene methanol. In this configuration, the current response of WE_2 was fully determined by the performance of WE_1 located upstream. Indeed, the time delay required for the perturbation generated by WE_1 to cross the distance separating the two electrodes is related to the in-situ flow rate [44]. As an example, the corresponding chronoamperometric responses monitored at a flow rate of 0.1 μL min^{-1} were reported in Figure 4B. They were also compared to the simulated responses accounting for all the experimental parameters including the diffusion coefficient of ferrocene methanol ($D = 7.6 \times 10^{-6}$ cm^2 s^{-1}) [37]. The rather good agreement observed between experimental and theoretical responses of WE_2 validated definitely the experimental control of the flow rate. Moreover, the steady-state residual current monitored at WE_2 demonstrated the complete abatement of ferrocene methanol in relation to the thin-layer regime expected at such a flow rate.

3.4 Evaluation of antioxidant capacity from individual AO solutions

A flow rate of 0.1 μLmin^{-1} was finally selected to evaluate antioxidant capacity from synthetic samples since this value fulfilled the criteria of thin-layer regime for all AOs considered. It could be also imposed with the adequate precision. Measurements were performed in solutions of individual AO (GA, CA, AA and T). The three potentials mentioned above, 0.66, 1.12 and 1.19 V/Ref, were applied to monitor the current responses at a single microchannel electrode. Figure 5 shows the chronoamperometric responses measured experimentally in buffer solution alone and in a solution of 0.5 mM CA. Since the current response in buffer was found to be dependent on the applied potential, this result confirmed again the need to correct the response from the capacitive and residual contribution of the currents. Following such a procedure, the time delay to reach steady-state currents was reduced to a few seconds (approximately 2s) as expected under these hydrodynamic regimes for process controlled by diffusion-convection [38]. The corrected currents agreed extremely closely with those simulated whatever the potential considered. However, the quality of the fits along the responses was better for currents close to the steady-state values. Indeed, the subtraction of currents is an approximate procedure since Faradaic and capacitive contributions are physicochemical processes that are intimately convoluted [38]. Furthermore, data at short time scale were not fully reproducible.
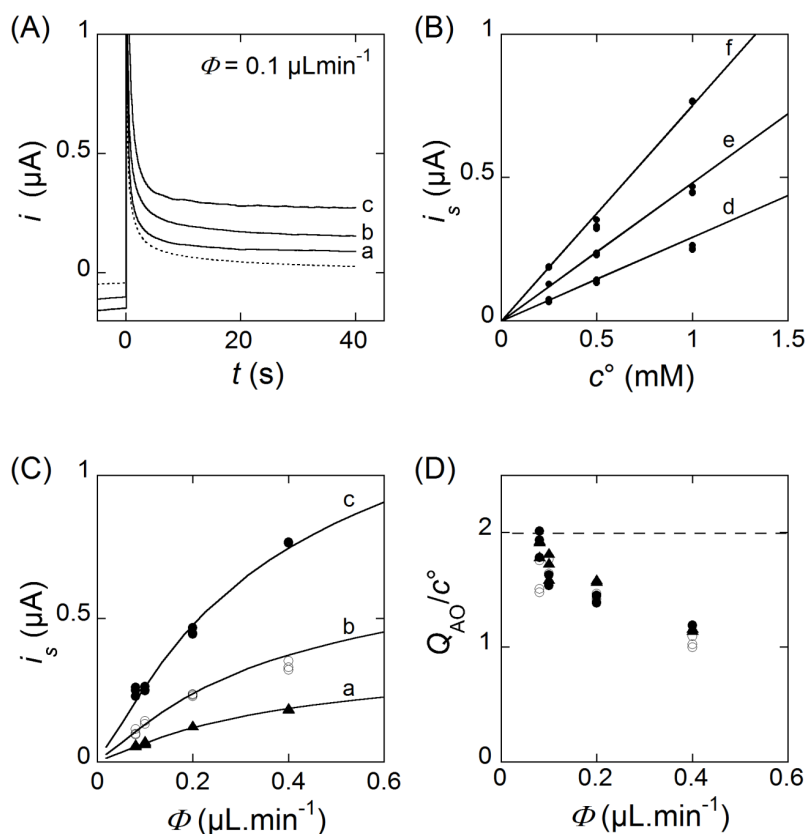
Figure 3: (A) Experimental chronoamperometric responses (solid lines) obtained in trolox solutions at different concentrations: 0.25 (a), 0.5 (b) and 1mM (c). The dotted line represents the response recorded in 0.1 M buffer solution. (B) Influence of trolox concentration on the steady-state current i_s for three volumic flow rates $\Phi = 0.1$ (d), 0.2 (e) and 0.4 µL min^{-1} (f). (C) Influence of the volumic flow rate Φ on the steady-state current i_s for three concentrations of trolox as in (A). (D) Experimental values of Q_{AO}/c^0 estimated from data in (C) as a function of volumic flow rate Φ. The dashed line corresponds to the predicted value of Q_{AO}/c^0 with $Q_{AO}/c^0 = n = 2$. In (A-C), $E = 1.12$ V/Ref. In (B-C), the experimental currents (symbols) are subtracted from background currents and compared to predicted ones obtained by numerical simulations (solid lines).

Similar experiments were also performed with 0.5 mM GA, AA and T solutions (data not shown). The experimental values of the ratio Q_{AO}/c^0 were reported in Figure 6 and compared with the predicted ones. They were in good accordance for each AO. The experimental values were lower than the predicted ones, by nearly 17 % at 0.66 V/Ref and by 10 % at higher potentials 1.12 and 1.19 V/Ref. These discrepancies are probably due to the fact that the current plateau of each AO is not fully reached at 0.66 V/Ref (Figure 2). Under these circumstances, the electrochemical reactions are partially limited by the kinetics of electron transfer. Therefore, Eqs. (7)-(8) do not any longer apply even when a thin layer regime is locally achieved at the electrode with lower concentration gradients. One must underline that n can still be estimated in this situation by taking into account the kinetics, *i.e.*, the difference between applied potential and half wave potential of each AO. Nevertheless, these

evaluations were not carried out here. Since they depend on the nature of the AOs and ultimately on the composition of samples, they were beyond the scope of the present investigation.
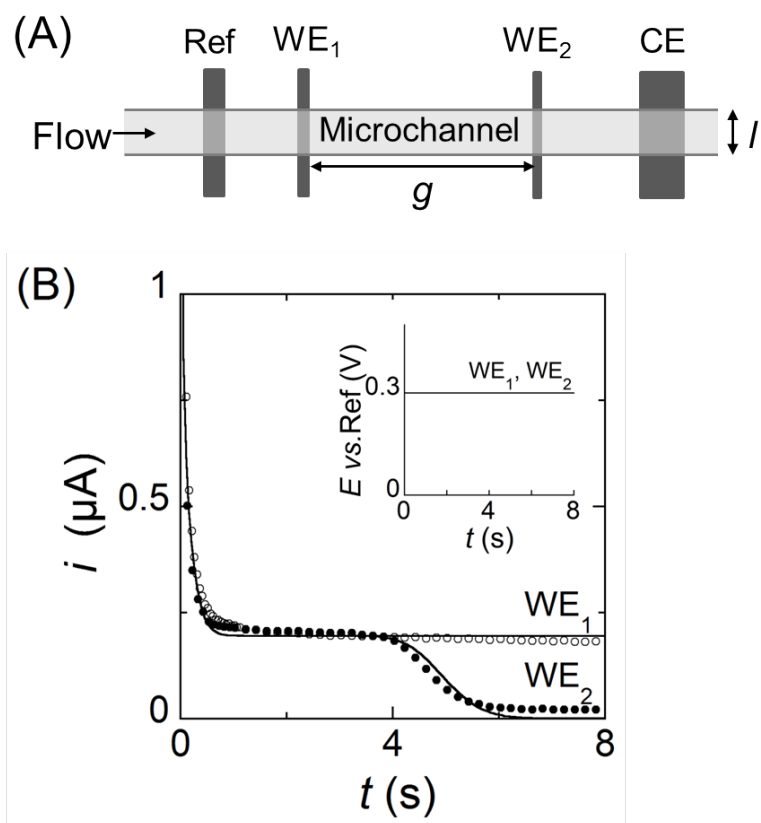
Figure 4: (A) Top view of the microfluidic device showing the relative positions of the two working electrodes WE_1 and WE_2. (B) Chronoamperometric responses recorded at WE_1 and WE_2 operating in generator-generator mode. Comparison between experimental (symbols) and theoretical currents (solid lines) in 1.2 mM ferrocene methanol / 0.1M supporting electrolyte. Electrode widths $w_1 = w_2 = 197$ µm, gap distance $g = 800$ µm, channel height $h = 20$ µm and channel width $l = 500$ µm. $F = 0.1$µL min^{-1}, $E = 0.3$ V/Ref and $D = 7.6 \times 10^{-6}$ cm^2 s^{-1}.

3.5 Evaluation of global antioxidant capacity from AO mixtures

In order to validate this new electrochemical procedure, measurements of antioxidant capacity were also performed following the same procedure with mixtures of two, three or four different AOs. The solutions were prepared with equimolar concentrations of each AO to achieve a total concentration of 0.5 mM. Figure 7 shows the values of global antioxidant capacity evaluated from steady-state currents in each mixture. They were compared to the values of Q_{AO} defined in case of AO mixtures by:

$$Q_{AO} = \sum n_i c_i \qquad (9)$$

where n_i and c_i are respectively the number of electron and concentration of individual AO in the mixture. As in Figure 6, a rather good agreement is observed between data even if experimental values obtained at 0.66 V/Ref were systematically lower than at 1.12 and 1.19 V/Ref. As already mentioned, this result is consistent with the oxidation of individual AO that mostly occurs above 0.66 V/Ref.

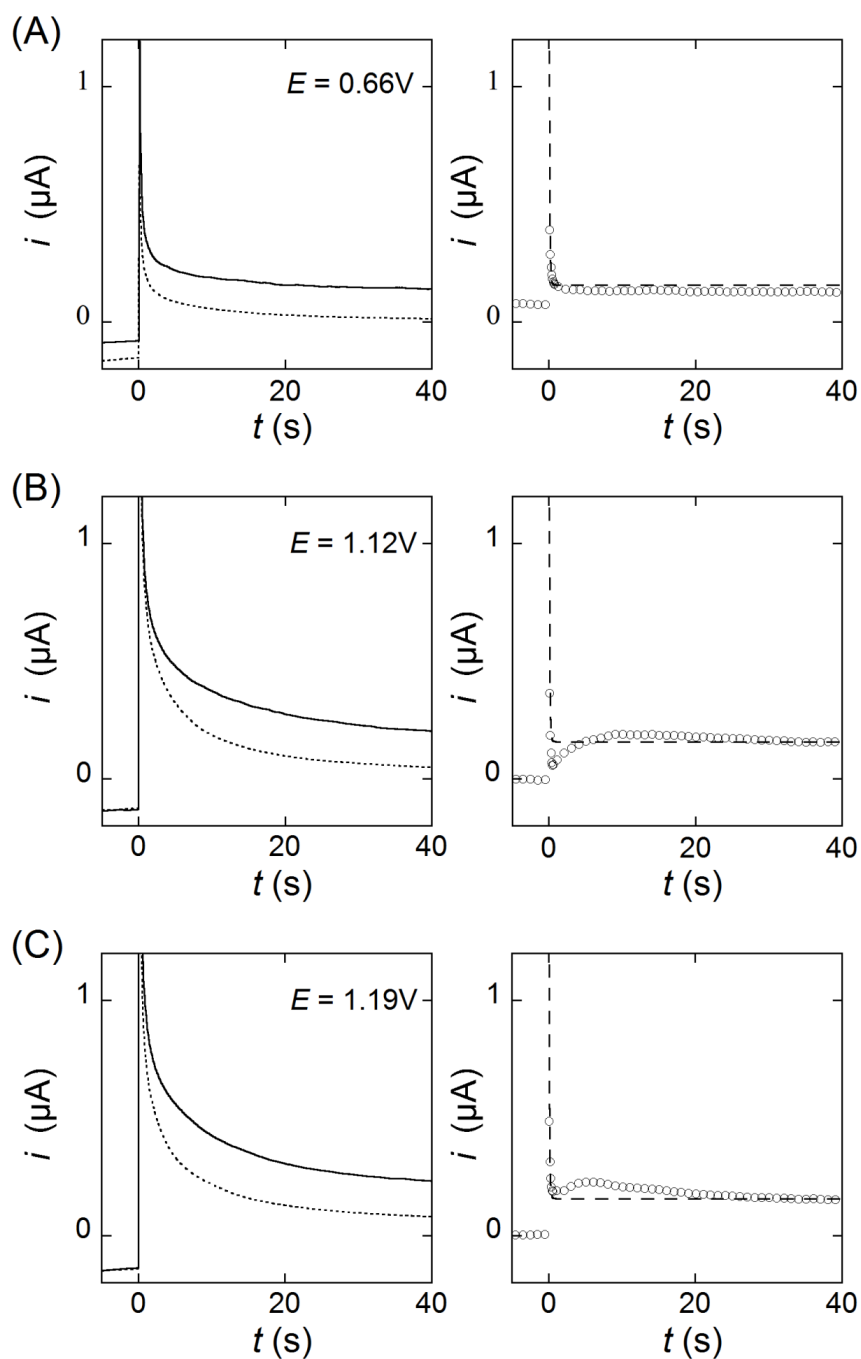**Figure 5:** Experimental chronoamperometric responses recorded in 0.5 mM CA (solid lines) and in buffer solution (dotted lines) at different applied potentials. (A) E = 0.66 V/Ref. (B) E = 1.12 V/Ref. (C) E = 1.19 V/Ref. In (A-C), the currents subtracted from capacitive and residual currents (○) are compared to the predicted currents (dashed lines) obtained by numerical simulations. F = 0.1 μL min^{-1}.

The good agreement observed at higher potentials shows that this analytical procedure is appropriate for evaluating antioxidant capacity of samples of unknown compositions, provided that the electrochemical reactions involved are fully controlled by the mass transport [37]. These results based on these different mixtures demonstrate that the individual diffusion coefficients of AO or number of electron exchanged during their oxidation have no influence on the determination of antioxidant capacity. The accuracy of this evaluation is guaranteed also if residual currents are subtracted from the global currents, in particular when the operating potentials are close from the oxidation of the medium.
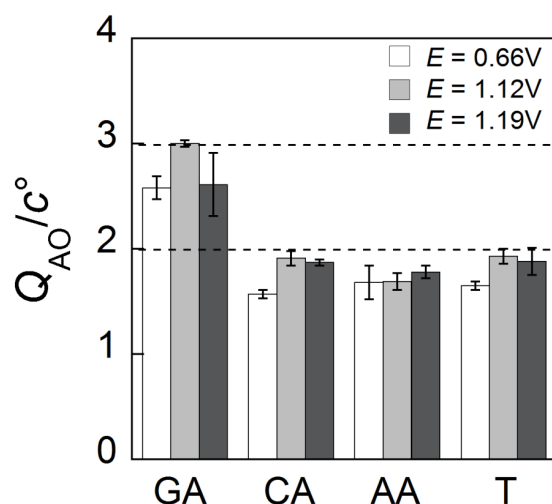
Figure 6: Experimental values of Q_{AO}/c^0 estimated from steady-state currents in 0.5 mM AO solutions after subtraction of residual currents. $F = 0.1 \mu L min^{-1}$. The predicted values (dashed lines) are equal to $Q_{AO}/c^0 = n = 3$ for GA and to $Q_{AO}/c^0 = n = 2$ for AA, CA and T. Uncertainties correspond to standard deviations of 3 successive measurements. CA+T (▲), GA+T (△), AA+CA+GA (□), AA+CA+GA+T (■).

3.6 Comparison with a method based on electrolysis

 Finally, some of these results were compared with others reported in a previous work [29]. The latter were obtained from coulometric experiments carried out with similar AOs mixtures. Under these experimental conditions, partial electrolysis were performed in a conventional electrochemical cell during an operating time of several minutes (through the RACE method) [29]. Figure 8 shows that the performances achieved in both situations were comparable with discrepancies ranging from 10 to 15 %. This comparison between data demonstrates clearly the great benefit of using microchannel electrodes to quantify antioxidant capacity while keeping identical or even better performances. Only very low samples volumes are required (*i.e.*, a few nanoliters) leading to fast determinations (*i.e.*, in a few seconds). Besides, the short duration of measurements should avoid long-time interferences

between oxidized species due the large degree of oxidized AOs and the formation of oxidized products during the electrochemical process.
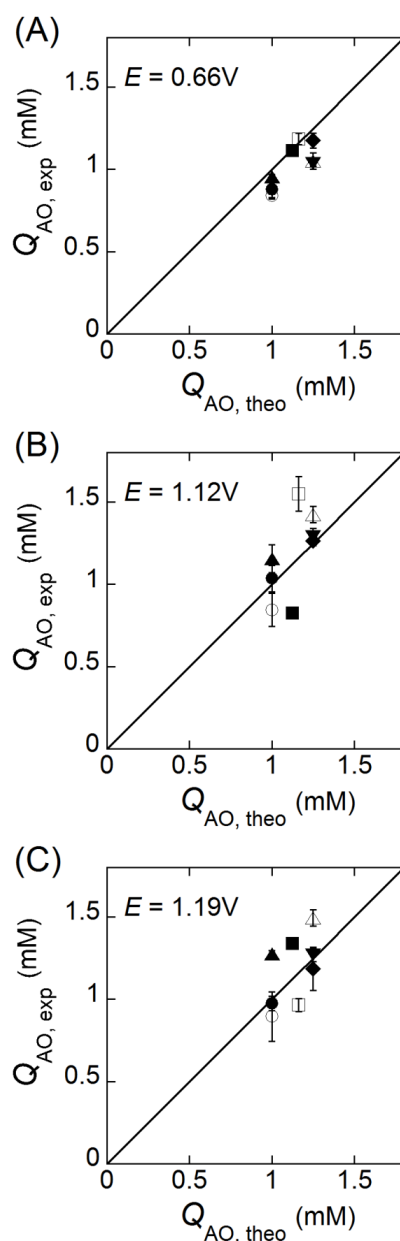
Figure 7: Comparison between experimental $Q_{AO, exp}$ and predicted $Q_{AO, theo}$ values of global antioxydant capacity for several mixtures of AO and different applied potentials. (A) $E = 0.66$ V/Ref. (B) $E = 1.12$ V/Ref. (C) $E = 1.19$ V/Ref. In (A-C) $\sum c_i = 0.5$ mM and $F = 0.1$ µLmin^{-1}. Uncertainties correspond to standard deviations of 3 successive measurements. The straight lines represent the equality $Q_{AO, exp} = Q_{AO, theo}$. AO Mixtures with AA+T ($\circ$), AA+CA ($\bullet$), AA+GA ($\blacklozenge$), CA+GA ($\blacktriangledown$),
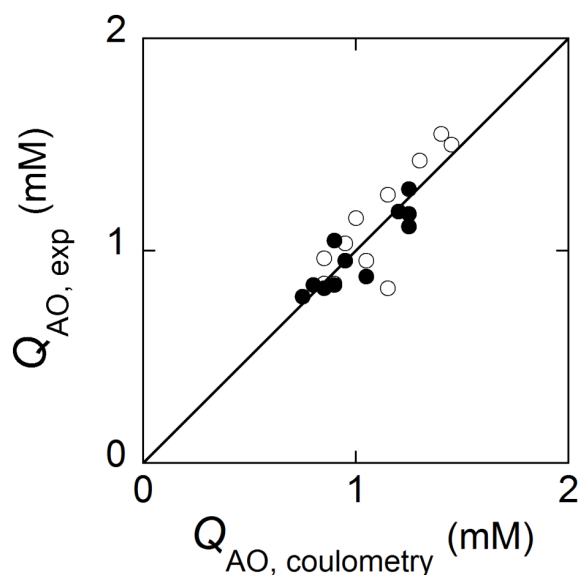
Figure 8: Comparison between experimental antioxidant capacity $Q_{AO, exp}$ evaluated at a microchannel electrode (data from figures 6 and 7) and antioxidant capacity $Q_{AO, coulometry}$ assessed from coulometric experiments[29] with same AO mixtures. The data in (●) correspond to $Q_{AO, exp}$ and $Q_{AO, coulometry}$ obtained respectively at E = 0.66 V/Ref and 0.8 V/(Ag.AgCl 3M KCl). The data in (○) correspond to $Q_{AO, exp}$ and $Q_{AO, coulometry}$ obtained respectively at E = 1.12 V/Ref and 1.2 V/(Ag.AgCl 3M KCl). The straight line represents the equality $Q_{AO, exp} = Q_{AO, coulometry}$.

4. Conclusion

These results clearly demonstrated the validity of this novel electrochemical procedure for evaluating total antioxidant capacity of samples. From one side, the selection of the operating potentials, which determine the analytical selectivity of the method, can easily simulate the oxidation power of many ROS like $O_2^{\bullet-}$ and H_2O_2. On the other side, the use of a microchannel electrodes provide all the benefits of confined environments such as the handling of low solution volumes and the set-up of fast electrochemical measurements. Under specific operating conditions, a thin layer regime may be established at the microchannel electrode that allows antioxidant capacity of AOs mixtures or samples to be analyzed without making any prior assumptions about their composition. This approach was validated by performing measurements with synthetic mixtures of AOs having dissimilar diffusion coefficients and involving different number of electron stoichiometries during their oxidation. This novel method paves the way to high performance antioxidant assays combining advantages of electrochemistry and microfluidics.

Acknowledgments

References

[1]   G.M. Whitesides, The origins and the future of microfluidics, Nature. 442 (2006) 368–373.

[2]   A. Arora, G. Simone, G.B. Salieb-Beugelaar, J.T. Kim, A. Manz, Latest Developments in Micro Total Analysis Systems, Anal. Chem. 82 (2010) 4830–4847.

[3]   A. Webster, J. Greenman, S.J. Haswell, Development of microfluidic devices for biomedical and clinical application, J. Chem. Technol. Biotechnol. 86 (2011) 10–17.

[4]   A. Escarpa, Food electroanalysis: sense and simplicity, Chem. Rec. 12 (2012) 72–91.

[5]   J.C. Jokerst, J.M. Emory, C.S. Henry, Advances in microfluidics for environmental analysis, Analyst. 137 (2012) 24–34.

[6]   C.I.D. Newman, B.C. Giordano, C.L. Copper, G.E. Collins, Microchip micellar electrokinetic chromatography separation of alkaloids with UV-absorbance spectral detection, Electrophoresis. 29 (2008) 803–810.

[7]   M. Hervas, M.A. Lopez, A. Escarpa, Integrated electrokinetic magnetic bead-based electrochemical immunoassay on microfluidic chips for reliable control of permitted levels of zearalenone in infant foods, Analyst. 136 (2011) 2131–2138.

[8]   C.N. Jayarajah, A.M. Skelley, A.D. Fortner, R.A. Mathies, Analysis of Neuroactive Amines in Fermented Beverages Using a Portable Microchip Capillary Electrophoresis System, Anal. Chem. 79 (2007) 8162–8169.

[9]   H. Ueno, J. Wang, N. Kaji, M. Tokeshi, Y. Baba, Quantitative determination of amino acids in functional foods by microchip electrophoresis, J. Sep. Sci. 31 (2008) 898–903.

[10]   M.J.A. Shiddiky, H. Park, Y.-B. Shim, Direct Analysis of Trace Phenolics with a Microchip: In-Channel Sample Preconcentration, Separation, and Electrochemical Detection, Anal. Chem. 78 (2006) 6809–6817.

[11]   M. Ávila, M. Zougagh, A. Escarpa, Á. Ríos, Fast single run of vanilla fingerprint markers on microfluidic-electrochemistry chip for confirmation of common frauds, Electrophoresis. 30 (2009) 3413–3418.

[12]   K.-S. Lee, M.J.A. Shiddiky, S.-H. Park, D.-S. Park, Y.-B. Shim, Electrophoretic analysis of food dyes using a miniaturized microfluidic system, Electrophoresis. 29 (2008) 1910–1917.

[13]   V. Blazek, R.A. Caldwell, Comparison of SDS gel capillary electrophoresis with microfluidic lab-on-a-chip technology to quantify relative amounts of 7S and 11S proteins from 20 soybean cultivars, Int. J. Food Sci. Technol. 44 (2009) 2127–2134.

[14]   G. Monti, L. De Napoli, P. Mainolfi, R. Barone, M. Guida, G. Marino, et al., Monitoring Food Quality by Microfluidic Electrophoresis, Gas Chromatography, and Mass Spectrometry Techniques: Effects of Aquaculture on the Sea Bass (Dicentrarchus labrax), Anal. Chem. 77 (2005) 2587–2594.

[15]   A.G. Crevillén, M. Ávila, M. Pumera, M.C. González, A. Escarpa, Food Analysis on Microfluidic Devices Using Ultrasensitive Carbon Nanotubes Detectors, Anal. Chem. 79 (2007) 7408–7415.

[16]   A.G. Crevillen, M. Pumera, M.C. Gonzalez, A. Escarpa, Towards lab-on-a-chip approaches in real analytical domains based on microfluidic chips/electrochemical multi-walled carbon nanotube platforms, Lab Chip. 9 (2009) 346–353.

[17] N. Kovachev, A. Canals, A. Escarpa, Fast and Selective Microfluidic Chips for Electrochemical Antioxidant Sensing in Complex Samples, Anal. Chem. 82 (2010) 2925–2931.

[18] P.S. Dittrich, K. Tachikawa, A. Manz, Micro Total Analysis Systems. Latest Advancements and Trends, Anal. Chem. 78 (2006) 3887–3908.

[19] S. Zhao, Y. Huang, Y.-M. Liu, Microchip electrophoresis with chemiluminescence detection for assaying ascorbic acid and amino acids in single cells, J. Chromatogr. A. 1216 (2009) 6746–6751.

[20] S. Zhao, X. Li, Y.-M. Liu, Integrated Microfluidic System with Chemiluminescence Detection for Single Cell Analysis after Intracellular Labeling, Anal. Chem. 81 (2009) 3873–3878.

[21] J.J.P. Mark, R. Scholz, F.-M. Matysik, Electrochemical methods in conjunction with capillary and microchip electrophoresis, J. Chromatogr. A. 1267 (2012) 45–64.

[22] Y. Chang, C. Zhao, Z. Wu, J. Zhou, S. Zhao, X. Lu, et al., Chip-based nanoflow high performance liquid chromatography coupled to mass spectrometry for profiling of soybean flavonoids, Electrophoresis. 33 (2012) 2399–2406.

[23] K. Tsukagoshi, T. Saito, R. Nakajima, Analysis of antioxidants by microchip capillary electrophoresis with chemiluminescence detection based on luminol reaction, Talanta. 77 (2008) 514–517.

[24] M. Kamruzzaman, A.-M. Alam, K.M. Kim, S.H. Lee, Y.H. Kim, G.-M. Kim, et al., Microfluidic chip based chemiluminescence detection of L-phenylalanine in pharmaceutical and soft drinks, Food Chem. 135 (2012) 57–62.

[25] J. Gao, X.-F. Yin, Z.-L. Fang, Integration of single cell injection, cell lysis, separation and detection of intracellular constituents on a microfluidic chip, Lab Chip. 4 (2004) 47–52.

[26] S. Ohla, P. Schulze, S. Fritzsche, D. Belder, Chip electrophoresis of active banana ingredients with label-free detection utilizing deep UV native fluorescence and mass spectrometry, Anal. Bioanal. Chem. 399 (2011) 1853–1857.

[27] A.J. Blasco, M.C.M.C. González, A. Escarpa, Electrochemical approach for discriminating and measuring predominant flavonoids and phenolic acids using differential pulse voltammetry: towards an electrochemical index of natural antioxidants, Anal. Chim. Acta. 511 (2004) 71–81.

[28] R.W. Hompesch, C.D. Garcia, D.J. Weiss, J.M. Vivanco, C.S. Henry, Analysis of natural flavonoids by microchip-micellar electrokinetic chromatography with pulsed amperometric detection, Analyst. 130 (2005) 694–700.

[29] R. Oliveira, J. Marques, F. Bento, D. Geraldo, P. Bettencourt, Reducing Antioxidant Capacity Evaluated by Means of Controlled Potential Electrolysis, Electroanalysis. 23 (2011) 692–700.

[30] R. Apak, S. Gorinstein, V. Böhm, K.M. Schaich, M. Özyürek, K. Güçlü, Methods of measurement and evaluation of natural antioxidant capacity/activity (IUPAC Technical Report), Pure Appl. Chem. 85 (2013) 957–998.

[31] M. Amatatongchai, O. Hofmann, D. Nacapricha, O. Chailapakul, A. DeMello, A microfluidic system for evaluation of antioxidant capacity based on a peroxyoxalate chemiluminescence assay, Anal. Bioanal. Chem. 387 (2007) 277–285.

[32] Z. Matharu, J. Enomoto, A. Revzin, Miniature Enzyme-Based Electrodes for Detection of Hydrogen Peroxide Release from Alcohol-Injured Hepatocytes, Anal. Chem. 85 (2013) 932–939.

[33] A. V Krylov, R. Sczech, F. Lisdat, Characterization of antioxidants using a fluidic chip in aqueous/organic media, Analyst. 132 (2007) 135–141.

[34] O. Makhotkina, P.A. Kilmartin, The use of cyclic voltammetry for wine analysis: Determination of polyphenols and free sulfur dioxide, Anal. Chim. Acta. 668 (2010) 155–165.

[35] H. Tiehua, G. Ping, H. Michael, Rapid Screening of Antioxidants in Pharmaceutical Formulation Development Using Cyclic Voltammetry - Potential And Limitations, Curr. Drug Discov. Technol. 1 (2004) 173–179.

[36] S. Shahrokhian, H.R. Zare-Mehrjardi, Application of thionine-nafion supported on multi-walled carbon nanotube for preparation of a modified electrode in simultaneous voltammetric detection of dopamine and ascorbic acid, Electrochim. Acta. 52 (2007) 6310–6317.

[37] C. Amatore, N. Da Mota, C. Sella, L. Thouin, Theory and Experiments of Transport at Channel Microband Electrodes under Laminar Flows. 1. Steady-State Regimes at a Single Electrode, Anal. Chem. 79 (2007) 8502–8510.

[38] C. Amatore, C. Lemmer, C. Sella, L. Thouin, Channel Microband Chronoamperometry: From Transient to Steady-State Regimes, Anal. Chem. 83 (2011) 4170–4177.

[39] C. Giacomelli, K. Ckless, D. Galato, F.S. Miranda, A. Spinelli, Electrochemistry of Caffeic Acid Aqueous Solutions with pH 2.0 to 8.5, J. Braz. Chem. Soc. 13 (2002) 332–338.

[40] S.M. Ghoreishi, M. Behpour, M. Khayatkashani, M.H. Motaghedifard, Simultaneous determination of ellagic and gallic acid in Punica granatum, Myrtus communis and Itriphal formulation by an electrochemical sensor based on a carbon paste electrode modified with multi-walled carbon nanotubes, Anal. Methods. 3 (2011) 636–645.

[41] Z. Taleat, M.M. Ardakani, H. Naeimi, H. Beitollahi, M. Nejati, H.R. Zare, Electrochemical Behavior of Ascorbic Acid at a 2,2′-[3,6-Dioxa-1,8-octanediylbis(nitriloethylidyne)]-bis-hydroquinone Carbon Paste Electrode, Anal. Sci. 24 (2008) 1039–1044.

[42] H. Masuhara, S. Kawata, F. Tokunaga, Preface, in: H. Masuhara, S. Kawata, F. Tokunaga (Eds.), Nano Biophotonics Sci. Technol. Proc. 3rd Int. Nanophotonics Symp. Handai, Elsevier, 2007.

[43] F. Sen, A.A. Boghossian, S. Sen, Z.W. Ulissi, J. Zhang, M.S. Strano, Observation of Oscillatory Surface Reactions of Riboflavin, Trolox, and Singlet Oxygen Using Single Carbon Nanotube Fluorescence Spectroscopy, ACS Nano. 6 (2012) 10632–10645.

[44] C. Amatore, M. Belotti, Y. Chen, E. Roy, C. Sella, L. Thouin, Using electrochemical coupling between parallel microbands for in situ monitoring of flow rates in microfluidic channels, J. Electroanal. Chem. 573 (2004) 333–343.

[45] A. Pépin, P. Youinou, V. Studer, A. Lebib, Y. Chen, Nanoimprint lithography for the fabrication of DNA electrophoresis chips, Microelectron. Eng. 61–62 (2002) 927–932.

[46] C. Amatore, N. Da Mota, C. Lemmer, C. Pebay, C. Sella, L. Thouin, Theory and Experiments of Transport at Channel Microband Electrodes under Laminar Flows. 2. Electrochemical Regimes at Double Microband Assemblies under Steady State, Anal. Chem. 80 (2008) 9483–9490.

[47] O. Scialdone, C. Guarisco, A. Galia, G. Filardo, G. Silvestri, C. Amatore, et al., Anodic abatement of organic pollutants in water in micro reactors, J. Electroanal. Chem. 638 (2010) 293–296.

[48]   S.G. Weber, W.C. Purdy, The behaviour of an electrochemical detector used in liquid chromatography and continuous flow voltammetry: Part 1. Mass transport-limited current, Anal. Chim. Acta. 100 (1978) 531–544.

[49]   D. Gilroy, B.E. Conway, Surface oxidation and reduction of platinum electrodes: Coverage, kinetic and hysteresis studies, Can. J. Chem. 46 (1968) 875–890.

3 Aromatic hydroxylation reactions by electrogenerated HO radicals: A kinetic study

Raquel Oliveira, Fátima Bento*, Dulce Geraldo

Department of Chemistry, Universidade do Minho, Campus de Gualtar 4710-057, Portugal

* Corresponding author T: +351 253604399; e-mail: fbento@quimica.uminho.pt

Abstract

The oxidation of benzoic acid (BA) and of 4-hydroxybenzoic acid (4-HBA) by galvanostatic electrolysis with simultaneous oxygen evolution, using BDD or Pt as anode materials is studied. Results concerning the oxidation kinetics as well as the identification and quantification of hydroxylated products are reported. First order kinetics are used to describe the consumption rates of both compounds despite of the anode material and of the applied current density. A simple kinetic model that accounts for the anode surface coverage by HO radicals is proposed. Based on this model it is possible to correlate the apparent rate constant of the organic consumption with kinetic parameter related to the organics reactivity and to the degree of the adsorption of HO radicals to the anode surface.

Keywords

1. Introduction

Hydroxyl radical (HO$^{\bullet}$), the most reactive species among oxygen radicals, is quite relevant in different fields, such as organic synthesis [1], oxidative stress studies [2] and environmental applications [3]. Reactions of HO$^{\bullet}$ with aromatic compounds have been extensively studied. It was demonstrated that addition reactions are more likely to occur than oxidation, despite the high reducing power of HO radical, $E^{\circ}(HO^{\bullet}, H^{+}/H_2O) = 2.72$ V, pH 0 [4] and $E^{\circ}(HO^{\bullet}/HO^{-}) = 1.89$ V [5], probably due to the large solvent reorganization following the electron transfer reactions.

The addition mechanism of HO$^{\bullet}$ was described as involving hydrogen atom abstraction and fast nucleophilic addition with the formation of a hydroxycyclohexadienyl radical that undergoes different reactions depending on the medium composition [6].

The production of HO radicals is an important issue that can be achieved by different approaches. Pulse radiolysis and flash photolysis are among the cleanest and most reproducible methods, yet their use is rather limited as the equipment required are not accessible to most research laboratories. In opposition, chemical methods based on disproportionation of peroxynitrous acid or on decomposition of hydrogen peroxide by metal ions, known as Fenton [7] or Fenton-like reactions [8] are the most spread method despite of fundamental questions concerning the enrollment of reagents in the oxidation process. A modification of the classic Fenton reaction, allowing for a controlled production of hydroxyl radicals, was achieved by electrochemical means. The electro-Fenton reaction allows for the generation of HO radical in a controlled manner by adjusting the homogeneous production of hydrogen peroxide and Fe(II) by means of the electrochemical reduction of oxygen and Fe(III), respectively [6,9]. Hydroxyl radicals are also formed by direct electro-oxidation of water as mediators of oxygen evolution reaction (Eqs. (1) and (2)). Although radicals formed by this process are adsorbed at the anode surface they can be involved in reactions with organic compounds as expressed by Eq. (3) [10]:

$$H_2O \rightarrow HO^{\bullet} + H^{+} + e^{-} \tag{1}$$

$$2\,HO^{\bullet} \rightarrow O_2 + 2H^{+} + 2e^{-} \tag{2}$$

$$R + \ nHO^{\bullet} \rightarrow \ products \tag{3}$$

Most of the work concerning the electrogeneration of hydroxyl radicals is aimed to the detoxification of effluents [11,12] where it is envisaged the total combustion of organic material. The reported experimental conditions include high oxidation power anodes, such as Sb-SnO$_2$ [13], PbO$_2$ [14] or BDD [15], high current densities, long electrolysis times and undivided electrochemical cells. Under these

conditions an efficient decrease of the chemical oxygen demand (COD) is usually attained as CO_2 is formed in a yield approaching 100% [3,16,17,18]. The benefits associated to this method of producing of HO radicals are important due to the simplicity of the required instrumentation and also because it does not require the use of any specific reagent. Despite its great success in environmental applications, the use of this method has not been explored in other important areas such as organic synthesis or oxidative stress studies.

This paper aims to demonstrate the potentiality of this method of production of HO radicals for other application besides the elimination of organics. Experiments were performed in experimental conditions that were selected to minimize the contribution from secondary reactions and from cathodic reactions, like low concentrations of organics, short electrolysis times and a two-compartment electrochemical cell. Benzoic acid and 4-hydroxybenzoic acid were chosen as model compounds as they are frequently used for characterizing HO radicals mediated reactions.

2. Experimental

2.1. Chemicals

All reagents employed were of analytical grade: 3-hydroxybenzoic acid (3-HBA), 2,3-dihydroxybenzoic acid (2,3-HBA), 2,4-dihydroxybenzoic acid (2,4-HBA), 2,5-dihydroxybenzoic acid (2,5-HBA), 2,6-dihydroxybenzoic acid (2,6-HBA), 2,3,4-trihydroxybenzoic acid (2,3,4-HBA), phosphoric acid, potassium dihydrogen phosphate and dipotassium hydrogen phosphate (all from ACROS Organics), potassium ferricyanide (José Gomes Santos), potassium chloride (Fluka), benzoic acid (BA; Prolabo), 2-hydroxybenzoic acid (2-HBA;Vaz Pereira), 4-hydroxybenzoic acid (4-HBA; BDH Chemicals), 3,4-dihydroxybenzoic acid (3,4-HBA; Aldrich), 3,4,5-trihydroxybenzoic acid (3,4,5-HBA; Sigma) and methanol (Fisher Scientific).

Phosphate buffer pH 7.0 was prepared by mixing adequate amounts of dipotassium hydrogen phosphate with potassium dihydrogen phosphate, whereas phosphate buffer pH 3.5 was prepared using potassium dihydrogen phosphate and phosphoric acid. The concentration of the buffer solutions was 0.15 M.

86

2.2. Electrochemical measurements

Voltammetric measurements and galvanostatic electrolyses were performed using a potentiostat (Autolab type PGSTAT30, Ecochemie) controlled by GPES 4.9 software provided by Ecochemie.

2.2.1. Cyclic voltammetry

Cyclic voltammetry experiments were carried out from -0.4 to 1.0 V vs Ag/AgCl, 3 M KCl at Pt disc (area 0.63 cm^2) and from 1.0 to 2.2 V vs Ag/AgCl, 3 M KCl at a BDD disc (area 0.63 cm^2) at a scan rate of 100 mV s^{-1}. The reference electrode was an Ag/AgCl, 3 M KCl electrode (CHl111, CH Instruments, Inc.). The counter electrode was a platinum wire.

2.2.2. Electrolyses

Galvanostatic electrolyses were carried out at 50, 268, 625 and 1250 A m^{-2} in a two compartments cell separated by a glass frit membrane. The volume of the anodic compartment was 9.0 ml and the solution was mechanically stirred with a magnetic stir bar (300 rpm). Pt and BDD materials were used as anode electrodes. The Pt anode (5.6 cm^2) is made of a piece (20 mm x 10 mm) of platinum gauze (52 mesh woven from 0.1 mm diameter wire, 99.9%, from Alfa Aesar). The BDD electrode (3.0 cm^2; 15 mm x 20 mm) characterized by a 800 ppm boron concentration and a BDD-film thickness of 2.7 μm, on a substrate of monocrystalline silicon, p-doped was purchased at Adamant Technologies, Switzerland. The area of the Pt working electrode was determined using a 1.00 mM of K$_3$Fe(CN)$_6$ in 0.1 M KCl, in a cronoamperometry experiment. The diffusion coefficient used was 7.63 x 10^{-6} cm^{2}s^{-1} [19]. Before each experiment anodes were electrochemically cleaned by applying a constant current according to its nature. The Pt anode was cleaned using 0.02 A in a 0.1 M phosphate buffer pH 3.5 during 600 s, whereas the BDD anode was cleaned using -0.01 A in a 0.1 M phosphate buffer pH 7.0 for the same period of time.

Apparent constant rate was determined by the average values of at least two electrolysis and its uncertainty was estimated through the standard deviation of the slope of the straight-lines Eq. (5).

2.3. HPLC

The reactions were monitored both by the concentration decrease of BA or of 4-HBA along time and by the quantification of hydroxylated products formed at 360 s. Hydroxylated compounds were selected as relevant reactive products as they are known to be the main products formed in the presence of oxygen, as demonstrated for BA reaction with HO radicals generated by radiolysis [20,21,22], by photochemistry [23,24] and by electro-Fenton reaction [25]. These products have also been detected as intermediaries in the photocatalytic degradation of BA induced by TiO_2 [26], in photo-Fenton oxidation of BA and in electrochemical oxidation of BA using BDD [18,27].

HPLC analyses were performed using a Jasco, PU-2080 Plus system equipped with a RP 18 column from Grace Smart (250 mm x 4.6 mm, 5 μm particle size) and Clarity HPLC software from Jasco. A flow rate of 0.6 ml min^{-1} and a loop of 20 μl were used. A mixture of methanol: water: phosphoric acid (60:39:1) (v/v) was used as mobile phase. The detection was made at 230 nm and the quantification was performed using standard curves for each substance.

3. Results and discussion

3.1. Voltammetry of benzoic acid and of 4-hydroxybenzoic acid at Pt and at BDD electrodes

The voltammetric responses of BA and of 4-HBA in phosphate buffer pH 3.5 at BDD and at Pt electrodes are presented in Fig. 1 A and B, respectively. The voltammogram of BA using BDD displays a not well-defined peak whereas the voltammogram of 4-HBA shows a well-defined peak at lower potentials. This result shows that the presence of the hydroxyl group in the aromatic ring favors the electron transfer reaction. Besides, these reactions are not reversible and the products formed tend to block the electrode surface decreasing the current in sequential runs (results not shown), as it was previously reported [18,28].

Voltammograms recorded for both compounds with the Pt electrode do not show a significant difference from those recorded in the blank solution. This result shows that the present experimental conditions did not allow the adsorption of BA or of 4-HBA for its subsequent oxidation, as it was previously demonstrated to occur under controlled conditions [29].
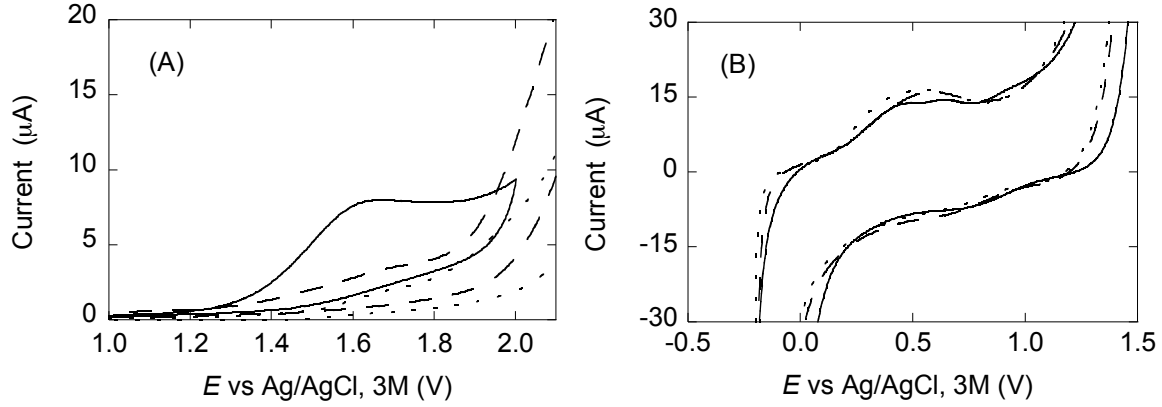
88

Figure 1. Cyclic voltammograms (100 mV s^{-1}) of benzoic acid 0.50 mM (– –) and of 4-hydroxybenzoic acid 0.50 mM (—) in 0.15 M phosphate buffer solution pH 3.5, and of the blank (---) obtained at: (A) BDD and (B) Pt electrodes.

3.2. Galvanostatic electrolysis

Two sets of galvanostatic electrolyses of BA (0.50 mM) were conducted in 0.15 M phosphate buffer pH 3.5 using either a BDD anode (A = 3.0 cm^2) or a Pt anode (A = 5.6 cm^2) at a current density of 625 A m^{-2}. The concentration decrease of BA, quantified by HPLC, is expressed by means of the concentrations ratio C/C_0 and plotted against the electrolysis time, where C is the concentration of BA and C_0 its initial concentration. Results are shown in Fig. 2 A. The concentration profiles obtained using both anode materials follow a first order kinetics characterized by an exponential decay of the concentration with time according to following equations:

$$C = C_0 \exp\left(-\frac{k_{app}A}{V}t\right)$$

(4)

$$\frac{1}{A}\ln\frac{C}{C_0} = -\frac{k_{app}}{V}t$$

(5)

where, A is the anode area, V is the volume of the solution in the anodic compartment, t is time and k_{app} is the apparent rate constant that characterizes the consumption of BA. While Eq. (4) is the most common form of expressing the concentration variation with time, we chose to represent our data by Eq.(5) to normalize the concentration ratio by the anode area in order to eliminate this variable that would induce changes in the slopes due to the difference of the areas of the anodes. As V is the same for all experiments carried out with both anodes, the value of the slopes can be compared directly as a measure of k_{app}. The slopes of the two straight-lines presented in Fig. 2 A are clearly different, (1.79 ± 0.03) x10^{-5} m s^{-1} for BDD and (3.6 ± 0.3) x10^{-6} m s^{-1} for Pt. The lower value obtained for Pt cannot be attributed to a partial blockage of this anode surface as the simultaneous oxygen evolution keeps the anode surface unobstructed. Therefore, this result indicates that k_{app} depends strongly on the anode

89

nature. Furthermore, the fact that BA oxidation is more effective when BDD is used, can be explained by the larger reactivity of this material for HO· mediated oxidations.

The former reported experiments were repeated using 4-HBA instead of BA. The obtained results are displayed in Fig. 2 B using an identical plot. In opposition to results from BA, for 4-HBA the slopes of both straight-lines are identical ($\approx$ (2.2±0.2) x 10^{-5} m s^{-1}, average value). In opposition to BA the k_{app} values seem not to depend on the anode material nature. Despite the use of an identical configuration of the electrochemical cell and that the solutions stirring was kept constant in all the experiments, it was not expectable that results from 4-HBA were independent on the nature of the anode material.

Comparing the slopes obtained for both compounds for the same anode material it can be concluded that k_{app} is related to nature of the organic compound. Furthermore, differences between k_{app} values are in agreement with the reactivity of the organic compounds, as k_{app} values are larger for 4-HBA (either using Pt or BDD) which is consistent with the larger reactivity of 4-HBA for electrophilic attack by HO· [6,30]. Besides, it can be notice that there is a differentiating/leveling effect concerning the anode oxidation power when BA or 4-HBA is used. The less reactive compound discriminate the oxidation power of the two anodes, while 4-HBA, the most reactive compound, is consumed with similar rates at both anodes.

3.3. Current density effect on the rate of organics oxidation

For a better understanding of the variables that affect k_{app} galvanostatic electrolyses were carried out with BA and 4-HBA at different current densities, between 50 and 1250 A m^{-2}, at both anodes. k_{app} values were calculated for all the experiments from the analysis of the concentration decrease with time. These values are reported in Fig. 3 as a function of the applied current density. For all current densities oxygen evolution was detected at the anodes, which potential varied between 1.8 V (i = 50 A m^{-2}) and 2.6 V (i = 1250 A m^{-2}) for Pt and between 2.8 V (i = 50 A m^{-2}) and 4.6 V (i = 1250 A m^{-2}) for BDD. Values of k_{app} for both compounds follow a linear relation with the current density with an intercept that is close to zero. This effect is quite remarkable as it is observed for the two compounds and the two anode materials. Both, the linear trend and the null intercept can lead to the following conclusions.
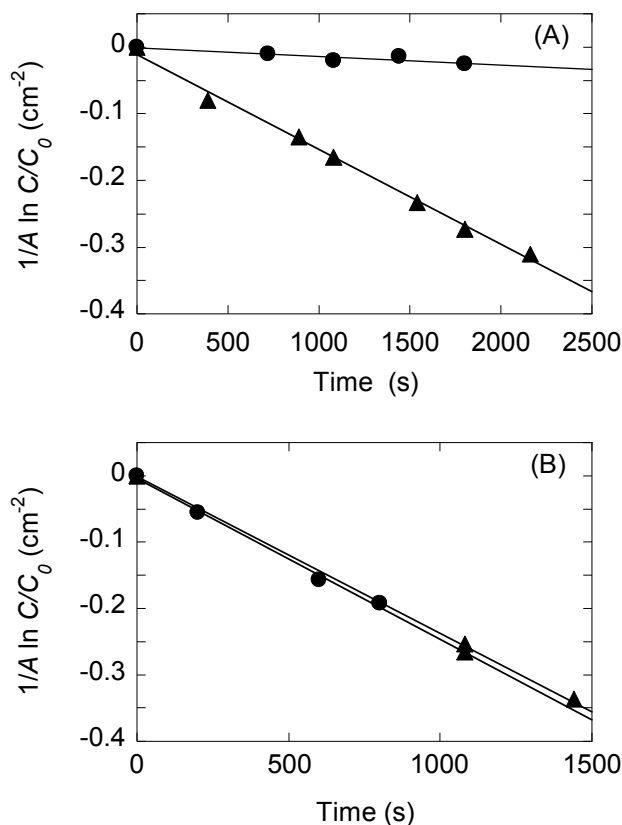
Figure 2. Plot of the concentration decrease during galvanostatic electrolyses, linearized and normalized to the anode area: (A) BA (C_0= 0.50 mM) at Pt anode (●) ($1/A$ ln(C/C_0) = -8.64 x 10^{-4} -3.60 x $10^{-4}t$, r=0.93) and at BDD anode (▲) ($1/A$ ln(C/C_0) = -1.08 x 10^{-2} - 1.79 x $10^{-3}t$, r=0.997) and (B) 4-HBA (C_0= 0.50 mM) at Pt anode (●) ($1/A$ ln(C/C_0) = -3.99 x 10^{-3} - 2.36 x $10^{-3}t$, r=0.998) and at BDD anode (▲) ($1/A$ ln(C/C_0) = -7.85 x 10^{-4} - 2.13 x $10^{-3}t$, r= 0.9994).

The fact that the intercept is almost zero means that when the current approaches zero (i.e. the water decomposition process vanishes) k_{app} tends to zero, which means that the oxidation of the organic compound does not occur, even if the anode potential is always above the oxygen evolution limit. This fact provides a clear evidence on the nature of the oxidation process, as a HO· mediated reaction and not by heterogeneous electron transfer.

The linear increase of k_{app} with the current density must be related to the increase of the surface concentration of HO radicals. The surface concentration of HO radicals must increase with the rate of the water decomposition as they are formed by this process (Eq. (1)). The importance of this effect is measured by the magnitude of the slopes. The fact that the magnitude of the slopes depend on the nature of the organic compound and of the anode material indicates that this parameter must incorporate variables associated with the reactivity of the organic species.
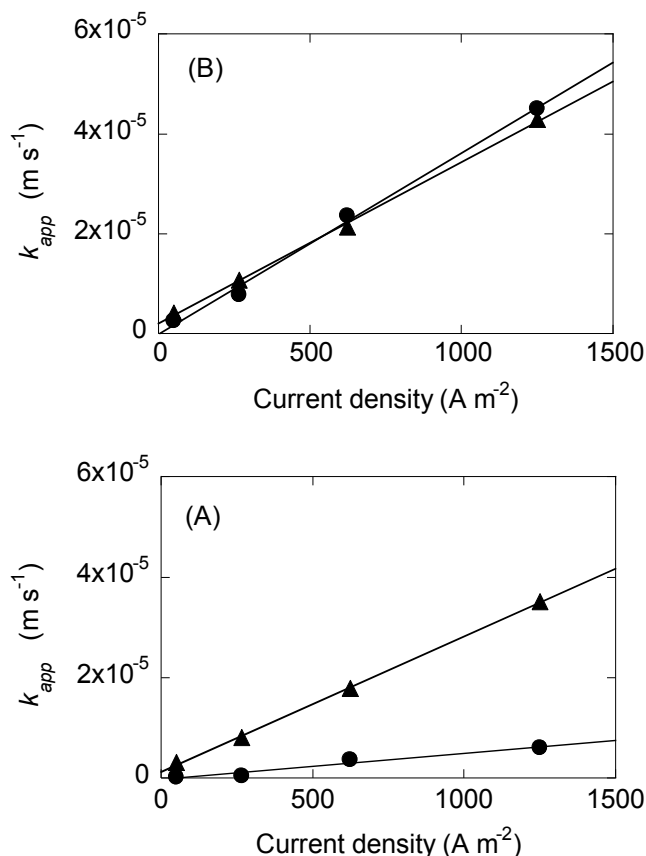
Figure 3. Effect of current density used in the galvanostatic electrolysis on the apparent rate constant for: (A) BA (C_0 = 0.50 mM) obtained at Pt anode (●) (k_{app} = -3.13 x 10^7 + 5.26 x 10^9 i, r= 0.98) and at BDD anode (▲) (k_{app} = 1.28 x 10^6 + 2.69 x 10^8 i, r= 0.997) and (B) for 4-HBA (C_0 = 0.50 mM) obtained at Pt anode (●) (k_{app} = -1.27 x 10^7 + 3.63 x 10^8 i, r= 0.998) and at BDD anode (▲) (k_{app} = 2.09 x 10^6 + 3.23 x 10^8 i, r=0.9992).

3.4. Analysis of hydroxylated products

Table 1 reports the results concerning the identification and quantification of the hydroxylated products formed by galvanostatic electrolysis of BA and 4-HBA with Pt and BDD at 360 s, for the current densities of 625 A m^{-2} and of 1250 A m^{-2}. The concentration products formed at lower current densities are not reported because they were above the detection limits.

The hydroxylated products formed, assigned by the position of the hydroxyl groups, were identified by comparison of the retention times with those of the standards. The concentration of each identified hydroxybenzoic derivative is expressed as a percentage of the total concentration of hydroxybenzoic products, $[P]/\Sigma[P]$ where the total concentration of hydroxylated products is expressed as Σ [P]. The yield of hydrxylated products is quantified by the parameter Σ $[P]/[R]_{conv}$ where $[R]_{conv}$ is the concentration of the organic that was converted to products. Although the conversion degree of BA and 4-HBA is quite different (according to the reported values of k_{app}) and despite the difference between

the anodes areas similar conclusions can be drawn concerning the effects of current density and of anode material on the yields of hydroxylated products.The amount of hydroxylated products formed when the Pt anode was used is higher than when the BDD anode was used, as it can be observed by the values of Σ [P] and of Σ [P]/[R]$_{conv}$ in Table 1. The fact that BDD seems to produce fewer hydroxylated compounds and at lower concentrations can be related to the higher activity of this anode material that might favor further oxidation of products into other forms, such as quinones, aliphatic acids and even CO_2.

On the other hand the increase of current density favors the formation of higher concentrations of hydroxylated products when Pt is used, while for BDD the concentration of products are similar for both current densities, even though higher amounts of the initial organic compound have been consumed. As a global trend the yield of hydroxylated species tend to decrease with the increase of current density indicating that hydroxylated products must be further oxidized.

Table 1. Identification of hydroxylated products of BA and 4-HBA formed by galvanostatic electrolysis after 360 s using either Pt or BDD anodes. The initial concentration of BA and 4-HBA was 0.50 mM. Quantification of the total concentration of hydroxylated products, Σ [P], and of the yield of hydroxylation Σ [P]/[R]$_{conv}$. [R]$_{conv}$ is the concentration of R that was converted to products and [P] is the concentration of each identified hydroxylated product.

R	i A m^{-2}	k$_{app}$ (10^{-5}) m s^{-1}		[R]$_{conv}$ mM		Σ [P] (10^{-2}) mM		Σ [P]/[R]$_{conv}$ %		x-HBA	[P]/ Σ[P] %	
		Pt	BDD	Pt	BDD	Pt	BDD	Pt	BDD		Pt	BDD
BA	625	0.360±0.003	1.79±0.03	0.0387	0.104	1.32	0.777	34	7	4-	37	45
										3,4,5-	63	55
	1250	0.61±0.02	3.51±0.03	0.0638	0.185	1.81	0.674	28	4	3-	-	8
										4-	31	44
										2,5-	22	-
										3,4-	29	-
										2,3,4-	18	-
										3,4,5-	-	48
4- HBA	625	2.4±0.4	2.13±0.08	0.287	0.268	1.11	0.0341	39	1	2,4-	1	-
										3,4-	46	43
										2,3,4-	18	-
										3,4,5-	35	57
	1250	4.5±0.4	4.3±0.9	0.401	0.393	1.32	0.0343	33	1	2,4-	8	-
										3,4-	44	90
										2,3,4-	25	10
										3,4,5-	24	-

3.5. Kinetic model for organics reaction with electrogenerated HO radicals

A quantitative analysis of the electrogenerated HO radicals reactions with organics must take into account the set of processes described by Eqs. (1)-(3), as previously demonstrated by Comninellis et al. [17,31]. If the organic consumption occurs solely by reaction with the HO radicals its rate of reaction can be expressed by the following rate law:

$$v_R = k_R \theta \Gamma_s C_R^E \tag{6}$$

where, v_R (mol m^{-2}s^{-1}) is the organic compound consumption rate, k_R (m^{3}mol^{-1}s^{-1}) the corresponding rate constant, θ the anode surface coverage by HO radicals, Γ_s (mol m^{-2}) the saturation concentration of this species and C_R^E (mol m^{-3}) is the concentration of the organic compound at the electrode surface. In order to calculate the surface concentration of HO radicals, $\theta\Gamma_s$, one has to consider the kinetics of formation (Eq. (1)) and of consumption of HO radicals, either in the formation of O_2 (Eq. (2)) or in the organics reaction (Eq. (3)). Considering that steady-state conditions are attained, an equilibrium is established between the rate of formation and the rates of consumption of these radicals:

$$v_{HO^\cdot} = 2v_{O_2} + n v_R \tag{7}$$

where $v_{HO}\bullet$ is the rate of formation of HO radicals by water dissociation (Eq. (8)) and v_{O_2} the rate of formation of O_2 (Eq. (9)) and n is the number of HO radicals used in the reaction with the organic compound:

$$v_{HO^\cdot} = \frac{i}{zF} \tag{8}$$

$$v_{O_2} = k_{O_2} \theta \Gamma_s \tag{9}$$

From Eqs. (6) to (9) the surface concentration of HO radicals at the anode can be expressed by:

$$\theta \Gamma_s = \frac{i}{zF(2k_{O_2} + nk_R C_R^E)} \tag{10}$$

The dependence of the surface coverage with the applied current and with the rate constants of the reactions described by Eqs. (2) and (3) was previously described by an equation similar to Eq. (10) [17,31].

Following Eq. (10) the rate of the organic consumption can be expressed by:

$$v_R = \frac{k_R i}{zF(2k_{O_2} + nk_R C_R^E)} C_R^E \tag{11}$$

or by:

$$v_R = \frac{i}{z\mathrm{F}\left(\dfrac{2k_{O_2}}{k_R} + nC_R^E\right)}C_R^E \tag{12}$$

Therefore the apparent rate constant can be defined as:

$$k_{app} = \frac{i}{z\mathrm{F}\left(\dfrac{2k_{O_2}}{k_R} + nC_R^E\right)} \tag{13}$$

This equation predicts that the rate of the organics consumption is related with the rate constant of O_2 formation, with the rate constant of the organics reaction, with the organics concentration and also with the number of HO radicals used in the organic reaction. Two limiting situations can be define depending on the relative magnitude of C_R^E toward k_{O_2}/k_R:

For $n\,C_R^E >> 2\,k_{O_2}/k_R$,

$$(k_{app})_0 = \frac{i}{z\mathrm{F}nC_R^E} \tag{14}$$

For $n\,C_R^E << 2\,k_{O_2}/k_R$,

$$(k_{app})_1 = \frac{i}{2z\mathrm{F}}\frac{k_R}{k_{O_2}} \tag{15}$$

Therefore, for higher concentrations of organics Eq. (14) predicts that the apparent rate constant is a function of the applied current, of the organics concentration and of the stoichiometric coefficient of the HO radical in Eq. (3). Under these circumstances k_{app} does not depend on the organics reactivity, k_R. This approximation can also be attained by disregarding the first term of Eq. (7), which means that the anode coverage by HO radicals depends entirely on the balance between the formation of HO· and its use by the organics oxidation. Furthermore, the organics oxidation rate is predicted to follow a zero order reaction ($v_R = i/n\mathrm{F}$).

In opposition, for low concentrations of organics the apparent rate constant given by Eq. (15) increases with the applied current and with k_R and decreases with k_{O_2}. In this situation the surface concentration of HO· is mainly controlled by the balance between the formation of HO· and its consumption in O_2 evolution. Moreover, reactions are expected to follow a first order kinetics.

The concentration effect on k_{app}, computed by means of Eq. (13) is reported in Fig. 4 A for n = 18, i = 1250 A m^{-2} and for different k_{O_2}/k_R values (5, 10, 25, 150 and 500 mol m^{-3}). The deviation of k_{app} from the two limiting situations described by Eq. (14) and Eq. (15) are reported in Fig. 4 B and C, where

these deviations are expressed in percentage of the limiting values $(k_{app})_0$ or $(k_{app})_1$. The selected value for n (=18) corresponds to the number of HO radicals needed to oxidize BA completely. This high number was considered as it corresponds to the less favorable situation for attaining the limiting condition expressed by Eq. (15), i.e. to verify a first order kinetics.

From the reported values in Fig. 4 A one can observe that k_{app} displays a strong dependence on both concentration and k_{O_2}/k_R. The concentration effect on k_{app} tends to be more significant for lower k_{O_2}/k_R ratios. For higher k_{O_2}/k_R values k_{app} tend to be approximately constant although dependent on the ratio k_{O_2}/k_R. The relative deviation of k_{app} from $(k_{app})_0$ (Fig. 4 B) is considerable for higher values of the ratio k_{O_2}/k_R despite of the concentration. In opposition, for 5 mM solutions deviations lower than 10% can be achieved if $k_{O_2}/k_R < 5$. On the other hand the deviations of k_{app} to $(k_{app})_1$ (Fig. 4 C) tend to decrease for the higher k_{O_2}/k_R, namely deviations lower than 10% are obtained for concentrations lower than 2 mM if $k_{O_2}/k_R \geq 150$.

The deviation between k_{app} and $(k_{app})_1$ for a concentration of 1 mM as a function of current density is illustrated in Fig. 5, where the k_{app} values (solid lines) are compared to $(k_{app})_1$ (dashed lines) for different k_{O_2}/k_R, i.e. 25, 150 and 500 mol m^{-3} and n = 18 (Fig. 5 A), whereas values for k_{O_2}/k_R = 150 mol m^{-3} for different n, namely 2, 9 and 18 are reported in Fig. 5 B. Although a linear relation is always obtained, the direct assessment of k_R/k_{O_2} from the slope can be erroneous depending on both k_{O_2}/k_R and n. The magnitude of these errors can be regarded through the discrepancy between the solid and the dashed lines for identical k_{O_2}/k_R (Fig. 5 A). Deviations of about 26%, 5.7% and 1.8% are observed for k_{O_2}/k_R equal to 25, 150 and 500 mol m^{-3}, respectively. On the other hand, for k_{O_2}/k_R = 150 mol m^{-3} deviations of 5.7%, 2.9% and 0.7% are observed for n equal to 18, 9, and 2, respectively.

Besides the effect of the current density on k_{app} related to the increase of the electrode surface coverage by HO radicals, the current increase can bring additional consequences related to the mass transport efficiency. The oxygen evolution leads to the formation of small bubbles at the electrode surface which produces an additional source of convection that will certainly disrupt the diffusion layer. Therefore the current density increase can lead to an increase of the mass transport rate. Two different situations can arise depending on the existence or not of a concentration polarization at the electrode surface. In the first situation the increase of current density will affect the concentration gradient, $C_R^S - C_R^E$ (where C_R^S is the bulk organics concentration), as convection will tend to homogenize solution. In opposition, when the concentration polarization can be neglected, i.e. $C_R^S = C_R^E$, k_{app} does

not depend on the diffusion rate of the organics toward the electrode and therefore the convection increase (due to oxygen bubbles formation) associated to the current density increase should not affect k_{app}.
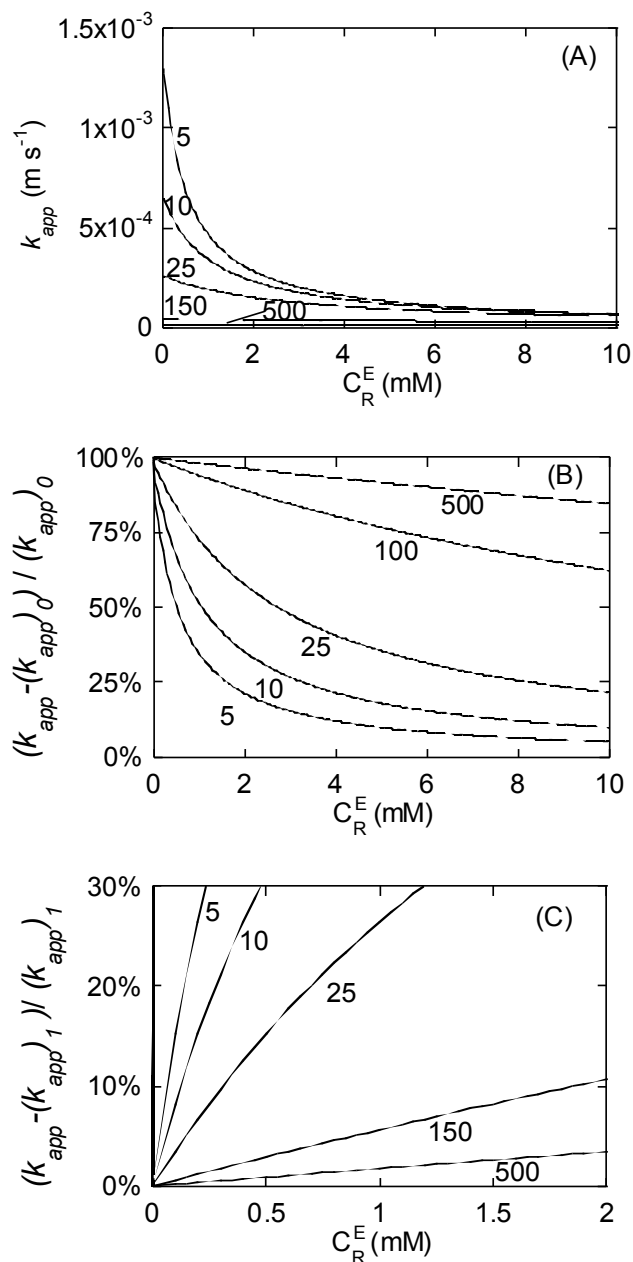
Figure 4. Effect of concentration on: (A) the apparent rate constant, k_{app}, (B) relative deviation of k_{app} from $(k_{app})_0$ and (C) relative deviation of k_{app} from $(k_{app})_1$ evaluated for $n = 18$, $i = 1250$ A m^{-2} and $k_{O_2}/k_R = 5, 10, 25, 150, 500$ mol m^{-3}.

Following the above development and considering that our experimental results followed first order kinetics, values of k_R/k_{O_2} were estimated from the experimental k_{app} of BA and of 4-HBA obtained using Pt or BDD at different current densities (Table 2). The ratio between the rate constants of the two

organic compounds, $k_{4\text{-}HBA}/k_{BA}$, for the same anode were estimated from $k_{4\text{-}HBA}/k_{O_2}$ and k_{BA}/k_{O_2} values. Although this ratio is independent of the current density it depends strongly on the anode material. For Pt (a low oxidation power anode) there is a higher ratio of $k_{4\text{-}HBA}/k_{BA}$ (= 6.8) showing that there is a considerable difference between the two rate constants, whereas for BDD (a high oxidation power anode) this ratio is lower (= 1.3).

Table 2. Values of k_{BA}/k_{O2} and *of* $k_{4\text{-}HBA}/k_{O2}$ estimated from k_{app} of BA and 4-HBA for the two anodes at different current densities. $k_{4\text{-}HBA}/k_{BA}$ corresponds to the ratio $(k_{4\text{-}HBA}/k_{O2})/(k_{BA}/k_{O2})$.

i (A m^{-2})	Pt			BDD		
	k_{BA}/k_{O_2} (10^{-3}) m^{3}mol^{-1}	$k_{4\text{-}HBA}/k_{O_2}$ (10^{-3}) m^{3}mol^{-1}	$k_{4\text{-}HBA}/k_{BA}$	k_{BA}/k_{O_2} (10^{-3}) m^{3}mol^{-1}	$k_{4\text{-}HBA}/k_{O_2}$ (10^{-3}) m^{3}mol^{-1}	$k_{4\text{-}HBA}/k_{BA}$
50	1.45±0.08	9.9±0.02	6.9	11.8±0.5	16±1	1.4
268	0.87±0.05	6±1	6.5	5.8±0.2	8±2	1.3
625	1.11±0.01	7±1	6.6	5.53±0.09	6.6±0.2	1.2
1250	0.94±0.02	6.9±0.6	7.4	5.42±0.05	7±1	1.2

It is also noticeable that the values of $k_{4\text{-}HBA}/k_{O_2}$ and k_{BA}/k_{O_2} obtained for 50 A m^{-2} are higher than those for the higher current densities. Despite this difference the value of the ratio $k_{4\text{-}HBA}/k_{BA}$ from 50 A m^{-2} is similar to those obtained from the other current densities. The fact that the lower values of $k_{4\text{-}HBA}/k_{O_2}$ and k_{BA}/k_{O_2} were obtained for the higher current densities is not expectable considering the convection increase associated to the higher rates of oxygen evolution that occurs at the higher current densities. Therefore it can be concluded that both O_2 formation and the organics reaction were not mass transport limited. Instead, this effect can be explained considering a hindrance of the electrode surface by the O_2 bubbles that is more important for higher current densities. This effect contributes to a reduction of the available anode surface leading to a decrease of k_{app}, and consequently of $k_{4\text{-}HBA}/k_{O_2}$ and k_{BA}/k_{O_2}, nonetheless the ratios $k_{4\text{-}HBA}/k_{BA}$ are not affected.
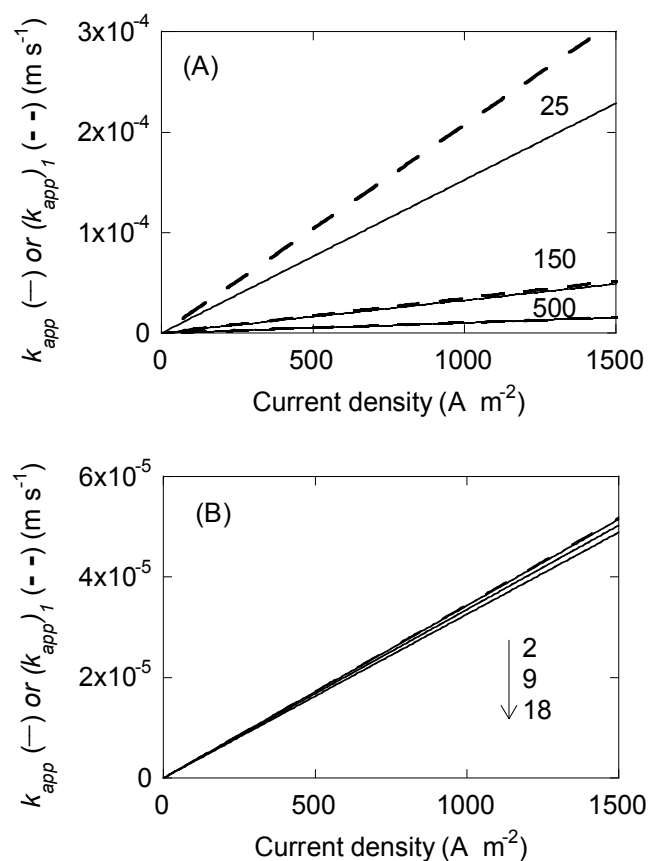
Figure 5. Effect of current density on k_{app} (solid lines) and on $(k_{app})_1$ (dashed lines) for $C_R^E = 1$ mM: (A) for $n = 18$ and $k_{O_2}/k_R = 25, 150, 500$ mol m^{-3} and (B) for $k_{O_2}/k_R = 150$ mol m^{-3} and $n = 2, 9, 18$.

4. Conclusions

The oxidation of BA and of 4-HBA by galvanostatic electrolysis with simultaneous oxygen evolution, using BDD or Pt as anode materials are examined. The products formed from the oxidation of the two organic compounds at the two anodes include hydroxylated derivatives that are typical of HO radicals reactions. The yields of hydroxylated products were rather low for BDD as compared with those obtained when the Pt anode was used. The concentration decrease of BA and of 4-HBA follows first order kinetics characterized by an apparent rate constant, k_{app}, that depends on the anode material and on the current density used in the electrolysis. The existence of a direct proportionality between k_{app} and the current density demonstrates that the reaction does not occur when the production of O_2 does not take place, despite the high potential of the anode in all experiments. Therefore it was concluded

that the oxidations of either BA or 4-HBA are started by HO radicals whose formation only takes place in conditions where O_2 is produced. A simple kinetic model that accounts for the anode surface coverage by HO radicals is proposed to interpret these results. This model predicts two limiting situations according to the magnitude of the organics concentration in comparison with the ratio of the rate constants k_{O_2}/k_R. For higher concentrations it is predicted that the rate of the organics consumption is independent of both its concentration and its reactivity, whereas for lower concentrations first order kinetics is envisaged. Based on this model the ratios k_{BA}/k_{O_2}, k_{4-HBA}/k_{O_2} and k_{4-HBA}/k_{BA} are estimated from experiments carried out with the two anode materials. The calculated reactivity ratio k_{4-HBA}/k_{BA} is higher than 1 as expected due to the higher reactivity of the hydroxylated derivative. Furthermore, a higher ratio is obtained for experiments carried out with platinum, which is also likely to occur due to the higher adsorption strength of HO radicals at this material, allowing for a better differentiation of the reactivity of organics.

Acknowledgments

References

[1]   T.F.S. Silva, K.V. Luzyanin, M.V. Kirillova, M.F.G. da Silva, L.M.D.R.S. Martins, A.J.L. Pombeiro, Novel Scorpionate and Pyrazole Dioxovanadium Complexes, Catalysts for Carboxylation and Peroxidative Oxidation of Alkanes, Advanced Synthesis & Catalysis 352 (2010) 171-187.

[2]   J.V. Hunt, R.T. Dean, S.P. Wolff, Hydroxyl Radical Production and Autoxidative Glycosylation - Glucose Autoxidation as the Cause of Protein Damage in the Experimental Glycation Model of Diabetes-Mellitus and Aging, Biochemical Journal 256 (1988) 205-212.

[3]   C. Comninellis, Electrocatalysis in the Electrochemical Conversion/Combustion of Organic Pollutants for Waste-Water Treatment, Electrochimica Acta 39 (1994) 1857-1862.

[4]   H.A. Schwarz, R.W. Dodson, Equilibrium between hydroxyl radicals and thallium(II) and the oxidation potential of hydroxyl(aq), The Journal of Physical Chemistry 88 (1984) 3643-3647.

[5]   D.T. Sawyer, J.L. Roberts, Hydroxide Ion - an Effective One-Electron Reducing Agent, Accounts of Chemical Research 21 (1988) 469-476.

[6]   M.A. Oturan, J. Pinson, Hydroxylation by Electrochemically Generated Oh Radicals - Monohydroxylation and Polyhydroxylation of Benzoic-Acid - Products and Isomers Distribution, Journal of Physical Chemistry 99 (1995) 13948-13954.

[7]   L.M. Dorfman, Reactivity of the hydroxyl radical in aqueous solutions [electronic resource] / Leon M. Dorfman and Gerald E. Adams, U.S. Dept. of Commerce, National Bureau of Standards, [Washington, D.C.] :, 1973.

[8]   J.A. Simpson, K.H. Cheeseman, S.E. Smith, R.T. Dean, Free-Radical Generation by Copper Ions and Hydrogen-Peroxide - Stimulation by Hepes Buffer, Biochemical Journal 254 (1988) 519-523.

[9]   A. Ventura, G. Jacquet, A. Bermond, V. Camel, Electrochemical generation of the Fenton's reagent: application to atrazine degradation, Water Research 36 (2002) 3517-3522.

[10] A. Kapalka, G. Foti, C. Comninellis, The importance of electrode material in environmental electrochemistry Formation and reactivity of free hydroxyl radicals on boron-doped diamond electrodes, Electrochimica Acta 54 (2009) 2018-2023.

[11] C.A. Martinez-Huitle, E. Brillas, Decontamination of wastewaters containing synthetic organic dyes by electrochemical methods: A general review, Applied Catalysis B-Environmental 87 (2009) 105-145.

[12] C.A. Martinez-Huitle, F. Hernandez, S. Ferro, M.A.Q. Alfaro, A. de Battisti, Electrochemical oxidation: An alternative for the wastewater treatment with organic pollutants agents, Afinidad 62 (2006) 26-34.

[13] C. Borras, C. Berzoy, J. Mostany, J.C. Herrera, B.R. Scharifker, A comparison of the electrooxidation kinetics of p-methoxyphenol and p-nitrophenol on Sb-doped SnO2 surfaces: Concentration and temperature effects, Applied Catalysis B: Environmental 72 (2007) 98-104.

[14] P.G. Keech, N.J. Bunce, Electrochemical oxidation of simple indoles at a PbO2 anode, Journal of Applied Electrochemistry 33 (2003) 79-83.

[15] J. Iniesta, P.A. Michaud, M. Panizza, G. Cerisola, A. Aldaz, C. Comninellis, Electrochemical oxidation of phenol at boron-doped diamond electrode, Electrochimica Acta 46 (2001) 3573-3578.

[16] A. Kapalka, G. Foti, C. Comninellis, Kinetic modelling of the electrochemical mineralization of organic pollutants for wastewater treatment, Journal of Applied Electrochemistry 38 (2008) 7-16.

[17] O. Simond, V. Schaller, C. Comninellis, Theoretical model for the anodic oxidation of organics on metal oxide electrodes, Electrochimica Acta 42 (1997) 2009-2012.

[18] F. Montilla, P.A. Michaud, E. Morallon, J.L. Vazquez, C. Comninellis, Electrochemical oxidation of benzoic acid at boron-doped diamond electrodes, Electrochimica Acta 47 (2002) 3509-3513.

[19] J.E. Baur, in: C.G. Zoski (Ed.), Handbook of Electrochemistry, Elsevier B.V, Amsterdam, 2007, pp. 829-848.

[20] I. Loeff, A.J. Swallow, On Radiation Chemistry of Concentrated Aqueous Solutions of Sodium Benzoate, Journal of Physical Chemistry 68 (1964) 2470-&.

[21] G.W. Klein, K. Bhatia, V. Madhavan, R.H. Schuler, Reaction of Oh with Benzoic-Acid - Isomer Distribution in Radical Intermediates, Journal of Physical Chemistry 79 (1975) 1767-1774.

[22] A.M. Downes, The Radiation Chemistry of Aqueous Solutions of [C-14]Benzoic and [C-14]Salicylic Acids, Australian Journal of Chemistry 11 (1958) 154-157.

[23] H.G.C. Bates, N. Uri, Oxidation of Aromatic Compounds in Aqueous Solution by Free Radicals Produced by Photo-Excited Electron Transfer in Iron Complexes, Journal of the American Chemical Society 75 (1953) 2754-2759.

[24] C.R.E. Jefcoate, J.R.L. Smith, R.O.C. Norman, Hydroxylation. Part IV. Oxidation of some benzenoid compounds by Fenton's reagent and the ultraviolet irradiation of hydrogen peroxide, Journal of the Chemical Society B: Physical Organic (1969) 1013-1018.

[25] M.A. Oturan, J. Pinson, Hydroxylation by Electrochemically Generated OH.bul. Radicals. Mono- and Polyhydroxylation of Benzoic Acid: Products and Isomer Distribution, The Journal of Physical Chemistry 99 (1995) 13948-13954.

[26] T. Velegraki, D. Mantzavinos, Conversion of benzoic acid during TiO2-mediated photocatalytic degradation in water, Chemical Engineering Journal 140 (2008) 15-21.

[27] T. Velegraki, G. Balayiannis, E. Diamadopoulos, A. Katsaounis, D. Mantzavinos, Electrochemical oxidation of benzoic acid in water over boron-doped diamond electrodes: Statistical analysis of key operating parameters, kinetic modeling, reaction by-products and ecotoxicity, Chemical Engineering Journal 160 (2010) 538-548.

[28] B. Louhichi, N. Bensalash, A. Gadri, Electrochemical oxidation of benzoic acid derivatives on boron doped diamond: Voltammetric study and galvanostatic electrolyses, Chemical Engineering & Technology 29 (2006) 944-950.

[29] R.M. Souto, J.L. Rodriguez, L. Fernandez-Merida, E. Pastor, Electrochemical reactions of benzoic acid on platinum and palladium studied by DEMS. Comparison with benzyl alcohol, Journal of Electroanalytical Chemistry 494 (2000) 127-135.

[30] M.I. Pariente, F. Martinez, J.A. Melero, J.A. Botas, T. Velegraki, N.P. Xekoukoulotakis, D. Mantzavinos, Heterogeneous photo-Fenton oxidation of benzoic acid in water: Effect of operating conditions, reaction by-products and coupling with biological treatment, Applied Catalysis B-Environmental 85 (2008) 24-32.

[31] G. Foti, C. Comninellis, Electrochemical oxidation of organics on iridium oxide and synthetic diamond based electrodes, in: R. White (Ed.), Modern Aspects of Electrochemistry, New York: Plenum Press, 2004, pp. 87-130.

4 Reactivity of hydroxy-containing aromatic compounds towards electrogenerated hydroxyl radicals

Raquel Oliveira, Nelson Pereira, Fátima Bento*, Dulce Geraldo

Department of Chemistry, Universidade do Minho, Campus de Gualtar 4710-057, Portugal

* Corresponding author T: +351 253604399; e-mail: fbento@quimica.uminho.pt

Abstract

A kinetic study on the oxidation of hydroxy-containing aromatic compounds by electrogenerated HO radical and simultaneous by direct electron transfer is presented. First order kinetics are used to describe consumption rates of hydroquinone, benzoic acid and of hydroxybenzoic acid derivatives by galvanostatic electrolysis with simultaneous oxygen evolution at a Pt electrode. Linear correlations were established from the effect of electrolyses current density on k_{app}. The meaning of the intercept and of the slope is analysed. A good agreement is found between intercept values and the apparent rate constants from potentiostatic electrolysis without O_2 evolution. Simultaneously, the slopes magnitude corroborate the relative reactivity order of species that was established considering the occurrence of positive charge densities on carbon atoms of the aromatic ring. Therefore, the present analysis provides kinetic information concerning both, the direct electron-transfer and the reaction with HO radical.

Keywords

1. Introduction

Electrochemical methods have proved to be adequate for the destruction of organics in aqueous media. A significant number of researchers has sought new electrode materials and improved reactors design to optimize mineralization indexes. Boron-doped diamond (BDD) was the most used anode material for this purpose [1–7], allowing to an efficient decrease of the TOC (total organic content) of aqueous solutions containing test compounds, such as phenol [8,9], benzoic acid [10,11], bisphenol A [12] or gallic acid [13]. The efficiency of organics destruction, by means of their electrooxidation with simultaneous oxygen evolution, was attributed to the formation of HO radicals as intermediaries of water electrooxidation [14–16]. The formation of this radical was detected in assays using anodes of Ti/IrO_2, Ti/SnO_2 and Pt using a radical trap [15]. The following mechanism was proposed for the oxidation of organics mediated by HO radicals [17].

$$H_2O \xrightarrow{k_{HO}} HO^\cdot + H^+ + e^- \tag{1}$$

$$2\,HO^\cdot \xrightarrow{k_{O_2}} O_2 + 2H^+ + 2e^- \tag{2}$$

$$R + nHO^\cdot \xrightarrow{k_{R,HO}} products \tag{3}$$
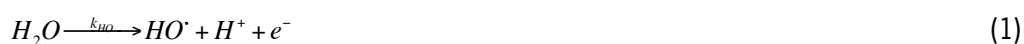
The adsorption of HO radicals at the anode surface has a significant effect on their reactivity. When they are strongly adsorbed they display lower reactivity, as it happens for Pt or IrO_2, whereas when the adsorption strength is weak, as it happens for BDD, the reactivity of electrogenerated radicals is important [7].

Although most of the available studies deal with high oxidation power anodes, the use of anodes with low oxidation power can have important applications particularly when a certain degree of selectivity is required for oxidation.

In a previous work [18] we have reported a kinetic study on the oxidation of two compounds (BA and 4-HBA) using BDD and Pt, where it was shown that consumption of species occurred mainly by reaction with electrogenerated HO radicals. Based on these results, a kinetic treatment was presented, considering the relative magnitude of the organics concentration towards $k_{R,HO}/k_{O_2}$, that allows the interpretation of concentrations decay during galvanostatic electrolysis.

In this work, a kinetic study on aromatic compounds oxidation by electrogenerated HO radical with simultaneous direct electron transfer is presented. The possibility of extending our previous analysis to electroactive compounds is quite relevant as a great number of organic compounds is electroactive, particularly the model compounds used in mineralization studies. Compounds used in this work were

selected regarding the direct electron transfer reaction features namely, the number of electrons involved (one or two) and the stability of the formed products (semiquinone radical or quinones). Kinetic data is analysed considering the presumed reactivity of these species suggested from charge density values on carbon atoms of the aromatic ring.

2. Experimental

2.1. Chemicals

All reagents employed were of analytical grade: benzoic acid (BA; Prolabo), 4-hydroxybenzoic acid (4-HBA; BDH Chemicals), 2,3-dihydroxybenzoic acid (2,3-HBA; ACROS Organics), 2,4-dihydroxybenzoic acid (2,4-HBA; ACROS Organics), 2,5-dihydroxybenzoic acid (2,5-HBA; ACROS Organics), 3,4,5-trihydroxybenzoic acid (3,4,5-HBA; Sigma), hydroquinone (HQ; May & Baker, Ltd), potassium chloride (Fluka), potassium ferrocyanide and potassium ferricyanide (José Gomes Santos), potassium dihydrogen phosphate and phosphoric acid (ACROS Organics). Methanol was of HPLC grade from Fisher Scientific.

2.2. HPLC

Oxidation reactions were monitored following the concentration decrease along galvanostatic electrolyses by HPLC. HPLC experiments were performed using a Jasco, PU-2080 Plus system equipped with a RP 18 column from Grace Smart (250 mm × 4.6 mm, 5 µm particle size) and using Clarity HPLC software from Jasco (Jasco 870 / UV detector). A flow rate of 0.6 ml min^{-1} and a loop of 20 µl were used. A mixture of methanol, water and phosphoric acid (60:39:1) (v/v) was used as mobile phase. The detection wavelength was selected according to species: 210 nm for 2,3-HBA and 2,4-HBA; 230 nm for BA, 4-HBA and 2,5-HBA; and 280 nm for 3,4,5-HBA and HQ. The quantification was performed using calibration curves.

2.3. Electrochemical measurements

Voltammetric measurements and galvanostatic / potentiostatic electrolyses were performed using a potentiostat (Autolab type PGSTAT30, Ecochemie) controlled by GPES 4.9 software provided by Ecochemie.

2.3.1. Cyclic voltammetry

Cyclic voltammetry experiments were carried out from -0.25 to 1.4 V using an undivided three-electrode cell. The working electrodes were of glassy carbon (GC; 3 mm diameter disk electrode, CHI104, CH Instruments, Inc.) and of Pt (EM-EDI, Radiometer Analytical). An Ag /AgCl, 3.0 M (CHI111, CH Instruments, Inc.) was used as reference electrode and a Pt wire as counter electrode. The surface of the GC electrode was cleaned between scans by polishing with polycrystalline diamond suspension (3F μm; Buehler) for ≈1 min. The Pt electrode was electrochemically cleaned in 0.10 M phosphate buffer pH 3.5 at the oxygen evolution region (0.02 A) during 600 s.

2.3.2. Electrolysis

Galvanostatic electrolyses were carried out using current densities from 50 to 1250 A m^{-2} in a two compartments cell separated by a glass frit membrane. The volume of the anodic compartment was 9.0 ml and the solution was mechanically stirred with a magnetic stir bar (300 rpm). The anode is made of a piece (20 mm × 10 mm) of Pt gauze (52 mesh woven from 0.1 mm diameter wire, 99.9%, from Alfa Aesar). Before each experiment the anode was cleaned electrochemically in 0.1 M phosphate buffer pH 3.5 during 600 s at a constant current of 0.02 A. The area of the Pt working electrode (5.6 cm^2) was determined in a chronoamperometry experiment using 1.00 mM of $K_3[Fe(CN)_6]$ in 0.1 M KCl [19].

Reported apparent rate constants from oxidation of hydroxybenzoic acid derivatives and of HQ were determined using data of at least two electrolyses and displayed uncertainties correspond to standard deviations.

2.4. Diffusion coefficients

Diffusion coefficients (D) were estimated from the slope of I_p vs. $v^{1/2}$ (regarding voltammetric data from 20 to 100 mV s^{-1}) for hydroxybenzoic acids derivatives whose first oxidation peaks involve a single electron. α values were estimated considering (E_p-$E_{p/2}$) = 48 / (α n) (Table 1). The number of electrons of the first oxidation peak in Table 1 were obtained from literature [20–23]. As the homogeneous rate constants were not known, the selection of the scan rates was based on the fit to a linear dependence

of I_p and $v^{1/2}$ in order to discard a pure kinetic behaviour (low scan rates) or distortions due to the capacitive current (higher scan rates). Despite a pure diffusion behavior is not assured the introduced uncertainty is known to be low for EC processes [24]. Validation of determined D values cannot be performed as there are not available D values for most of the compounds analysed. For 3,4,5-HBA the calculated value of D is in agreement with that reported elsewhere based on simulation results [22,25] with a deviation of 5%. Reported uncertainties were calculated using the standard deviation of the slope of I_p vs. $v^{1/2}$.

Table 1: Voltammetric data (regarding the first oxidation peak) of the different hydroxybenzoic acid derivatives, hydroquinone and of potassium hexacyanoferrate estimated from results in Figure 1. Diffusion coefficients of species whose first oxidation peak involves a single electron were determined by from the slope of I_p vs. $v^{1/2}$.

	E_p (V)	I_p (10^{-6}A)	E_p - $E_{p/2}$ (mV)	E_p^a - E_p^c (mV)	n	α	D (10^{-5} cm^2 s^{-1})
4-HBA	1.002 ± 0.004	7.36 ± 0.02	78	–	1 [20]	0.62	3.5 ± 0.1
2,3-HBA	0.496 ± 0.007	10.54 ± 0.07	69	–	1 [21]	0.70	3.6 ± 0.6
2,4-HBA	0.996 ± 0.006	9.56 ± 0.04	74	–	1 [20]	0.65	3.8 ± 0.3
2,5-HBA	0.430 ± 0.004	8.75 ± 0.04	51	135	2 [27]	a)	–
3,4,5-HBA	0.527 ± 0.001	7.72 ± 0.03	73	–	1 [22]	0.66	3.7 ± 0.2
HQ	0.477 ± 0.004	5.91 ± 0.03	71	288	2 [23]	a)	–
$[Fe(CN)_6]^{4-}$	0.281 ± 0.001	3.07 ± 0.02	60	65	1 [24]	b)	0.77 ± 0.03

a) ECEC mechanism

b) reversible electron transfer

2.5. Hydrodynamics characterization of the electrolysis cell

The mass transport efficiency of the electrochemical cell was characterized by analysis of j - t curves from electrolyses (1.2 V) of 0.50 mM K$_4$[Fe(CN)$_6$] in 0.15 M phosphate buffer pH 3.5 (Eq. (4)) [24] .

$$\frac{j}{j_0} = \exp\left(-\frac{k_{app} A}{V} t\right)$$

(4)

where, A is the anode surface area, V is the volume of the solution in the anodic compartment, k_{app} is the apparent rate constant that characterizes the consumption of the substrate and t is time. As oxidation of $[Fe(CN)_6]^{4-}$ is a very fast one-electron transfer, the process is mass transport controlled and therefore $k_{app} = k_m$:

$$k_m = \frac{D}{\delta}$$ (5)

where, k_m is the mass transport coefficient and δ is the diffusion-layer thickness.

From Eq. (5) $\delta = 2.53 \times 10^{-3}$ cm was determined using $k_m = 3.04 \times 10^{-3}$ cm s^{-1} (evaluated from j - t curve of potentiostatic electrolysis) and $D = 7.7 \times 10^{-6}$ cm^2 s^{-1} (from voltammograms recorded in 0.15 M phosphate buffer pH 3.5 and using Cottrell equation). Calculated values of D for $[Fe(CN)_6]^{4-}$ is in agreement with that reported [22,25].

2.6. Charge density calculations

Charge density values were calculated using MarvinSketch, a Java based chemical editor, provided by platform ChemAxon. Representation of molecules was drawn also using MarvinSketch.

3. Results and discussion

Electrogeneration of HO radicals from water occurs at potentials higher than those required for oxidation of most hydroxybenzoic acid derivatives, therefore it is expected that their direct oxidation occurs simultaneously with the oxidation via HO radicals. Characterization of voltammetric response of these compounds is consequently relevant for interpretation of their oxidation kinetics.

3.1 Cyclic voltammetry and potentiostatic electrolysis

Cyclic voltammetry of 4-HBA, 2,3-HBA, 2,4-HBA, 2,5-HBA, 3,4,5-HBA and HQ in phosphate buffer pH 3.5 was carried out at Pt and GC electrodes. Voltammograms of BA (both at Pt and at GC) and of 4-HBA (at Pt) are not significantly different from those of blank solution. For the other compounds, voltammograms recorded at Pt electrode are not well defined due to Pt oxide formation current (not shown). Fig. 1 reports voltammetric responses of 4-HBA, 2,3-HBA, 2,4-HBA, 2,5-HBA and 3,4,5-HBA at a GC electrode in phosphate buffer pH 3.5. Voltammogram of HQ is also reported in Fig. 1 as a reference compound. Table 1 contains voltammetric data from the first oxidation process (Ip, Ep, Ep-Ep/2 and Epa-Epc) as well as experimental values of D (section 2.4).Oxidation of the monohydroxybenzoic acid, 4-HBA, corresponds to a single electron transfer [20]. The peak potential, Ep, is very positive as compared to HQ peak potential and no significant reverse peak is noticeable The

oxidation process is assigned to the formation of a semiquinone and is accomplished by the abstraction of a proton. The semiquinone radical is very unstable and therefore its formation is followed by other reactions, including dimerization and polymerization [20,26].

Polyhydroxybenzoic acids with two or more HO groups can be oxidized by one or more electrons. This is clearly observed in the voltamograms of 2,3-HBA and of 3,4,5-HBA where the HO groups are in *ortho* position in respect to each other. In this configuration the semiquinone radical formed by the first electron-transfer reaction is further oxidized to quinone in a second process [21,22]. In this case the first oxidation is rather facilitated and occurs at a low potential, comparable to that of HQ. Nevertheless, no reverse.

peak is observed. Voltammogram of 2,4-HBA also displays two peaks (partially overlapped) that can correspond to two successive electron transfer processes. The first oxidation peak occurs at a potential comparable to that of 4-HBA and superior to that of 2,3-HBA and to that of 3,4,5-HBA. The HO groups in 2,5-HBA are located in *para* position in respect to each other, like in HQ and both compounds are oxidized in a single step involving the transfer of 2 electrons accomplished by the abstraction of 2 protons [23,27]. Although the processes are irreversible by an electrochemical perspective the formed quinone can be reduced back in the reverse scan.

As global trend, it can be remarked that voltammograms of species that enable the formation of a *para*-quinone (as for 2,5-HBA and HQ) display a single oxidation process with a reverse peak, while when a *ortho*-quinone can be formed oxidation occurs by two one-electron processes and without reverse peak (as for 2,3-HBA and 3,4,5-HBA). In both cases (formation of *ortho* or *para*-quinone) the first peak potential is rather low compared to that of species that do not afford the formation of quinones (as for 4-HBA and 2,4-HBA).

Potentiostatic electrolysis were carried out with BA, 4-HBA, 2,4-HBA, 2,3-HBA, 2,5-HBA, 3,4,5-HBA and HQ at 1.2 V. This potential is much higher than the peak potential of these species (of voltammograms recorded in carbon electrodes) but is lower than the required for oxygen evolution. Concentration decrease was monitored by HPLC and apparent rate constants were determined according to Eq. (6) that is characteristic of 1st order kinetics:

$$\frac{C}{C_0} = \exp\left(-\frac{k_{app} A}{V} t\right) \tag{6}$$

where, C is the concentration at a given time and C_0 is the initial concentration. Calculated values for the apparent rate constant for 2,3-HBA, 2,5-HBA, 3,4,5-HBA and HQ are presented in Table 2 as k^0_{app}. For BA and for 4-HBA current dropped to zero almost at the start of potentiostatic electrolysis,

indicating that electron transfer reaction did not occur at Pt. For 2,4-HBA an abrupt drop of current was observed at the first instants of potentiostatic electrolysis due to anode passivation probably due to formation of polymers at the electrode surface. Values of k_m calculated by means of Eq. (5), using D values reported in Table 1, are much higher than experimental k^0_{app} values (Table 2). The difference between these two parameters is quite significant and cannot be assigned to the inaccuracy of D values related to the presence of the coupled chemical reaction as previously discussed. The discrepancy between k_m and k^0_{app} provide a strong evidence that the electron transfer rate is low at the present conditions and the electrolysis rate is not limited by mass transport.

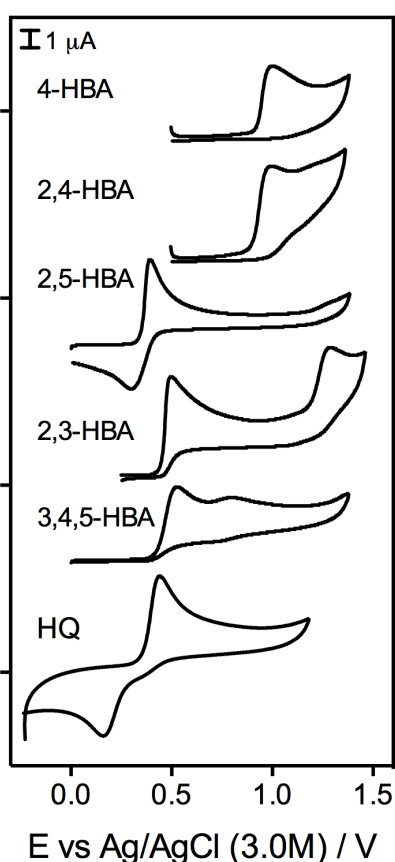**Figure 1:** Cyclic voltammograms (from top to bottom) of 0.50 mM 4-HBA, 2,4-HBA, 2,5-HBA, 2,3-HBA, 3,4,5-HBA and HQ in 0.15 M phosphate buffer solution pH 3.5, recorded at 20 mV s^{-1} using a GC electrode.

3.2 Galvanostatic electrolysis

Galvanostatic electrolyses of BA, hydroxybenzoic acid derivatives and of HQ (0.50 mM) in 0.15 M phosphate buffer pH 3.5 using Pt anode were conducted at a current density of 1250 A m^{-2} with

simultaneous oxygen evolution. Concentration decrease, expressed by means of the concentrations ratio C/C_0, was quantified by HPLC and is plotted against electrolysis time. Values of concentration decrease of BA and of 3,4,5-HBA are presented in Fig. 2. Curves displayed are fitted to experimental data considering Eq. (6).

Table 2: Apparent rate constants from potentiostatic electrolysis (k^0_{app}) and from galvanostatic electrolysis (k_{app}) at different current densities. Values of $(k_{app})_{j=0}$ correspond to the intercept of the straight lines in Fig. 4. The mass transport coefficient values (k_m) reported were calculated using $\delta = 2.53 \times 10^{-5}$ m (according to results from $[Fe(CN)_6]^{4-}$ reported in section 2.5.) and the diffusion coefficients of Table 1.

	1.2 V		50 (A m⁻²)	268 (A m⁻²)	625 (A m⁻²)	1250 (A m⁻²)	
	k^0_{app} (10^{-6} m s⁻¹)	$(k_{app})_{j=0}$ (10^{-6} m s⁻¹)	k_{app} (10^{-6} m s⁻¹)				k_m (10^{-6} m s⁻¹)
BA	a)	-0.3 ± 0.5	0.38 ± 0.05	1.21 ± 0.06	3.60 ± 0.03	6.10 ± 0.01	c)
4-HBA	a)	-0.1 ± 1.2	2.57 ± 0.06	8 ± 1	24 ± 4	45 ± 4	138 ± 21
2,3-HBA	18.2 ± 0.6	21 ± 1	21.1 ± 0.5	30 ± 2	37 ± 4	52 ± 3	142 ± 31
2,4-HBA	b)	9.8 ± 0.2	11 ± 2	22 ± 1	41 ± 3	67 ± 3	150 ± 26
2,5-HBA	19.0 ± 0.5	21.5 ± 0.7	22 ± 2	27 ± 3	34 ± 3	46 ± 2	d)
3,4,5-HBA	30 ± 8	30 ± 2	32 ± 2	39 ± 3	45 ± 4	66 ± 6	146 ± 23
HQ	38.2 ± 0.4	38 ± 1	39.6 ± 0.3	47 ± 1	53 ± 2	73 ± 4	d)

a) no faradaic current was measured
b) not possible to measure due to the anode passivation during potentiostatic electrolysis.
c) not determined as no voltammetric response was obtained.
d) not calculated as the 1st peak corresponds to a ECEC mechanism.

Concentrations decrease of 3,4,5-HBA can be assigned to its oxidation by electrogenerated HO radicals and also by direct electron-transfer, while for BA is mainly due to oxidation by HO radicals (as there is no evidence of direct electron transfer by voltammetric studies). Experimental k_{app} value of 3,4,5-HBA

$(66 \times 10^{-6}$ m s^{-1}) is quite different from that of BA $(6.10 \times 10^{-6}$ m s^{-1}) and is considerable lower than the calculated mass transport coefficient, k_m $(146 \times 10^{-6}$ m s^{-1}). Values of k_m are much higher than experimental k_{app} values for all the analyzed hydroxybenzoic acid derivatives (Table 2). If the process was controlled by mass transport k_{app} values should be higher than the calculated k_m values using the δ obtained from potentiostatic electrolyses without O$_2$ evolution. Due to bubbles formation, convection is increased and thus δ must be thinner, what would imply a higher mass transport efficiency, in opposition to what is observed. These results provide an unequivocal indication that k_{app} is not limited by mass transport. Instead k_{app} provides a measure of the rate of whole oxidation reactions associated to the consumption of species, by direct electron transfer and by electrogenerated HO radicals.
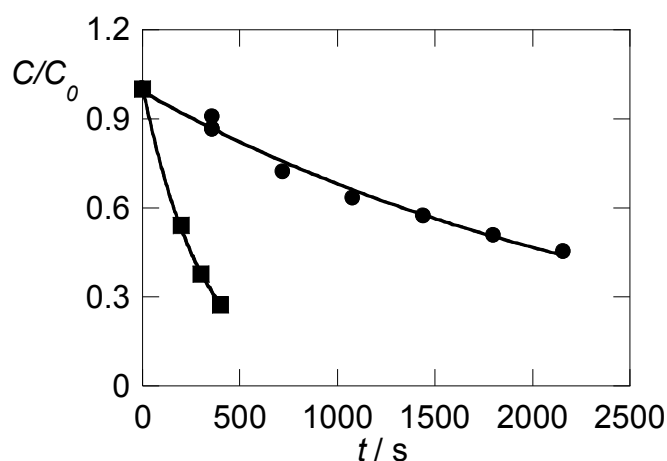

Figure 2: Concentration decrease during galvanostatic electrolyses (Pt anode at 1250 A m^{-2}) of 0.50 mM solutions: (●) BA $(C/C_0 = \exp((-3.8 \pm 0.1) \times 10^{-4}\ t)$, r = 0.99) and (■) 3,4,5-HBA $(C/C_0 = \exp((-3.6 \pm 0.2) \times 10^{-3}\ t)$, r = 0.99). Equations and curves were obtained by regression analysis.

3.3 Current density effect

The effect of current density on the consumption of 2,4-HBA is illustrated in Fig. 3, where C/C_0 values against time are reported for 50, 268, 625 and 1250 A m^{-2}. All galvanostatic electrolyses were performed with simultaneous O$_2$ evolution. Experimental k_{app} values are reported in Table 2 together with the corresponding values of other hydroxybenzoic acid derivatives and of HQ. An increase of k_{app} with current density is evident for all the compounds studied. The origin of this variation cannot be attributed to an increase of mass transport rate associated to a raise of oxygen bubbles formation as the processes are not mass transport limited, as explained in the previous section. Therefore this variation must be related to the kinetic variables that control the oxidation rates of these compounds.

As consumption of hydroxybenzoic acid derivatives can be due to direct electron transfer as well as to reaction with HO radicals, Eq. (7) must be considered in addition to Eq. (3):

$$R - ne^- \xrightarrow{k_{R,e}} products \tag{7}$$

Therefore the rate of consumption of species results from the contribution of these two processes:

$$v_R = v_{R,HO} + v_{R,e} \tag{8}$$

where $v_{R,HO}$ is the rate of the reaction with HO radicals and $v_{R,e}$ is the rate of the oxidation by electron transfer. Eq. (8) can be rewritten as:

$$v_R = (k_{R,HO}\,\theta\,\Gamma_s + k_{R,e})\,C_R \tag{9}$$

where, $k_{R,HO}$ is the apparent rate constant of the reaction with HO radicals (Eq. (3)), $\theta\,\Gamma_s$ is the HO radical surface concentration at the anode, $k_{R,e}$ is the electron transfer rate constant (Eq. (7)) and C_R is the concentration of the species. Hence k_{app} in Eq. (6) corresponds to:

$$k_{app} = k_{R,HO}\,\theta\,\Gamma_s + k_{R,e} \tag{10}$$

Analysis of k_{app} variation with current density must take into account the effect of j on each variable in Eq. (10). Whereas $k_{R,HO}$ and Γ_s (saturation concentration of HO radicals) should not be affected by current density, the anode coverage degree, θ, and the heterogeneous rate constant $k_{R,e}$ can depend on it.

The heterogeneous rate constant $k_{R,e}$ may increase with current density if the reaction is not diffusion limited as it is the present case. Although in voltammetric experiments a diffusion control regime was achieved for all species for $E > 1.04$ V, in electrolysis a diffusion control regime was not attained because the diffusion layer is thinner due to forced convection. Therefore the increase of $k_{R,e}$ may occur if the anode potential increases with j. Indeed, when current density is varied from 50 to 268 A m^{-2} the potential increase is not negligible in opposition to what happens for the subsequent variations of current density (from 268 to 628 and from 628 to 1250 A m^{-2}) as the slope of E - j curves tend to zero for $j \geq 268$ A m^{-2} (results not shown). Thus variation of $k_{R,e}$ could only explain an increase of k_{app} for the lower concentration densities. However, as the augmentation of k_{app} is considerable for higher current densities, the variation of $k_{R,e}$ cannot be overall justified by $k_{R,e}$ increase.

On the other hand, the rate of formation of HO radicals (Eq. (1)) is controlled by j [28]:

$$v_{HO^\cdot} = \frac{j}{z\mathrm{F}} \tag{11}$$

Furthermore, in conditions of low C_R it was demonstrated that [18]:

$$\theta\Gamma_s = \frac{j}{2z\mathrm{F}k_{O_2}} \tag{12}$$

116

where, k_{O_2} is the rate constant of O_2 formation (Eq. (2)).

From Eq. (12) it is expected that the surface concentration of HO radicals increases steadily with j. As a consequence of this concentration increase, and based on Eq. (10) it is foreseen a linear variation of k_{app} with j:

$$k_{app} = \frac{1}{2zF} \frac{k_{R,HO}}{k_{O_2}} j + k_{R,e} \tag{13}$$

The observation of this linear trend implies that $k_{R,e}$ does not vary significantly with j.
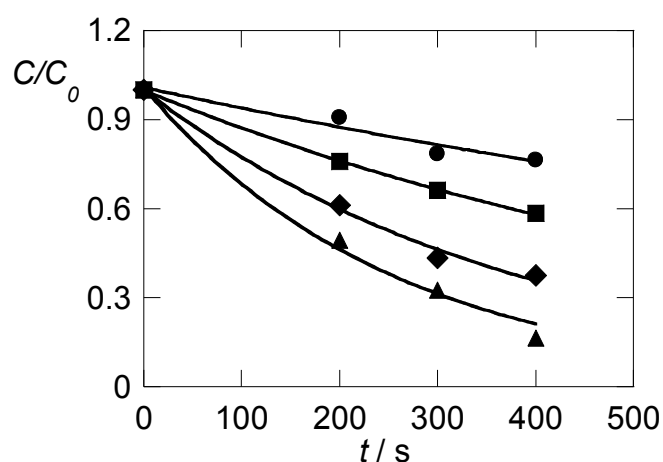

Figure 3: Concentration decrease during galvanostatic electrolyses of 2,4-HBA ($C_0 = 0.50$ mM) at a Pt anode: (●) 50 A m^{-2} ($C/C_0 = \exp ((-0.7 \pm 0.1) \times 10^{-3} t)$, r = 0.99), (■) 268 A m^{-2}, ($C/C_0 = \exp ((-1.36 \pm 0.02) \times 10^{-3} t)$, r = 0.999), (◆) 628 A m^{-2}, ($C/C_0 = \exp ((-2.6 \pm 0.2) \times 10^{-3} t)$, r = 0.99) and (▲)1250 A m^{-2}, ($C/C_0 = \exp ((-3.9 \pm 0.5) \times 10^{-3} t)$, r = 0.99). Equations and curves were obtained by regression analysis.

3.4 Correlation between apparent rate constant and current density

In Fig. 4 the apparent rate constant of BA, hydroxybenzoic acid derivatives and of HQ are plotted against current density. Open symbols (k^0_{app}) correspond to potentiostatic electrolyses (E = 1.2 V), whereas solid symbols (k_{app}) correspond to galvanostatic electrolyses. Straight lines were obtained from regression analysis considering only k_{app} values.

Plots in Fig. 4 for all species display linear trends of k_{app} vs. j as predicted by Eq. (13). The magnitudes of the intercept differ significantly among them. While a null intercept is found for BA and 4-HBA, noteworthy intercepts are found for all the other species. The origin of the intercept can be explained as follows. As current density approaches zero the amount of O_2 produced vanishes and no HO radicals will be generated; therefore the oxidation reaction will only take place by direct electron transfer. The

fact that zero intercepts are found for BA and 4-HBA means that no significant consumption of these species is observed in the absence of HO radicals, which is consistent with the absence of a voltammetric response at Pt. Besides, the match between the straight lines intercept and k^0_{app} values from potentiostatic electrolysis (open symbols) provides a clear evidence that the intercept is a measure of the apparent rate constant of oxidation via direct electron transfer. The similarity between the experimental (k^0_{app}) and extrapolated $(k_{app})_{j=0}$ (Fig. 4(a) and Table 2) is also an evidence that $k_{R,e}$ was not significantly affected by current density increase (see section 3.3).

The meaning of the slope of k_{app} vs. j was thoroughly discussed by us in a previous work considering different conditions (i.e. different magnitude of C_R wi $k_{R,HO} / (2zF k_{O_2})$ th regard to $k_{O_2} / k_{R,HO}$) [18]. In brief, the slope is a measure of the degree of susceptibility of k_{app} to an increase of HO radicals concentration at the anode, that is related to the relative magnitude of $k_{R,HO}$ towards k_{O_2} .

When pseudo-first order kinetics is achieved (characterized by a logarithmic concentration decay along time) the slope of k_{app} vs. j is given by $k_{R,HO} / (2zF k_{O_2})$ (Eq. (13)). Values of $k_{R,HO} / k_{O_2}$ displayed in Table 3 were calculated from slopes of plots in Fig. 4.

Analysis of the intercept and slope contributions to k_{app} can provide important insight on the reactivity of the species accordingly to the meaning of each parameters.

3.5. Kinetic data analysis

As discussed in sections 3.3 and 3.4 the rates of consumption of all species are much below the calculated values assuming mass transport control (Table 2), demonstrating that important kinetic hindrances are present.

Regarding the contribution of direct electron transfer reaction for the global oxidation, evaluated through the extrapolated $(k_{app})_{j=0}$, the obtained values depended on the nature of species. Moreover, a correlation of 0.87 was observed between $(k_{app})_{j=0}$ and the reciprocal of E_p. This serendipitous correlation can be explained considering that both variables are affected by a common parameter, i.e. the exchange current density (j_0). Low j_0 values can be at the origin of high E_p and simultaneously of low electron transfer rates. 4-HBA and 2,4-HBA display simultaneously the higher E_p and the lower $(k_{app})_{j=0}$, at the same time 2,3-HBA, 2,5-HBA, 3,4,5-HBA and HQ exhibit lower E_p and have higher values of $(k_{app})_{j=0}$. A better correlation between these two variables is difficult to attain since potential parameters reflect not only the kinetic but also the thermodynamic properties of a system [29], whereas $(k_{app})_{j=0}$ reflects exclusively kinetic features.
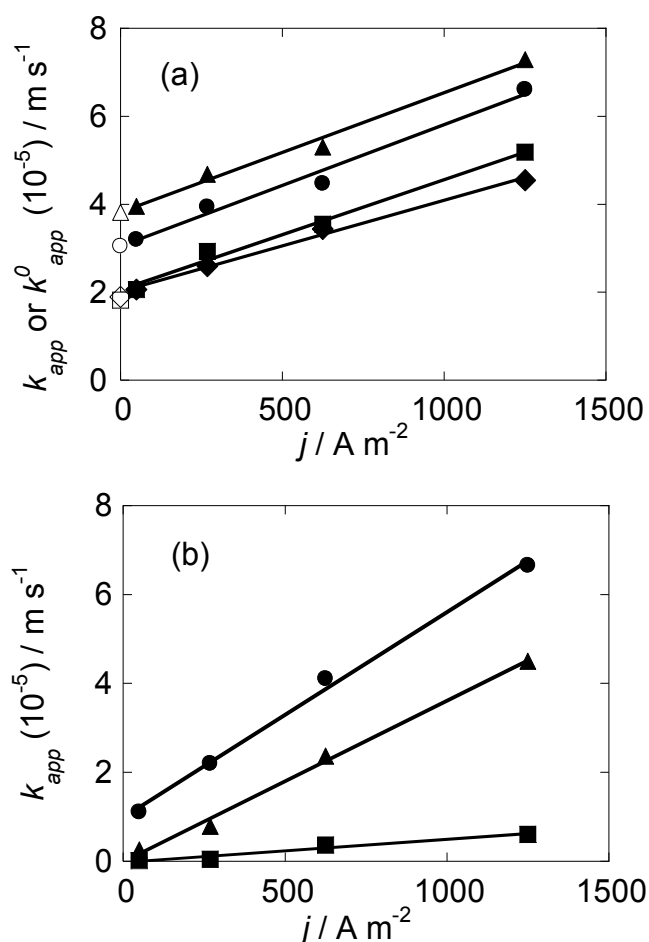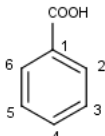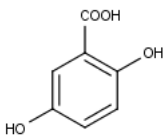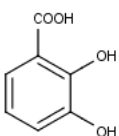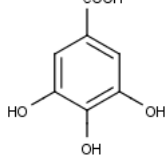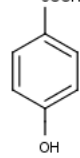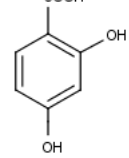
Figure 4: Effect of current density on the rate of consumption of: (a) (●) 3,4,5-HBA, (■) 2,3-HBA, (◆), 2,5-HBA, (▲) HQ; (b) (■) BA, (▲) 4-HBA, (●) 2,4-HBA. Solid symbols (k_{app}) correspond to electrolyses with simultaneous oxygen evolution whereas open symbols (k^0_{app}) correspond to electrolyses carried out at E = 1.2 V (vs. Ag / AgCl, 3.0 M).

The evaluated ratios $k_{R,HO}/k_{O_2}$ are listed in Table 3 along with structural representation of the HBA derivatives and with charge density values on the carbon atoms of the aromatic ring. The increase of $k_{R,HO}/k_{O_2}$ does not follow the number of HO groups of the molecule since the three most reactive species comprise a tri-, a mono- and a di-hydroxybenzoic acid derivative. Alternatively, this kinetic parameter must be related to electronic properties of the species that can control reactions between HO radical and aromatic compounds. The presence of HO groups bonded to the aromatic ring induces negative charge densities on the carbon atoms of the ring. Considering the electrophilic nature of HO radical, the presence of negative charge densities on carbon atoms of the aromatic ring bonded to a hydrogen atom favours hydroxylation reaction resulting from HO radical electrophilic attack [30,31]. A relative reactivity order is proposed taking in consideration the number of negatively charged carbons as well as the magnitude of the charge density at positions where an HO group can be added (Table 3).

The six compounds studied can be divided into three groups. The less reactive BA (with lower $k_{R,HO}/k_{O_2}$) exhibits positive charge densities at C2, C4 e C6 and slightly negative charge densities (almost null) at C3 and C5. The species 2,3-HBA and 2,5-HBA, more reactive than BA (higher $k_{R,HO}/k_{O_2}$), have one carbon with a significant negative charge density at C5 (-0.026) and C3 (-0.039), respectively. The most reactive species 3,4,5-HBA, 4-HBA and 2,4-HBA have two carbons with negative charge density. 3,4,5-HBA, the less reactive of these three compounds, displays the lower charge densities (-0.010, -0.010); 4-HBA (with higher $k_{R,HO}/k_{O_2}$) has intermediary charge densities (-0.039, -0.039) and 2,4-HBA the most reactive species exhibits the highest charge densities (-0.083, -0.063).

Table 3: Values of $k_{R,HO}/k_{O_2}$ calculated for benzoic acid and for hydroxybenzoic acid derivatives from the slope of k_{app} vs. j using Eq. (13). Values of charge density are reported for carbon atoms from the aromatic ring that are bonded to a hydrogen atom. Negative values of charge density are in bold.

$k_{R,HO}/k_{O_2}$ (10⁻³ m³ mol⁻¹)		0.94 ± 0.08	4.0 ± 0.8	4.7 ± 0.4	5.3 ± 0.5	7.0 ± 0.4	8.9 ± 0.4
	C2	0.058			-0.010	0.059	
	C3	-0.002	-0.039			-0.039	-0.083
Charge density	C4	0.049	0.014	0.008			
	C5	-0.002		-0.026		-0.039	-0.063
	C6	0.058	0.013	0.026	-0.010	0.059	0.058

4. Conclusions

Apparent rate constants were determined from the consumption of seven hydroxy-containing aromatic compounds. These values are much lower than the calculated considering mass transport control and depend on the nature of species, demonstrating that electrolyses rates are controlled by the kinetics of oxidation reactions. Values of k_{app} were found to increase linearly with the current density of galvanostatic electrolysis with simultaneous O_2 evolution. The intercept, $(k_{app})_{j=0}$, of the linear dependence between k_{app} and j matches the apparent rate constant of potentiostatic electrolysis without O_2 evolution. Thus, $(k_{app})_{j=0}$ was deemed as a measure of the apparent rate constant of oxidation by direct electron transfer. From the slope of k_{app} vs. j values of $k_{R,HO}/k_{O_2}$ were determined for all species. These ratios of rate constants provide information concerning the reactivity of the species towards OH radicals. A good agreement between $k_{R,HO}/k_{O_2}$ values and the occurrence of negative charge densities on carbon atoms of the aromatic ring was observed. The consistency between the determined kinetic ratios and electronic properties of molecules substantiates the presented methodology for the kinetic study of oxidation by electrogenerated HO radical with simultaneous direct electron transfer.

References

[1] M. Panizza, G. Cerisola, Application of diamond electrodes to electrochemical processes, Electrochim. Acta. 51 (2005) 191–199.

[2] M. Panizza, A. Kapalka, C. Comninellis, Oxidation of organic pollutants on BDD anodes using modulated current electrolysis, Electrochim. Acta. 53 (2008) 2289–2295.

[3] A. Kapalka, G. Fóti, C. Comninellis, Investigations of electrochemical oxygen transfer reaction on boron-doped diamond electrodes, Electrochim. Acta. 53 (2007) 1954–1961.

[4] F. Montilla, P.A. Michaud, E. Morallón, J.L. Vázquez, C. Comninellis, Electrochemical oxidation of benzoic acid at boron-doped diamond electrodes, Electrochim. Acta. 47 (2002) 3509–3513.

[5] M. Panizza, G. Cerisola, Direct And Mediated Anodic Oxidation of Organic Pollutants, Chem. Rev. 109 (2009) 6541–6569.

[6] X. Zhu, M. Tong, S. Shi, H. Zhao, J. Ni, Essential Explanation of the Strong Mineralization Performance of Boron-Doped Diamond Electrodes, Environ. Sci. Technol. 42 (2008) 4914–4920.

[7] A. Kapałka, G. Fóti, C. Comninellis, Kinetic modelling of the electrochemical mineralization of organic pollutants for wastewater treatment, J. Appl. Electrochem. 38 (2008) 7–16.

[8] J. Iniesta, P.A. Michaud, M. Panizza, G. Cerisola, A. Aldaz, C. Comninellis, Electrochemical oxidation of phenol at boron-doped diamond electrode, Electrochim. Acta. 46 (2001) 3573–3578.

[9] M. Mascia, A. Vacca, A.M. Polcaro, S. Palmas, J.R. Ruiz, A. Da Pozzo, Electrochemical treatment of phenolic waters in presence of chloride with boron-doped diamond (BDD) anodes: Experimental study and mathematical model, J. Hazard. Mater. 174 (2010) 314–322.

[10] B. Louhichi, N. Bensalash, A. Gadri, Electrochemical Oxidation of Benzoic Acid Derivatives on Boron Doped Diamond: Voltammetric Study and Galvanostatic Electrolyses, Chem. Eng. Technol. 29 (2006) 944–950.

[11] T. Velegraki, G. Balayiannis, E. Diamadopoulos, A. Katsaounis, D. Mantzavinos, Electrochemical oxidation of benzoic acid in water over boron-doped diamond electrodes: Statistical analysis of key operating parameters, kinetic modeling, reaction by-products and ecotoxicity, Chem. Eng. J. 160 (2010) 538–548.

[12] Y. Cui, X. Li, G. Chen, Electrochemical degradation of bisphenol A on different anodes, Water Res. 43 (2009) 1968–1976.

[13] M. Panizza, G. Cerisola, Electrochemical degradation of gallic acid on a BDD anode, Chemosphere. 77 (2009) 1060–1064.

[14] C.A. Martinez-Huitle, F. Hernandez, S. Ferro, M.A.Q. Alfaro, A. de Battisti, Electrochemical oxidation: An alternative for the wastewater treatment with organic pollutants agents, Afinidad. 62 (2006) 26–34.

[15] C. Comninellis, Electrocatalysis in the electrochemical conversion/combustion of organic pollutants for waste water treatment, Electrochim. Acta. 39 (1994) 1857–1862.

[16] J.L. Wang, L.J. Xu, Advanced Oxidation Processes for Wastewater Treatment: Formation of Hydroxyl Radical and Application, Crit. Rev. Environ. Sci. Technol. 42 (2012) 251–325.

[17] A. Kapałka, G. Fóti, C. Comninellis, A. Kapalka, G. Foti, The importance of electrode material in environmental electrochemistry: Formation and reactivity of free hydroxyl radicals on boron-doped diamond electrodes, Electrochim. Acta. 54 (2009) 2018–2023.

[18] R. Oliveira, F. Bento, D. Geraldo, Aromatic hydroxylation reactions by electrogenerated HO radicals: A kinetic study, J. Electroanal. Chem. 682 (2012) 7–13.

[19] R. Oliveira, J. Marques, F. Bento, D. Geraldo, P. Bettencourt, Reducing Antioxidant Capacity Evaluated by Means of Controlled Potential Electrolysis, Electroanalysis. 23 (2011) 692–700.

[20] K.E. Yakovleva, S.A. Kurzeev, E. V Stepanova, T. V Fedorova, B.A. Kuznetsov, O. V Koroleva, Characterization of plant phenolic compounds by cyclic voltammetry, Appl. Biochem. Microbiol. 43 (2007) 661–668 LA – English.

[21] R. Liu, B. Goodell, J. Jellison, A. Amirbahman, Electrochemical Study of 2,3-Dihydroxybenzoic Acid and Its Interaction with Cu(II) and H2O2 in Aqueous Solutions: Implications for Wood Decay, Environ. Sci. Technol. 39 (2004) 175–180.

[22] S.M. Ghoreishi, M. Behpour, M. Khayatkashani, M.H. Motaghedifard, Simultaneous determination of ellagic and gallic acid in Punica granatum, Myrtus communis and Itriphal formulation by an electrochemical sensor based on a carbon paste electrode modified with multi-walled carbon nanotubes, Anal. Methods. 3 (2011) 636–645.

[23] M. Quan, D. Sanchez, M.F. Wasylkiw, D.K. Smith, Voltammetry of Quinones in Unbuffered Aqueous Solution: Reassessing the Roles of Proton Transfer and Hydrogen Bonding in the Aqueous Electrochemistry of Quinones, J. Am. Chem. Soc. 129 (2007) 12847–12856.

[24] A.J. Bard, L.R. Faulkner, Electrochemical Methods: Fundamentals and Applications, 2nd ed., Wiley, New York, 2001.

[25] J.E. Baur, 19 - Diffusion Coefficients, in: C.G.Z.B.T.-H. of Electrochemistry (Ed.), Elsevier, Amsterdam, 2007: pp. 829–848.

[26] L.F. Ferreira, L.M. Souza, D.L. Franco, A.C.H. Castro, A.A. Oliveira, J.F.C. Boodts, et al., Formation of novel polymeric films derived from 4-hydroxybenzoic acid, Mater. Chem. Phys. 129 (2011) 46–52.

[27] D. Nematollahi, H. Khoshsafar, Investigation of electrochemically induced Michael addition reactions. Oxidation of some dihydroxybenzene derivatives in the presence of azide ion, Tetrahedron. 65 (2009) 4742–4750.

[28] O. Simond, V. Schaller, C. Comninellis, Theoretical model for the anodic oxidation of organics on metal oxide electrodes, Electrochim. Acta. 42 (1997) 2009–2012.

[29] C. Amatore, Principles and Methods. Basic Concepts, in: M. Baizer, H. Lund (Eds.), Org. Electrochem., M. Dekker, New York, 1991: pp. 11–119.

[30] B. Lee, M. Lee, Prediction of Hydroxyl Substitution Site (s) of Phenol , Monochlorophenols and 4-Chloronitrobenzene by Atomic Charge Distribution Calculations, Bull. Korean Chem. Soc. 30 (2009) 4–7.

[31] S.M. Mukherji, S.P. Singh, R.P. Kapoor, R. Dass, Organic Chemistry, in: Org. Chem. Vol. II, 2nd ed., New Age International, 2012: pp. 146–188.

5 Electrogenerated HO radical reactions: the role of competing reactions on the degradation kinetics of hydroxy-containing aromatic compounds

Raquel Oliveira, Dulce Geraldo, Fátima Bento*

Department of Chemistry, Universidade do Minho, Campus de Gualtar 4710-057, Portugal

* Corresponding author T: +351 253604399; e-mail: fbento@quimica.uminho.pt

Abstract

The rate of degradation of an aromatic compound by electrogenerated HO radicals is investigated considering the effect of the presence of other species, that can either be a reaction product of the target compound or not. The effect of the actual reaction products is also analysed. The action of these secondary species is integrated in a general model that accounts for the dependency of the anode coverage by HO radicals on the concentration and reactivity of HO radical scavengers. From the magnitude of the effect of competing reactions the reactivity of a set of hydroxybenzoic acid derivatives was estimated by the product between the stoichiometric coefficients and the rate constants. A possible mechanistic interpretation is provided to explain the unexpected high values of the stoichiometric coefficients estimated that largely exceed the number of radicals required for the species mineralization.

Keywords

1. Introduction

Hydroxyl radical is one of the most powerful oxidant. Although it is best known for its deleterious action against cell components in oxidative stress [1], its application in the destruction of pollutants is particularly valuable regarding environmental friendly technologies [2]. Regardless of the research/ application field, the understanding of HO radical reactions is of great interest.

The generation of HO radicals is carried out in most laboratories by the so-called Fenton or Fenton-type reactions that use metal ions such as Fe(II) or Cu(II) to reduce H_2O_2 [3,4]. Despite the simplicity and accessibility of such methods, alternative ways have been suggested for this purpose, including the sono-Fenton [5], photo-Fenton [6], the electro-Fenton [7,8], sono-electro-Fenton [9] and photo-electro-Fenton [10,11]. Besides, HO radicals can also be generated by the photolysis of H_2O_2 [12] or by sonolysis [13] or radiolysis of water [2,14].

Electrochemical techniques are also used to generate of HO radicals. Following the identification of hydroxylated products [15] or using spin traps, as N,N-dimethyl-p-nitrosoaniline [16] or 5,5-dimethyl-1-pyrroline-N-oxide [17], the formation of HO radicals verified during the electrooxidation of water at different anode materials, such as Pt, IrO_2, SnO_2 and BDD. Besides the well known advantages of electrochemical techniques, e.g. low cost and easy automation, the degree of adsorption of the electrogenerated HO radicals at the anode can be controlled by the nature of the anode material. According to the adsorption strength of electrogenerated HO radicals to the anode surface [15,16] both the extent and rate of oxidation reactions can be varied. While quasi-free HO radicals are formed at BDD (boron doped diamond) anodes, strongly adsorbed HO radicals are formed at Pt anodes [18].

The generation of strongly adsorbed HO radicals can be rather interesting for comparing the reactivity of different species [19] or else for mechanistic studies. As the oxidation tends to be more selective, less reactive intermediaries can be stabilized. This possibility can be exploited in order to identify these intermediaries or to obtain information on secondary or competing reactions.

In the present work we present a kinetic study on the consumption of aromatic compounds that aims to elucidate the role of competing reactions. As HO radical is not selective it can react with a given compound and simultaneously with its reaction products. Besides, in natural systems (e.g. biological or wastewater) organic molecules occur in more or less complex mixtures. Therefore competing reactions cannot be avoid.

2. Experimental

2.1. Chemicals

All reagents employed were of analytical grade. Benzoic acid (BA; Prolabo), 2-hydroxybenzoic acid (2-HBA;Vaz Pereira), 4-hydroxybenzoic acid (4-HBA; BDH Chemicals) and 2,3-dihydroxybenzoic acid (2,3-HBA; ACROS Organics). Potassium chloride (Fluka), potassium ferricyanide (José Gomes Santos), potassium dihydrogen phosphate and phosphoric acid (ACROS Organics). Methanol was of HPLC grade from Fisher Scientific.

Solutions were prepared in 0.15 M buffer containing potassium dihydrogen phosphate and phosphoric acid pH 3.2.

2.2. HPLC

Oxidation reactions were monitored following the concentration decrease along galvanostatic electrolyses by HPLC. HPLC experiments were performed using a Jasco, PU-2080 Plus system equipped with a RP 18 column from Grace Smart (250 mm × 4.6 mm, 5 μm particle size) and using Clarity HPLC software from Jasco (Jasco 870 / UV detector). A flow rate of 0.6 ml min^{-1} and a loop of 20 μl were used. A mixture of methanol, water and phosphoric acid (60:39:1) (v/v) was used as mobile phase. The detection wavelength was selected according to species: 210 nm for 2-HBA and 2,3-HBA and 230 nm for BA and 4-HBA. The quantification was performed using calibration curves.

2.4. Electrolysis

Galvanostatic electrolysis were carried out (using a potentiostat Autolab type PGSTAT30, Ecochemie) at 1250 A m^{-2} in a two compartments cell separated by a glass frit membrane. Volume of anodic compartment is 9.0 ml and solution was mechanically stirred with a magnetic stir bar (300 rpm). Anode is made of a piece (20 mm ×10 mm) of Pt gauze (52 mesh woven from 0.1 mm diameter wire, 99.9%, from Alfa Aesar). Before each experiment the anode was electrochemically cleaned in the phosphate buffer solution pH 3.2 during 600 s at a constant current of 0.02 A. The area of the Pt working electrode (5.6 cm^2) was determined in a chronoamperometry experiment using 1.00 mM of $K_3[Fe(CN)_6]$ in 0.1 M KCl [20].

3. Results and discussion

Using Pt anodes fairly oxidized, in conditions where HO radicals are produced by oxidation of water, the consumption of aromatic compounds is not limited by mass transport, but by the kinetics of charge transfer and by the kinetics of reaction with HO radicals. The apparent rate constants, k^0_{app}, of degradation of aromatic compounds are related to the reactivity of the species, according to eq. 1 and to eq. 2 for non-electroactive and for electroactive compounds, respectively [19].

$$k^0_{app} = \frac{j}{zF}\left(\frac{1}{\frac{2k_{O_2}}{k_{S,HO}}+n_S[S]}\right) \tag{1}$$

$$k^0_{app} = \frac{j}{zF}\left(\frac{1}{\frac{2k_{O_2}}{k_{S,HO}}+n_S[S]}\right)+k_{S,e} \tag{2}$$

Where k_{O_2} is the rate constant of the reaction of O_2 evolution (according to eq. A.2, of appendix), $k_{S,HO}$ is the rate constant of the consumption of a species S by reaction with HO radicals adsorbed at the anode surface (according to eq. A.4), n_S is the stoichiometric coefficient, $k_{S,e}$ is the rate constant of the oxidation of S by direct electron transfer, z is the number of electrons involved in the electrogeneration of HO radical, j is the current density of the galvanostatic electrolysis and F is the Faraday constant. The fact that k^0_{app} keeps constant during the electrolysis of a number of aromatic compounds, despite the consumption of the compound, was taken as an indicator that $n_S[S]$ would be much smaller than $2k_{O_2} / k_{S,HO}$. On the basis of this consideration, values of $k_{S,HO} / k_{O_2}$ were evaluated from the slope of the representation of k^0_{app} vs j. Indeed, as k^0_{app} was independent of the instantaneous concentration of the organic species S it means that the HO surface concentration kept constant during the electrolysis. Although this approach suited our previous results [15,19] it is not adequate to interpret the new evidences provided by experimental data presented herein regarding the occurrence of competing reactions. The oxidation of a target compound in the presence of a second species, that can either be a reaction product of the target compound or not is considered in sections 3.1 and 3.2. The effect of the actual reaction products is also analysed (section 3.3) in experiments where the oxidation of a single starting compound is carried out at different initial concentrations, covering two orders of magnitude, so that the concentration of the formed products can also vary significantly.

3.1. Kinetic analysis of benzoic acid reaction with HO radicals in the presence of 2-hydroxybenzoic acid or of 4-hydroxybenzoic acid

The consumption of benzoic acid (BA) by galvanostatic electrolysis along time is displayed in Fig. 1A and 1B. The initial concentration of BA was 0.50 mM in all experiments. Circles correspond to results from solutions containing only BA as the starting compound, whereas triangles correspond to data obtained from solutions where BA is mixed with 2-HBA (Fig. 1A) or with 4-HBA (Fig. 1B). The independent variable τ in Fig. 1 is time normalized for the geometric ratio of the cell V/A.

The solid line adjusted to circles was simulated using eq. A.13 and describes the concentration decay of BA (C^0_{BA} = 0.50 mM) in the absence of any other added organic compound. A value of 2331 mol m^{-3} is assigned to $(2\,k_{O_2} + CS)\,/\,k_{BA,HO}$ in eq. A.13. The parameter CS, defined by eq. A.14, concerning BA oxidation can be expressed as:

$$CS = n_{BA}k_{BA,HO}[BA] + \sum n_{P_{BA,i}}k_{P_{BA,i},HO}[P_{BA,i}] \qquad (3)$$

where $k_{BA,HO}$ is the rate constant of BA reaction with HO radical and n_{BA} is the corresponding stoichiometric coefficient; $P_{BA,i}$ (i = 1, 2,..., n) is a reaction intermediary or product formed directly from the oxidation of BA or from the oxidation of a BA product, $n_{P_{BA,i}}$ is the stoichiometric coefficient of the reaction of $P_{BA,i}$ with HO radicals which rate constant is $k_{P_{BA,i},HO}$ and $[P_{BA,i}]$ is its concentration.

The fact that BA consumption is described by a pseudo-first order reaction indicates that k^0_{app} remains approximately constant along time. Considering eq. A.13 this result can be a consequence of one of the following situations. First, the magnitude of k_{O_2} is much larger than that of *CS* and even if *CS* can vary along time, the sum $2\,k_{O_2} + CS$ keeps constant. On the other hand, if CS is comparable to k_{O_2}, it must remain constant despite the consumption of BA. Considering eq. 3, in order that *CS* remains constant the decrease of the rate of consumption of HO radicals by reaction with BA (first parcel of eq. 3) must be compensated by the increase of its rate of consumption by reaction with the formed intermediaries or products P$_{BA,i}$ (second parcel of eq. 3).

The consumption of benzoic acid from the two mixtures (BA +2-HBA or BA + 4-HBA) show identical features (Fig. 1) in the sense that the concentration decay is slower than the observed in solutions where BA is the single starting compound and that the concentration decrease does not follow an exponential function. These observations were interpreted considering that the reaction of BA with electrogenerated HO radicals was significantly slowed down due to the competition between both organic compounds towards electrogenerated HO radicals. The fact that k_{app} (the rate constant of BA consumption in the presence of a second organic compound) is lower than k^0_{app} (rate constant of BA

consumption in the absence of any added organic compound) is a direct consequence of the lower concentration of HO radicals in the presence of two organics that can react with these radicals. Therefore, 2-HBA or 4-HBA provide a kind of protective effect towards the consumption of BA by HO radicals. This protective effect tends to decrease along time given that the consumption of BA tend to accelerate vis-a-vis the predicted by a constant k_{app}. This is illustrated in Fig. 1 by comparing the dotted with the dashed lines.

These lines are simulated using eq. B.10 (dotted lines) or eq. B.8 (dashed lines) that assumes that the concentration of HO radical at the electrode surface is influenced not only by the presence of the two organic compounds initially present in the solution (BA + 2-HBA or BA + 4-HBA) but also by the products of reaction of these compounds ($P_{BA,i}$ and $P_{2\text{-}HBA,i}$, or $P_{BA,i}$ and $P_{4\text{-}HBA,i}$). The only difference between the two equations is that for eq. B.8 (dashed lines) k_{app} is constant while for eq. B.10 (dotted lines) k_{app} diminishes along time.
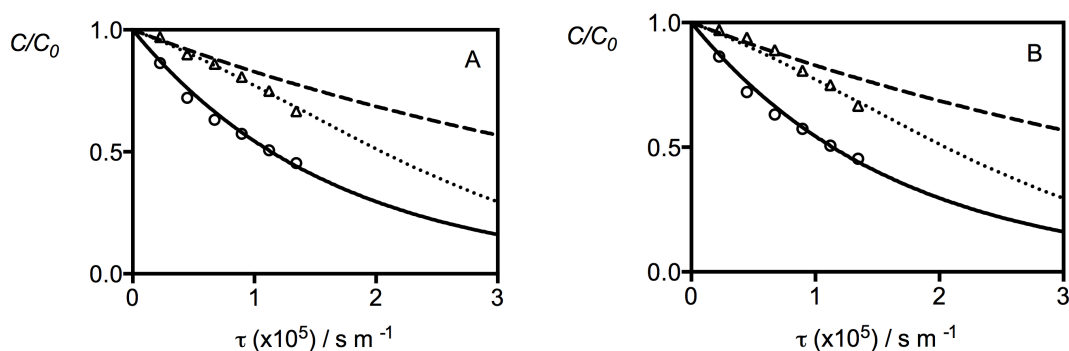
Figure 1: Concentration decrease of BA along time, C^0_{BA} = 0.50 mM, electrolysis conducted at j = 1250 A m^{-2} alone (○) and in the presence (△) of 0.50 mM: 2-HBA (A) or 4-HBA (B). Experimental data are plotted together with simulation curves: using eq. A.13 (solid line), using eq. B.10 (dotted line) and using eq. B.8 (dashed line). Simulation parameters: $(2\,k_{O_2} + CS) / k_{BA,HO}$ = 2331 mol m^{-3}, $\overline{n_{2\text{-}HBA,P_{2\text{-}HBA}} k_{2\text{-}HBA,P_{2\text{-}HBA}}} / k_{BA,HO}$ = 1060 mol m^{-3}, $k_{C(2\text{-}HBA,P)}$ = 3.5 x 10^{-5} m s^{-1} (A) and $(2\,k_{O_2} + CS) / k_{BA,HO}$ = 2331 mol m^{-3} $\overline{n_{4\text{-}HBA,P_{4\text{-}HBA}} k_{4\text{-}HBA,P_{4\text{-}HBA}}} / k_{BA,HO}$ = 36250 mol m^{-3} $k_{C(4\text{-}HBA,P)}$ = 5.0 x 10^{-6} m s^{-1} (B).

In eq. B.8 the initial concentration of the species R (2-HBA or 4-HBA), C^0_R ($C^0_{2\text{-}HBA}$ or $C^0_{4\text{-}HBA}$), is taken as an measure of the total concentration of the species that are able to react with HO radicals C_R (defined by eq. B.4), assuming that the decrease of [R] is compensated by the increase of [$P_{R,i}$].

At short times, $\tau < 1 \times 10^5$ s m^{-1}, experimental data are adequately simulated by this equation demonstrating that there was no significant decrease of the total concentration $C^0_{2\text{-}HBA}$ and $C^0_{4\text{-}HBA}$.

In eq. B.10 it is considered that the total concentration of the species that are able to react with HO radicals decrease with time (by a first order rate reaction with a rate constant of $k_{C(R,P)}$) (eq. B.5). The parameters used in the simulation are listed in the legend of Fig.1. where $\overline{n_{2\text{-}HBA,P_{2\text{-}HBA}} k_{2\text{-}HBA,P_{2\text{-}HBA}}}$ and $\overline{n_{4\text{-}HBA,P_{4\text{-}HBA}} k_{4\text{-}HBA,P_{4\text{-}HBA}}}$ are the average values of the product between the stoichiometric coefficients and the rate constants of 2-HBA and 4-HBA respectively.

3.2. Kinetic analysis of 2,3- hydroxybenzoic acid reaction with HO radicals in the presence of 4-hydroxybenzoic acid

Results of concentration decrease of 2,3-HBA are reported in Fig.2 in a similar study to that reported in the previous section. The experimental conditions used for the electrolyses are similar regarding the electrolysis cell, current density and concentrations of the organic compounds. Concerning the electrolyses of 2,3-HBA as a single starting organic compound (circles), results are similar to those obtained for BA, as an exponential decay is observed even though the consumption of 2,3-HBA is much faster than that of BA (compare the electrolysis time scales of Fig. 1 and Fig. 2). Based on this evidence, identical conclusions can be drawn concerning the establishment of a steady concentration of HO radicals at the anode surface along the electrolysis of 2,3-HBA. The solid line fitted to experimental data in Fig. 2 was simulated using Eq. A.15 in the same manner as it is done for BA.

Results from the electrolysis of 2,3-HBA (displayed as triangles) show that its consumption in the presence of 4-HBA slows down appreciably. The concentration decrease follow an exponential decay with an apparent rate constant, k_{app}, lower than the k^0_{app} of 2,3-HBA. As with BA, experimental data were simulated using eq. B.9 and eq. B.11. The curves adjusted using both equations fit quite well to experimental data, showing that the protective effect of 4-HBA does not decrease noticeably in the experimental time range. It should be mentioned that the value of the rate constant used to describe the decrease of $C^0_{4\text{-}HBA}$ along time ($k_{C(4\text{-}HBA,P)}$ = 5.0 x 10^{-6} m s^{-1}) was identical to that used for BA in the previous section.

These results, in conjunction with the reported in section 3.1 for BA, demonstrate that k_{app} is susceptible to the occurrence of further reactions involving HO radicals. Furthermore, depending of the time span of the experiments, the effect can be rather constant or may decrease along time.
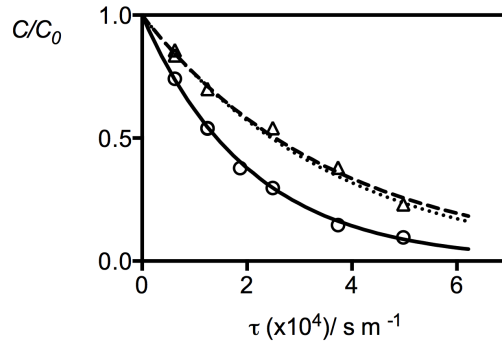
Figure 2: Concentration decrease of 2,3-HBA, C_0= 0.50 mM during a galvanostatic electrolysis at 1250 A m^{-2} in the absence ($\bigcirc$) and in the presence ($\triangle$) of 4-HBA. Experimental data are plotted together with simulated curves considering eq. A.15 using (solid line), eq. B.11 (dotted line) and eq. B.9 (dashed line) and using the following kinetic parameters: $(2\,k_{O_2} + CS)\,/\,k_{2,3\text{-}HBA,HO} = 419$ mol m^{-3}, $\overline{n_{4\text{-}HBA,P_{2\text{-}HBA}}k_{4\text{-}HBA,P_{2\text{-}HBA}}}\,/\,k_{2,3\text{-}HBA,HO} = 1906$ mol m^{-3}, $k_{C(4\text{-}HBA,P)} = 5.0 \times 10^{-6}$ m s^{-1}, $k_{2,3\text{-}HBA,e} = 21 \times 10^{-6}$ m s^{-1}.

In order to validate the model and assumptions used to deduce eq. B.8, eq. B.9, eq.B.10 and eq. B.11 used to fit experimental data in Fig. 1 and Fig. 2, additional experiments were carried out regarding the consumption of 2,3-HBA in the presence of different concentrations of 4-HBA. According to our assumptions k_{app} should decrease with regard to k^0_{app} with the increasing concentration of 4-HBA. Eq. B.12 predicts a linear relation between the reciprocal of the variation of the apparent rate constant $(\Delta k_{app} = k^0_{app} - k_{app})$ and the reciprocal of the total concentration $C^0_{4\text{-}HBA}$. Indeed, experimental data obtained from 0.50 mM 2,3-HBA with concentrations of 4-HBA ranging from 0.08 mM to 3.00 mM show an excellent agreement with the predicted trend. By means of a linear regression, values of intercept and slope were estimated for the straight-line represented in Fig. 3. According to eq. B.12, the intercept corresponds to (zF/j) $(2\,k_{O_2} + CS)\,/\,k_{2,3\text{-}HBA,HO}$ and allow to estimate a value of 431 mol m^{-3} for $(2\,k_{O_2} + CS)\,/\,k_{2,3\text{-}HBA,HO}$, that is comparable to 419 mol m^{-3} used to simulate the experimental data in Fig. 2 concerning an initial concentration of 4-HBA of 0.50 mM. Regarding the meaning of the slope given by Eq. B.12, and combining the values of the slope and intercept (intercept^2/slope) a value of 1992 mol m^{-3} is estimated for $\overline{n_{4\text{-}HBA,P_{4\text{-}HBA}}k_{4\text{-}HBA,P_{4\text{-}HBA}}}\,/\,k_{2,3\text{-}HBA,HO}$ that is similar to the value (1906 mol m^{-3}) used to simulate the experimental results in Fig. 2.

3.3. Effect of the presence of the actual reaction products

The formation of reaction products that can react with HO radicals was pointed out above as the reason for obtaining constant values of k^0_{app}. In terms of the model used to simulate experimental data this effect is accounted by the term CS that is defined by eq. A.14. The increase of concentration of the

reaction products along the electrolysis could therefore compensate the concentration decrease of the initial organic compound, thus keeping CS constant during an electrolysis. However considering electrolyses with different concentrations of the starting organic compound, it is expected that the value of k^0_{app} from each electrolyses is different due to the variation of CS with C^i_S (eq.A.16). The concentration decrease of BA, 2-HBA, 4-HBA and 2,3-HBA from electrolyses conducted at different initial concentrations is shown in Fig. 4. Despite the magnitude of the initial concentration, that was varied between 0.05 to 5.00 mM, exponential concentration decreases are observed, that are characteristic of pseudo-first order reactions. Results also indicate a pronounced dependency between the rate of consumption of each compound and its initial concentration. The more effective concentration decreases were obtained for lower initial concentrations, i.e. for the lower values of CS, what is in accordance with the predicted by eq. A.13 and eq. A.15. This effect is more pronounced for the non-electroactive BA and 4-HBA [15]. Indeed this fact can be easily understood, since for electroactive species only the parcel of k^0_{app} associated to the reaction involving HO radicals, $k^0_{app,HO}$, is affected by the variation of the initial concentration, while the rate constant of the direct electron transfer reaction, $k_{S,e}$, does not depend on the species concentration.
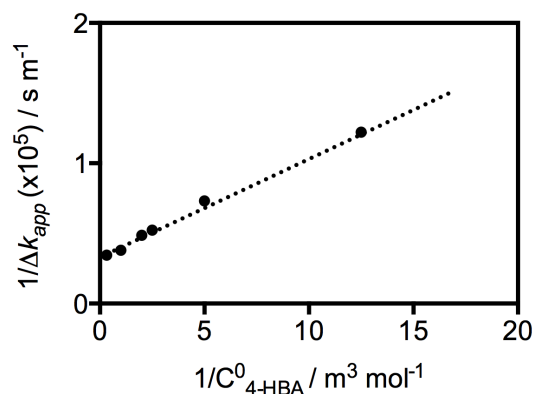
Figure 3: Representation of the reciprocal of the variation of k_{app} of 0.50 mM 2,3-HBA as a function of the reciprocal of concentration of 4-HBA. Dotted line is obtained by linear regression ($1/\Delta k_{app} = (3.3 \pm 0.1) \times 10^4 + (7.2 \pm 0.2) \times 10^3 \, 1/C^0_{4-HBA}$).

The dependency of k^0_{app} on the initial concentration of the species in each electrolysis is illustrated in Fig. 5. Concerning the non-electroactive species (Fig. 5A and Fig.5C) the representation is $1/k^0_{app}$ vs C^0_S (eq. A.22), whereas for the electroactive species the corresponding representation (Fig. 5B and Fig.5D) is $1/k^0_{app,HO}$ vs C^0_S (eq. A.24).Values of $k^0_{app,HO}$ were calculated by $k^0_{app} - k_{S,e}$ where values of $k_{S,e}$ were estimated from the intercept of k^0_{app} vs j [19]. The obtained linear correlations are quite good for the four aromatic compounds, demonstrating that the parameters ascribed to the intercept and to the

slope remain constant despite the change of the initial concentration. Considering the relations expressed by eq. A.22 and eq. A.24, from the intercept it can be estimated the value of $k_{S,HO} / k_{O_2}$. Values of $k_{S,HO} / k_{O_2}$ for BA, 2-HBA, 4-HBA and 2,3-HBA are presented in Table 1, together with our previous estimations [19] evaluated directly from the slope of the representation of k^0_{app} vs j (considering that the magnitude of k_{O_2} is much larger than the concentration term). Despite the introduced error in our previous estimations, the proposed reactivity order did not change considering the present results.
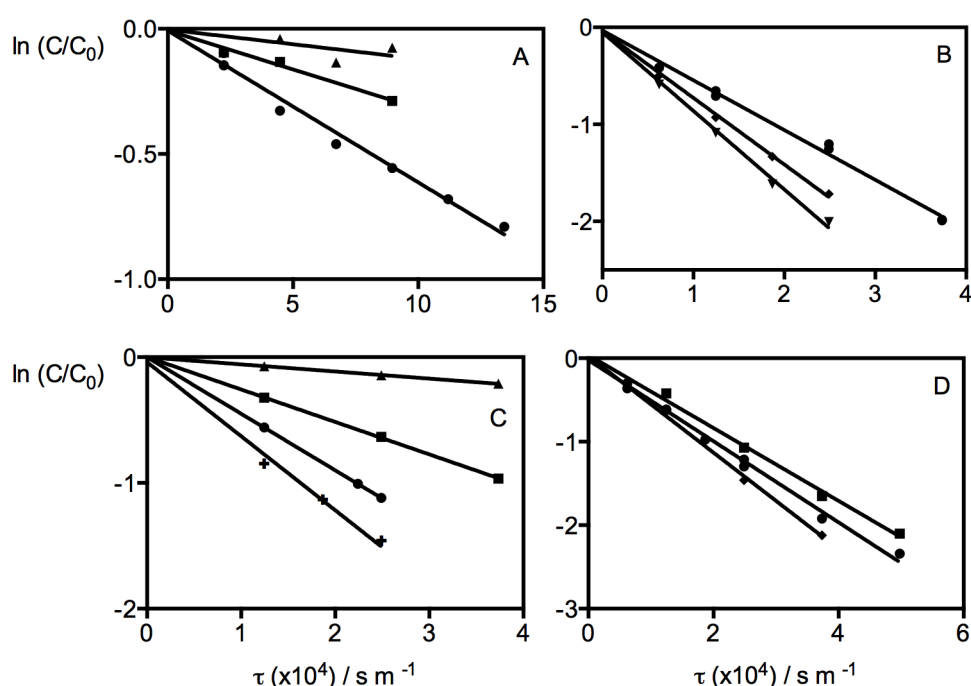
Figure 4: Concentration decrease during galvanostatic electrolyses at 1250 A m^{-2} of BA (A), 2-HBA (B), 4-HBA (C) and 2,3-HBA (D) at different concentrations: 5.00 mM (▲), 1.00 mM (■), 0.50 mM (●), 0.25 mM (✚), 0.10 mM (◆) and 0.05 mM (▼).

From the slope of $1/ k^0_{app,HO}$ vs C^0_S values of $\overline{n_{S,P} k_{S,P}} / k_{S,HO}$ (= $\overline{n_{S,P}} \; \overline{k_{S,P}} / k_{S,HO}$) can be obtained. This amount corresponds to the product of the average stoichiometric coefficients by the average rate constants, regarding the original species S and products P, divided by the rate constant of S. An estimation of the average stoichiometric coefficients, $\overline{n_{S,P}}$, can be obtained by assuming that $\overline{k_{S,P}} / k_{S,HO} \approx 1$. The error of this estimation depends on the relative weight of $k_{S,HO}$ on the calculation of $\overline{k_{S,P}}$, (eq. A.19). As this average value is calculated by a weighted arithmetic mean, regarding the concentrations of each species, the correspondence between $\overline{k_{S,P}}$ and $k_{S,HO}$ can be fairly accepted for

low conversion levels of S. On the other side, for experimental data that include high conversion levels of S, the error of this approximation should not exceed one order of magnitude. This assumption is made considering the differences between the values of $k_{S,HO} / k_{O_2}$ (Table 1). Besides, if the difference between $k_{S,HO}$ and $\overline{k_{S,P}}$ is significantly large, a steady k^0_{app} will certainly not be obtained. As this was not the case for any of the analysed set of data (in Fig. 4), we can therefore accept the assumption of $\overline{k_{S,P}} / k_{S,HO} \approx 1$.

The estimated values of $\overline{n_{S,P}}$ for BA, 2-HBA, 4-HBA and 2,3-HBA are displayed in Table 1. The quite unexpected high values obtained for $\overline{n_{S,P}}$ require some reflection and careful analysis concerning a possible mechanistic interpretation of this evidence.
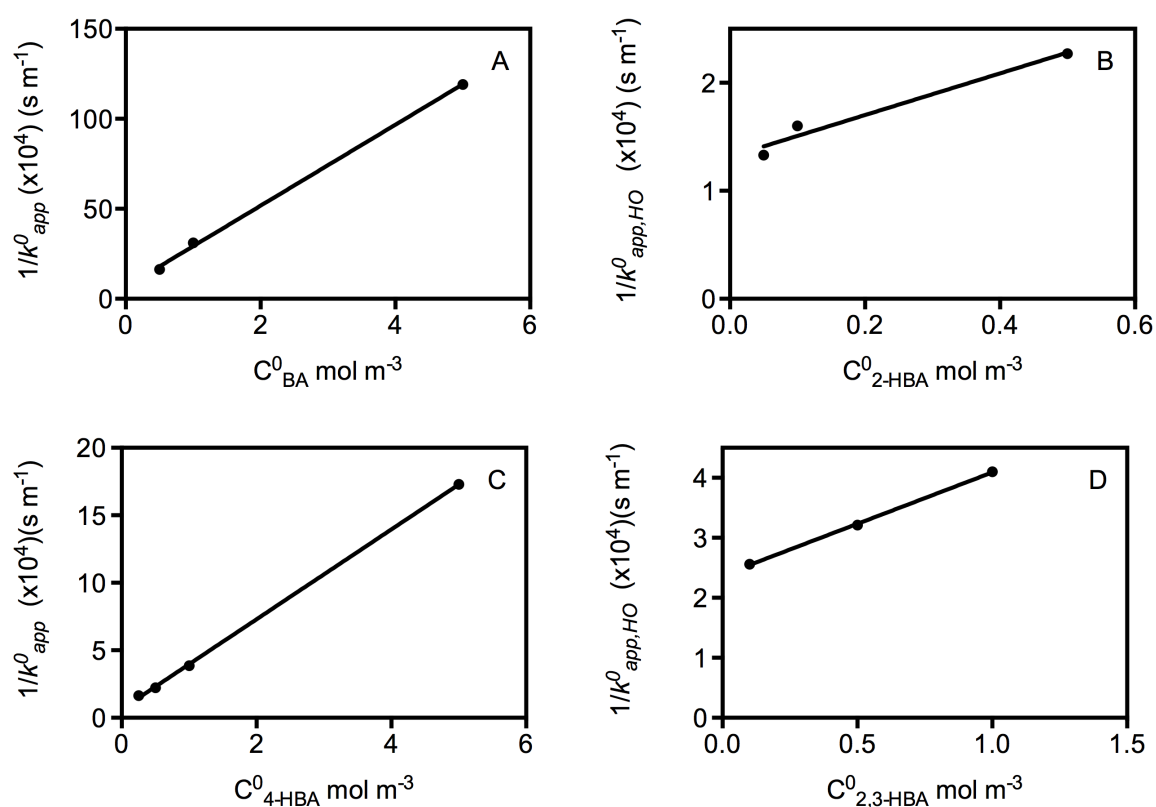
Figure 5: Representation of the reciprocal of k^0_{app} vs the initial concentration for: BA (A), and 4-HBA (C); and of the reciprocal of $k^0_{app,HO}$ vs the initial concentration for: 2-HBA (B) and 2,3-HBA (D).

3.4 Mechanistic interpretation of the HO radical stoichiometric coefficients

The amazingly high values of $\overline{n_{S,P}}$, that range from 190 (from 2-HBA) to 2,900 (from BA), can only be explained considering that reaction products and intermediaries formed by reaction with HO radicals

are involved in subsequent reactions that make possible to regenerate reactive species that persist in scavenging HO radicals.

Table 1. Values of $k_{S,HO}/k_{O2}$ reported in literature and values of $k_{S,HO}/k_{O2}$ and $\overline{n_{SP}}$ calculated from the intercept and from the slope of $k_{app,HO}^{-1}$ vs C^O_{AO}.

	$k_{S,HO}/k_{O2}$ ($10^{-3}\,m^3\,mol^{-1}$)[19]	$k_{s,HO}/k_{O2}$ ($10^{-3}\,m^3\,mol^{-1}$)	$\overline{n_{SP}}$ (10^2)
BA	0.941 ± 0.008	2.3 ± 0.7	29.0 ± 0.9
2-HBA	-	13.0 ± 0.9	1.9 ± 0.4
4-HBA	7.0 ± 0.4	24 ± 4	4.32 ± 0.05
2,3-HBA	4.7 ± 0.4	6.49 ± 0.07	2.22 ± 0.06

Aromatic compounds with aromatic rings such as BA or 4-HBA are readily attacked by hydroxyl radicals giving a variety of free radical aromatic species as it is shown in scheme 1. There are several reports describing the reaction of aromatic compounds with HO radical [15,19,21]. The addition of HO radicals to these type compounds gives hydroxycyclohexadienyl radical intermediates that are easily oxidized to give several hydroxylated derivatives (scheme 1). The 4-HBA is one of the major products isolated from the oxidation of BA [15]. This is probably due to the stability of the corresponding hydroxycyclohexadienyl radical. Dehydration of the hydroxycyclohexadienyl radicals can also occur giving a BA radical that can be decarboxylate or can regenerate BA. Benzoic acid can also be obtained by an addition-elimination mechanism from hydroxycyclohexadienyl radicals. As the reactivity of electrogenerated HO radicals can be quite low, as a result of the strong adsorption strength at Pt, the rate of HO radical addition to aromatic ring can be lower than that of elimination or dehydration reactions. As a result, the number of HO radicals involved in the reaction, $\overline{n_{S,P}}$, can exceed the number of radicals required for the species mineralization.
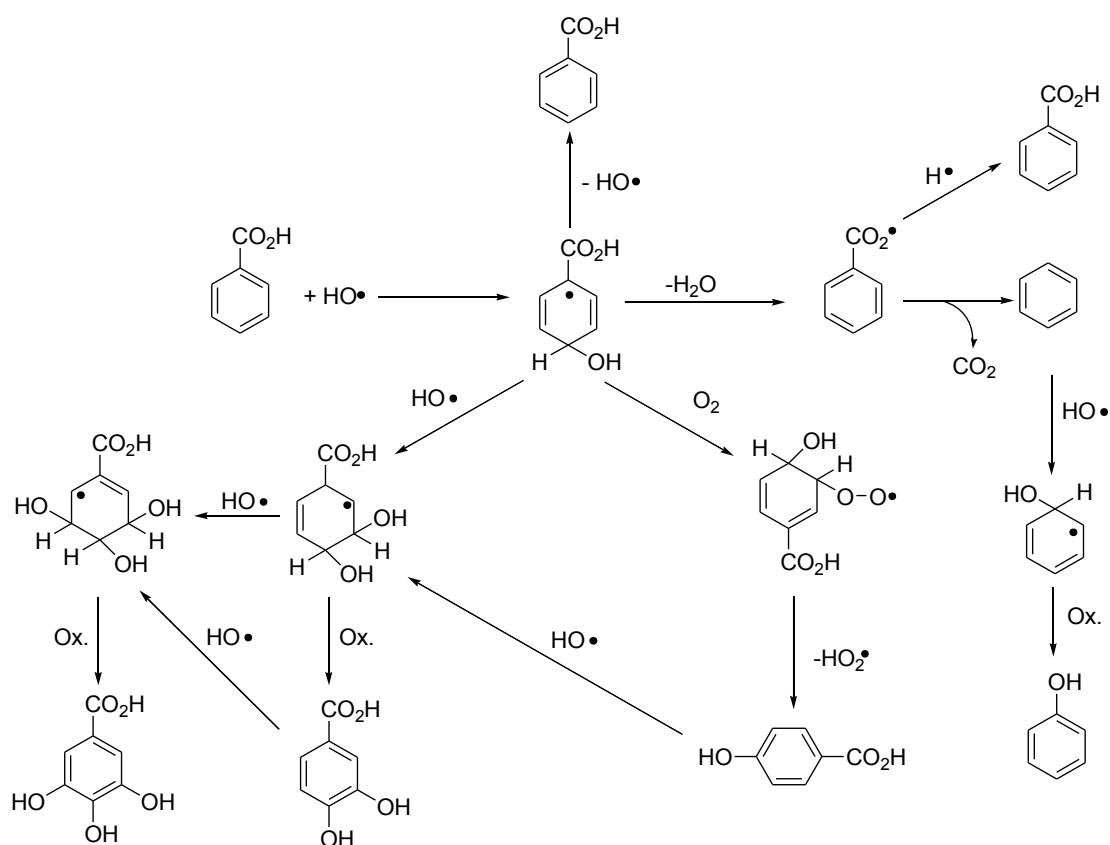
Scheme 1. Possible reactions involved in the attack of hydroxyl radicals to benzoic acid.

4. Conclusion

The rate of consumption of aromatic compounds by electrogenerated HO radicals depends strongly on the presence of other species that are potential HO radicals scavengers. The effect of the presence of 4-HBA on the apparent rate constants of BA and 2,3-HBA and the effect of the presence of 2- HBA on the apparent rate constant of BA was similar, in the sense that a substantial decrease in the rate of consumption of BA and of 2,3-HBA was noticed. The magnitude of this effect was shown to depend not only on the concentration of the radical scavenger but also on its reactivity towards HO radical, that was characterized by $\overline{n_{R,P}\,k_{R,P}}$, i.e. by the average value of the product between the stoichiometric coefficients and the rate constants of reactions of R and its reaction products with HO radicals.

The products formed from the reaction between aromatic compounds and HO radicals can themselves be HO radicals scavengers and therefore compete with the reactant for these radicals. This assumption was considered and validated to explain the apparent disagreement between the dependency of apparent rate constants (k^0_{app}) on the concentration of each species. While k^0_{app} depended on the initial concentration of the species, k^0_{app} remained constant during each electrolysis (despite the concentration decrease). By considering that the HO radical concentration is controlled by both,

starting species and reaction products, an expression was deduced that allows to estimate important reactivity parameters such as $k_{S,HO} / k_{O_2}$ (ratio between the rate constant of reaction of S with HO radical and the rate constant of O_2 formation) and $\overline{n_{S,P}}$ (average stoichiometric coefficients regarding the original species S and products and intermediaries P). The high values estimated for $\overline{n_{S,P}}$, from all the analysed compounds (BA, 2-HBA, 4-HBA and 2,3-HBA), indicates that elimination or dehydration reactions can play an important role in stabilizing reaction intermediaries in conditions where the availability of HO radicals (with sufficient energy to react, as a result of their strong adsorption strength at Pt) is quite low.

Appendix A

The consumption of an organic compound, S, by galvanostatic electrolysis, with simultaneous O_2 evolution is considered in view of the following conditions and assumptions:

- The starting compound reacts with electrogenerated HO radicals and originate products that may also react with these radicals;
- The starting compound and its reaction products may be electroactive;
- The rate of all reactions (including the heterogeneous charge transfer) is slow relative to diffusion, so that concentration polarization can be neglected.

The consumption of organic compounds by galvanostatic electrolysis, with simultaneous O_2 evolution, is related to the formation of HO radical, as an intermediary species, according to eq. A.1 and eq. A.2 [22,23].

$$H_2O \rightarrow HO^{\bullet} + H^+ + e^-$$ (A.1)

$$2\ HO^{\bullet} \xrightarrow{k_{O_2}} O_2 + 2H^+ + 2e^-$$ (A.2)

The rate of formation of radicals, v_{HO}, is controlled by the current density j (A m^{-2}), according to equation A.3 [22] [23].

$$v_{HO} = \frac{j}{zF}$$ (A.3)

where z corresponds to the stoichiometric factor and F to the Faraday constant. The reaction between HO radicals and a chemical species, S, is expressed by equation A.4. As the products formed by this

reaction may also be react with HO radicals in subsequent reactions, eq. A.5 must be considered as well:

$$S + n_S HO^\bullet \xrightarrow{k_{S,HO}} P_{S,i} \qquad\qquad (A.4)$$

$$P_{S,i} + n_{P_{S,i}} HO^\bullet \xrightarrow{k_{P_{S,i},HO}} P_{S,n} \qquad\qquad (A.5)$$

where $P_{S,i}$ (i = 1, 2, ..., n) corresponds to intermediaries or chemical species formed by direct or subsequent reactions of S with HO radicals and $k_{S,HO}$ and $k_{P_{S,i},HO}$ are the corresponding rate constants.

The rate of formation of HO radicals in steady state conditions can be defined as:

$$v_{HO^\bullet} = 2v_{O_2} + n_S v_{S,HO} + \sum n_{P_{S,i}} v_{P_{S,i},HO} \qquad\qquad (A.6)$$

where v_{O_2}, the rate of formation of oxygen according to equation A.2, can be defined as follows:

$$v_{O_2} = k_{O_2} \Gamma\theta \qquad\qquad (A.7)$$

where $\Gamma\theta$ corresponds to the surface concentration of HO radicals at the anode surface; θ is the surface coverage degree and Γ the saturation concentration of this species (mol m^{-2}). The rate of reaction between the chemical species S and the HO radical is defined by:

$$v_{S,HO} = k_{S,HO}[S]\Gamma\theta \qquad\qquad (A.8)$$

Considering eq. A.3, eq A.7 and eq A.8, eq. A.6 can therefore be rewritten as follows:

$$\frac{j}{zF} = 2k_{O_2}\Gamma\theta + n_S k_{S,HO}[S]\Gamma\theta + \sum n_{P_{S,i}} k_{P_{S,i},HO}[P_{S,i}]\Gamma\theta \qquad\qquad (A.9)$$

or in an equivalent form:

$$\Gamma\theta = \frac{j}{zF} \frac{1}{2k_{O_2} + n_S k_{S,HO}[S] + \sum n_{P_{S,i}} k_{P_{S,i},HO}[P_{S,i}]} \qquad\qquad (A.10)$$

Combining equations A.10 and A.8 it is possible to defined the consumption rate trough equation A.11:

$$v_{S,HO} = \frac{j}{zF} \frac{k_{S,HO}}{2k_{O_2} + n_S k_{S,HO}[S] + \sum n_{P_{S,i}} k_{P_{S,i},HO}[P_{S,i}]}[S] \qquad\qquad (A.11)$$

According to equation A.11 the apparent rate constant associated to the consumption of S is described by the expression:

$$k_{app}^0 = \frac{j}{zF} \frac{k_{S,HO}}{2k_{O_2} + n_S k_{S,HO}[S] + \sum n_{P_{S,i}} k_{P_{S,i},HO}[P_{S,i}]} \qquad\qquad (A.12)$$

A simplified expression equivalent to equation A.12 can be defined as:

$$k_{app}^0 = \frac{j}{zF} \frac{1}{(2k_{O_2} + CS)/k_{S,HO}} \qquad\qquad (A.13)$$

By defining the quantity CS as follows:

$$CS = n_S k_{S,HO}[S] + \sum n_{P_{S,i}} k_{P_{S,i},HO}[P_{S,i}] \qquad \text{(A.14)}$$

Eq. A.13 must incorporate an additional term concerning the consumption of the species by direct electron transfer, $k_{S,e}$, for species that are electroactive [19].

$$k_{app}^0 = \frac{j}{zF} \frac{1}{(2k_{O_2} + CS)/k_{S,HO}} + k_{S,e} \qquad \text{(A.15)}$$

At each moment the sum of the concentration of the species S and the concentration of all the products $P_{S,i}$ is equal to C_S^i, according to eq. A.16.

$$C_S^i = [S] + \sum [P_{S,i}] \qquad \text{(A.16)}$$

where C_S^i is related to the initial concentration of S, C_S^0, by:

$$C_S^i = C_S^0 \, e^{-k_{C(S,P)}t} \qquad \text{(A.17)}$$

where $k_{C(S,P)}$ is the rate constant that expresses the decay of concentration of the species, either S ou $P_{S,i}$ that can act as HO radical scavengers.

Eq. A.18 is defined combining eq. A.14 with eq. A.16:

$$\overline{n_{S,P}k_{S,P}} = \frac{CS}{C_S^i} \qquad \text{(A.18)}$$

This equation defines a weighted arithmetic mean of the product between the stoichiometric coefficients and the rate constants of reactions (considering both species S and products $P_{s,i}$), where the weigh is the concentration of each species.

In circumstances where a constant CS is predicted (i.e. the concentration decay follow a exponential trend), $C_S^i = C_S^0$. This situation is likely to occur for short times where the extent of mineralization or ring cleavage is low. Thus, eq. A.18 can be replaced by:

$$\overline{n_{S,P}k_{S,P}} = \frac{CS}{C_S^0} \qquad \text{(A.19)}$$

The apparent rate constant can therefore be rewritten as,

$$k_{app}^0 = \frac{j}{zF} \frac{1}{(2k_{O_2}/k_{S,HO} + \overline{n_{S,P}k_{S,P}}C_S^0/k_{S,HO})} \qquad \text{(A.20)}$$

for a non-electroactive species or, as

$$k_{app}^0 = \frac{j}{zF} \frac{1}{(2k_{O_2}/k_{S,HO} + \overline{n_{S,P}k_{S,P}}C_S^0/k_{S,HO})} + k_{S,e} \qquad \text{(A.21)}$$

for an electroactive species.

For a non-electroactive species, a linear relation can be established between the reciprocal of k_{app}^0 with C_S^0, as follows:

$$\frac{1}{k_{app}^0} = \frac{zF}{j}\left(\frac{2k_{O_2}}{k_{S,HO}} + \frac{\overline{n_{S,P}k_{S,P}}}{k_{S,HO}}C_S^0\right)$$ (A.22)

For an electroactive species, it is defined:

$$k_{app,HO}^0 = k_{app}^0 - k_{S,e}$$ (A.23)

and a relation similar to A.22 can then also be defined:

$$\frac{1}{k_{app,HO}^0} = \frac{zF}{j}\left(\frac{2k_{O_2}}{k_{S,HO}} + \frac{\overline{n_{S,P}k_{S,P}}}{k_{S,HO}}C_S^0\right)$$ (A.24)

Appendix B

The consumption of an organic compound, S, by galvanostatic electrolysis, with simultaneous O_2 evolution is considered in the presence of a second organic species, R, that compete with S to the electrogenerated HO radicals. The conditions and assumptions considered are similar to those presented in appendix A.

The reaction between HO radicals with the chemical species, R, as well as with the reaction products or intermediaries of R, $P_{R,i}$ (i = 1, 2, ..., n), can be described by equations similar to eq. A.4 and eq. A.5. For these reactions the rate constants are $k_{R,HO}$ and $k_{P_{R,i},HO}$ and the corresponding stoichiometric coefficients are n_R and $n_{P_{R,i}}$.

In steady state conditions the rate of formation of HO radicals is be defined by eq. B.1, that includes all the processes involving formation / consumption of HO radicals already considered in eq. A.6 as well as reactions with the species R and $P_{R,i}$:

$$v_{HO^\cdot} = 2\,v_{O_2} + n_S v_{S,HO} + \sum n_{P_{S,i}} v_{P_{S,i},HO} + n_R v_{R,HO} + \sum n_{P_{R,i}} v_{P_{R,i},HO}$$ (B.1)

Therefore, the apparent rate constant for the reaction of S with electrogenerated HO radicals in the presence of R can be defined as:

$$k_{app} = \frac{j}{zF}\frac{k_{S,HO}}{2k_{O_2} + n_S k_{S,HO}[S] + \sum n_{P_{S,i}} k_{P_{S,i},HO}[P_{S,i}] + n_R k_{R,HO}[R] + \sum n_{P_{R,i}} k_{P_{R,i},HO}[P_{R,i}]}$$ (B.2)

in a similar way as for eq.A.12.

Defining the quantity CR as:

$$CR = n_R k_{R,HO}[R] + \sum n_{P_{R,i}} k_{P_{R,i},HO}[P_{R,i}]$$ (B.3)

and $C_R^{'}$ as:

$$C_R^i = [R] + \sum [P_{R,i}] \tag{B.4}$$

where C_R^i is related to the initial concentration of R, C_R^0, by:

$$C_R^i = C_R^0\, e^{-k_{C(R,P)}t} \tag{B.5}$$

where $k_{C(R,P)}$ is the rate constant that express the decay of concentration of the species, either R or $P_{R,i}$ that can act as HO radical scavengers.

Eq. B.6 is therefore defined combining eq. B.3 with eq. B.4:

$$\overline{n_{R,P}k_{R,P}} = \frac{CR}{C_R^i} \tag{B.6}$$

Similarly to eq. A.18, eq. B.6 defines a weighted arithmetic mean of the product between the stoichiometric coefficients and the rate constants of reactions.

For short times, the extent of mineralization or ring cleavage is low and a constant CR is predicted, therefore $C_R^i = C_R^0$:

$$\overline{n_{R,P}k_{R,P}} = \frac{CR}{C_R^0} \tag{B.7}$$

The apparent rate constant for short times can thus be defined attending to eq. B.2, eq. B.3 and eq. B.7:

$$k_{app} = \frac{j}{zF}\, \frac{1}{\dfrac{2k_{O_2} + CS}{k_{S,HO}} + \dfrac{\overline{n_{R,P}k_{R,P}}}{k_{S,HO}} C_R^0} \tag{B.8}$$

for non-electroactive species, or by:

$$k_{app} = \frac{j}{zF}\, \frac{1}{\dfrac{2k_{O_2} + CS}{k_{S,HO}} + \dfrac{\overline{n_{R,P}k_{R,P}}}{k_{S,HO}} C_R^0} + k_{S,e} \tag{B.9}$$

for the case of electroactive species.

For long times, the apparent rate constant is defined on the basis of eq. B.2, eq. B.3 and eq. B.6:

$$k_{app} = \frac{j}{zF}\, \frac{1}{\dfrac{2k_{O_2} + CS}{k_{S,HO}} + \dfrac{\overline{n_{R,P}k_{R,P}}}{k_{S,HO}} C_R^0\, e^{-k_{C(R,P)}t}} \tag{B.10}$$

for non-electroactive species, or by:

$$k_{app} = \frac{j}{zF}\, \frac{1}{\dfrac{2k_{O_2} + CS}{k_{S,HO}} + \dfrac{\overline{n_{R,P}k_{R,P}}}{k_{S,HO}} C_R^0\, e^{-k_{C(R,P)}t}} + k_{S,e} \tag{B.11}$$

for the case of electroactive species.

The effect of the presence of the species R can therefore be evaluated from the variation of the apparent rate constants as $\Delta k_{app} = k^0_{app} - k_{app}$. Considering the difference between eq. A.20 and eq. B.8

or the difference between eq. A.21 and eq. B.9, eq. B.12 is defined for both electroactive and non-electroactive species.

$$\frac{1}{\Delta k_{app}} = \frac{ZF}{j}\left(\frac{2k_{O_2}+CS}{k_{S,HO}} + \left(\frac{2k_{O_2}+CS}{k_{S,HO}}\right)^2 \frac{k_{S,HO}}{n_{R,P}k_{R,P}}\frac{1}{C_R^0}\right)$$ (B.12)

Acknowledgments

References

[1]   B. Lipinski, Hydroxyl radical and its scavengers in health and disease., Oxid. Med. Cell. Longev. 2011 (2011) 1–9.

[2]   J.L. Wang, L.J. Xu, Advanced Oxidation Processes for Wastewater Treatment: Formation of Hydroxyl Radical and Application, Crit. Rev. Environ. Sci. Technol. 42 (2012) 251–325.

[3]   J.J. Pignatello, E. Oliveros, A. MacKay, Advanced Oxidation Processes for Organic Contaminant Destruction Based on the Fenton Reaction and Related Chemistry, Crit. Rev. Environ. Sci. Technol. 36 (2006) 1–84.

[4]   B.. Ou, M.. Hampsch-Woodill, J.. Flanagan, E.K.. K. Deemer, R.L.. L. Prior, D.. Huang, Novel fluorometric assay for hydroxyl radical prevention capacity using fluorescein as the probe, J. Agric. Food Chem. 50 (2002) 2772–2777.

[5]   J. Lin, Y. Ma, Oxidation of 2-Chlorophenol in Water by Ultrasound/Fenton Method, J. Environ. Eng. 126 (2000) 130–137.

[6]   S.M. Kumar, Degradation and mineralization, of organic contaminants by Fenton and photo-Fenton processes: Review of mechanisms and effects of organic and inorganic additives, Res. J. Chem. Environ. 15 (2011) 96–112.

[7]   E. Brillas, I. Sirés, M.A. Oturan, Electro-Fenton Process and Related Electrochemical Technologies Based on Fenton's Reaction Chemistry, Chem. Rev. 109 (2009) 6570–6631.

[8]   P. V Nidheesh, R. Gandhimathi, Trends in electro-Fenton process for water and wastewater treatment: An overview, Desalination. 299 (2012) 1–15.

[9]   M.A. Oturan, I. Sirés, N. Oturan, S. Pérocheau, J.-L. Laborde, S. Trévin, Sonoelectro-Fenton process: A novel hybrid technique for the destruction of organic pollutants in water, J. Electroanal. Chem. 624 (2008) 329–332.

[10]   R. Salazar, M.S. Ureta-Zanartu, Mineralization of Triadimefon Fungicide in Water by Electro-Fenton and Photo Electro-Fenton, Water Air soil Pollut. 223 (2012) 4199–4207.

[11]   A. Babuponnusami, K. Muthukumar, Advanced oxidation of phenol: A comparison between Fenton, electro-Fenton, sono-electro-Fenton and photo-electro-Fenton processes, Chem. Eng. J. 183 (2012) 1–9.

[12]   J.L. France, M.D. King, J. Lee-Taylor, Hydroxyl (OH) radical production rates in snowpacks from photolysis of hydrogen peroxide (H2O2) and nitrate (NO3−), Atmos. Environ. 41 (2007) 5502–5509.

[13]   L. Villeneuve, L. Alberti, J.-P. Steghens, J.-M. Lancelin, J.-L. Mestas, Assay of hydroxyl radicals generated by focused ultrasound, Ultrason. Sonochem. 16 (2009) 339–344.

[14]   W. Bors, C. Michel, Antioxidant capacity of flavanols and gallate esters: pulse radiolysis studies, Free Radic. Biol. Med. 27 (1999) 1413–1426.

[15]   R. Oliveira, F. Bento, D. Geraldo, Aromatic hydroxylation reactions by electrogenerated HO radicals: A kinetic study, J. Electroanal. Chem. 682 (2012) 7–13.

[16]   C. Comninellis, Electrocatalysis in the electrochemical conversion/combustion of organic pollutants for waste water treatment, Electrochim. Acta. 39 (1994) 1857–1862.

[17]   B. Marselli, J. Garcia-Gomez, P.-A. Michaud, M.A. Rodrigo, C. Comninellis, Electrogeneration of Hydroxyl Radicals on Boron-Doped Diamond Electrodes, J. Electrochem. Soc. . 150 (2003) D79–D83.

[18]   A. Kapałka, H. Baltruschat, C. Comninellis, Electrochemical Oxidation of Organic Compounds Induced by Electro-Generated Free Hydroxyl Radicals on BDD Electrodes, in: Synth. Diam. Film., John Wiley & Sons, Inc., 2011: pp. 237–260.

[19]   R. Oliveira, N. Pereira, D. Geraldo, F. Bento, Reactivity of hydroxy-containing aromatic compounds towards electrogenerated hydroxyl radicals, Electrochim. Acta. 105 (2013) 371–377.

[20]   A.J. Bard, L.R. Faulkner, Electrochemical Methods: Fundamentals and Applications, 2nd ed., Wiley, New York, 2001.

[21]   M.A. Oturan, J. Pinson, Hydroxylation by Electrochemically Generated OH.bul. Radicals. Mono- and Polyhydroxylation of Benzoic Acid: Products and Isomer Distribution, J. Phys. Chem. 99 (1995) 13948–13954.

[22]   O. Simond, V. Schaller, C. Comninellis, Theoretical model for the anodic oxidation of organics on metal oxide electrodes, Electrochim. Acta. 42 (1997) 2009–2012.

[23]   A. Kapałka, G. Fóti, C. Comninellis, Kinetic modelling of the electrochemical mineralization of organic pollutants for wastewater treatment, J. Appl. Electrochem. 38 (2008) 7–16.

6 Radical scavenging activity of antioxidants evaluated by means of electrogenerated HO

radical

Raquel Oliveira, Dulce Geraldo, Fátima Bento*

Centro de Química, Universidade do Minho, Campus de Gualtar 4710-057 Braga, Portugal

* Corresponding author Tel.: +351 253604399; e-mail: fbento@quimica.uminho.pt

Abstract

A method is proposed and tested concerning the characterization of antioxidants by means of their reaction with electrogenerated HO radicals in galvanostatic assays with simultaneous O_2 evolution, using a Pt anode fairly oxidized. The consumption of a set of species with antioxidant activity, ascorbic acid (AA), caffeic acid (CA), gallic acid (GA) and trolox (T), is described by a first order kinetics. The rate of the processes is limited by the kinetics of reaction with HO radicals and by the kinetics of charge transfer.

Information regarding the scavenger activity of antioxidants was estimated by the relative value of the rate constant of the reaction between antioxidants and HO radical, $k_{AO,HO} / k_{O_2}$. The number of HO radicals scavenged per molecule of antioxidant was also estimated as ranging from 260 (ascorbic acid) to 500 (gallic acid). The method was applied successfully in the characterization of the scavenger activity of ascorbic acid in a green-tea based beverage.

Keywords

1. Introduction

Oxidative stress is a condition of biological systems where there is a imbalance between the amount of reactive oxygen species (ROS) and the ability of antioxidants to eliminate this species and/or repair the caused damage [1]. Hydroxyl radical is undoubtedly the most deleterious species among ROS that can be formed *in vivo*, being able to react with most cellular constituents including lipids, proteins and DNA. The implication of hydroxyl radical in the pathogenesis of conditions, such as Parkinson's and Alzheimer's diseases [2], cancer [3], and aging [4] has been suggested. Studies concerning identification of oxidative damages originated by hydroxyl radical, recognition of oxidative stress markers, or evaluation of the potential action of specific molecules as antioxidants require the *in vitro* generation of this radical. The use of pulse radiolysis or ultraviolet photolysis is quite convenient for this purpose although these methods are not accessible in most laboratories. For characterizing the HO radical scavenging activity of antioxidants, either isolated or in complex samples, radicals generation is conducted by several methods including Fenton [4–6], Fenton-like [7,8], electro-Fenton [9,10], or organic Fenton [11] among others. Despite the differences between these methods the use of chemical precursors is a common denominator.

Electrochemical generation of hydroxyl radicals can provide a significant contribution in this area as it does not require the use of any specific reagent. The resulting benefits are varied, but of particular relevance is the minimization of interferences from chemical species that are alien to the system under study.

In the oxygen evolution reaction by electrooxidation of water, according to Eq. (1) and Eq. (2), hydroxyl radicals are generated as intermediary species adsorbed at the anode surface [12,13].

$$H_2O \rightarrow HO^\bullet + H^+ + e^- \tag{1}$$

$$2\ HO^\bullet \xrightarrow{k_{O_2}} O_2 + 2H^+ + 2e^- \tag{2}$$

Where the rate of HO radicals formation, v_{HO}, is controlled by the current density of the electrolysis, j (A m^{-2}), according to Eq. (3).

$$v_{HO} = \frac{j}{zF} \tag{3}$$

The adsorption degree of these radicals at the anode surface depends on the anode material. Weakly adsorbed radicals at boron dopped diamond or at PbO_2 were successfully used for organic compounds mineralization [12,13]. In opposition, HO radicals strongly adsorbed at Pt were used to characterize the reactivity of aromatic compounds with respect to these radicals [14,15]. The consumption of aromatic

compounds in galvanostatic electrolysis, using Pt anodes fairly oxidized, is not limited by mass transport, but by the kinetics of charge transfer and by the kinetics of reaction with HO radicals [14,15]. The apparent rate constant, k^0_{app}, obtained for the aromatic compounds consumption was related to the reactivity of the species, according to Eq. (4) and to Eq. (5) for non-electroactive and for electroactive compounds, respectively [14,15]:

$$k_{app} = \frac{j}{zF} \left(\frac{1}{\frac{2k_{O_2}}{k_{S,HO}} + n_S[S]} \right) \qquad (4)$$

$$k_{app} = \frac{j}{zF} \left(\frac{1}{\frac{2k_{O_2}}{k_{S,HO}} + n_S[S]} \right) + k_{S,e} \qquad (5)$$

where k_{O_2} is the rate constant of the O_2 evolution reaction following the recombination of HO radicals, $k_{S,HO}$ is the rate constant of the reaction between species S and HO radicals adsorbed at the anode and n_S is the number of HO radicals scavenged by S. The constant $k_{S,e}$ is the rate constant of the oxidation of S by direct electron transfer, z is the number of electrons involved in the electrogeneration of HO radical and j is the current density of the galvanostatic electrolysis.

For both electroactive and non-electroactive compounds, a linear correlation was found between the apparent rate constant of the species consumption and current density. Whereas non-electroactive compounds displayed a null intercept, the intercept from electroactive species was found to be a measure of the rate constant of the species oxidation by direct electron transfer.

In this work it is demonstrated that electrogenerated HO radicals can be used for antioxidants characterization concerning their radical scavenging ability. Four well-known species recognized by their antioxidant activity are used as well as a commercial green-tea based beverage.

2. Experimental

2.1. Chemicals

All reagents employed were of analytical grade. Caffeic acid (CA) was provided by Fluka, gallic acid (GA), L-ascorbic acid (AA) and 6-hydroxy-2,5,7,8-tetramethylchroman-2-carboxylic acid (trolox, T) by Sigma-Aldrich. Phosphoric acid and potassium dihydrogen phosphate were obtained from ACROS

Organics whereas acetic acid and methanol of HPLC grade was from Fisher Scientific. Potassium ferrocyanide and potassium ferricyanide were provided by José Gomes Santos.

Antioxidant solutions were prepared in pH 3.5 0.15 M buffer containing potassium dihydrogen phosphate and phosphoric acid.

2.2. HPLC

Oxidation reactions were monitored following the concentration decrease along galvanostatic electrolyses by HPLC. HPLC experiments were performed using a Jasco, PU-2080 Plus system equipped with a RP 18 column from Grace Smart (250 mm × 4.6 mm, 5 μm particle size) and using Clarity HPLC software from Jasco (Jasco 870 / UV detector). The loop was 20 μl. The flow rate selected was 0.6 ml min^{-1} for AA, GA and CA and 0.8 ml min^{-1} for T and for tea samples. A mixture of methanol, water and phosphoric acid (60:39:1) (v/v) was used as mobile phase for GA, CA and T and a mixture of water, methanol and acetic acid (94:5:1) (v/v) was used for AA and tea samples.

The detection wavelength was selected according to the species: 280 nm for GA and CA, 254 nm for AA and tea samples, and 210 nm for T. The quantification was performed using calibration curves.

2.3. Electrochemical measurements

Voltammetric measurements and galvanostatic / potentiostatic electrolyses were performed using a potentiostat (Autolab type PGSTAT30, Ecochemie) controlled by GPES 4.9 software provided by Ecochemie.

2.3.1. Cyclic voltammetry

Cyclic voltammetry was performed using as working electrode a glassy carbon electrode (GC, 3 mm disk diameter, CHI104, CH Instruments, Inc.) and a Pt electrode (3 mm diameter, EM-EDI, Radiometer Analytical). The reference electrode was a Ag/AgCl/3 M KCl (CHI111, CH Instruments, Inc.) and the counter electrode was a Pt wire. All experiments were carried out using an undivided three-electrode cell.

The GC electrode surface was cleaned between scans by polishing with polycrystalline diamond suspension (3F μm) for about 1 min. The Pt anode was electrochemically cleaned between runs in the

blank solution (0.15 M phosphate buffer pH 3.5) by two different ways. In one procedure (P1), the electrode was submitted to three potential scans, from -0.4 V to 1.2 V, whereas in the other procedure (P2) the electrode was submitted to a galvanostatic treatment at the oxygen evolution region (0.02 A for 600 s). Procedure P2 is identical to the anode conditioning performed before each electrolysis as described below. In order to analyse the effect of the oxidation state of the anode surface on the electron transfer kinetics, voltammograms were recorded after each electrochemical cleaning procedure. After the cleaning procedure P1, cyclic voltammograms were recorded from -0.4 V to 0.7 V at 100 mV s^{-1}. In order to avoid the removal of the oxide layer formed during the cleaning procedure P2, cyclic voltammograms were recorded from 0 V to 1.2 V in the direct scan and from 1.2 V to -0.4 V in the reverse scan, at 100 mV s^{-1}.

2.3.2. Electrolysis

Galvanostatic electrolyses were carried out at different current densities from 50 to 1250 A m^{-2} and potentiostatic electrolyses were conducted at 1.2 V. All electrolyses were performed in a two compartments cell separated by a glass frit membrane. Volume of anodic compartment is 9.0 ml and solution was mechanically stirred with a magnetic stir bar (300 rpm). Anode is made of a piece (20 mm ×10 mm) of Pt gauze (52 mesh woven from 0.1 mm diameter wire, 99.9%, from Alfa Aesar). Before each experiment the anode was electrochemically cleaned in the blank solution during 600 s at a constant current of 0.02 A. The area of the Pt working electrode (5.6 cm^2) was determined in a chronoamperometric experiment using 1.00 mM of K$_3$[Fe(CN)$_6$] in 0.1 M KCl [16].

2.4. Hydrodynamic characterization of the electrolysis cell

The characterization of the mass transport efficiency of the electrolysis assays was performed by analysis of j - t curves from electrolysis (1.2 V) of 0.50 mM K$_4$[Fe(CN)$_6$] in 0.15 M phosphate buffer pH 3.5 using Eq. (6):

$$\frac{j}{j_0} = \exp\left(-\frac{k^0_{app} A}{V} t\right) \tag{6}$$

where, A is the anode surface area, V is the volume of the solution in the anodic compartment, k^0_{app} is the apparent rate constant that characterizes the consumption of the substrate in a potentiostatic electrolysis and t is time.

156

The diffusion-layer thickness δ is determined by Eq. (7) considering that oxidation of $[Fe(CN)_6]^{4-}$ is mass transport limited, i.e. $k^0_{app} = k_m$:

$$k_m = \frac{D}{\delta} \qquad\qquad (7)$$

where, k_m is the mass transport coefficient and D is the diffusion coefficient. A value of $\delta = 2.53 \times 10^{-3}$ cm was determined using $k_m = 3.04 \times 10^{-3}$ cm s^{-1} (evaluated from j - t curve of potentiostatic electrolysis) and $D = 7.7 \times 10^{-6}$ cm^2 s^{-1} (from voltammograms recorded in 0.15 M phosphate buffer pH 3.5 and using Cottrell equation).

2.5. Sample characterization

A commercial beverage of green tea enriched with lemon juice (Pleno tisanas) was analysed. The sample was characterized by cyclic voltammetry using a GC electrode. Voltammetry was carried out in solutions prepared by dilution of the original sample with phosphate buffer pH 3.5. Voltammograms recorded from the 1:2 diluted sample displayed two waves ($(E_{1/2})_1 = 169$ mV and $(E_{1/2})_2 = 335$ mV vs Ag/AgCl, 3 M KCl). From the area under voltammograms integrated from 0 V to 1.4 V a total concentration of 3.5 ± 0.3 mM of T equivalent was estimated for the undiluted tea sample by interpolation in a calibration curve [17].

The HPLC characterization of the sample is presented in Figure 1. Despite the large amount of small peaks detected, ascorbic acid was the only antioxidant detected from the set of antioxidants analysed.
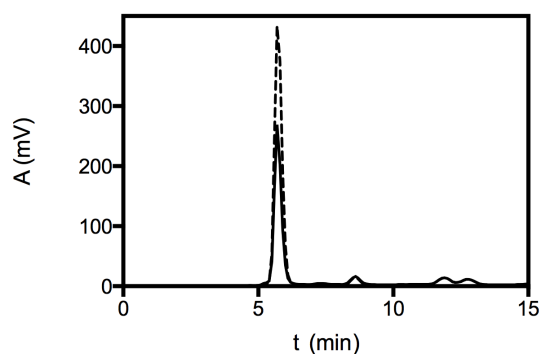

Figure 1: Chromatographic profile of: (full line) sample of commercial green tea-based beverage and (dashed line) sample enriched with ascorbic acid.

3. Principle of the method

The proposed method for evaluation of antioxidant activity is based on the kinetic characterization of the reaction between antioxidants (AOs) and electrogenerated HO radicals highly adsorbed at a Pt anode, during a galvanostatic electrolysis with simultaneous O_2 evolution. The species consumption is analysed in view of the following conditions and assumptions:

1. The starting compound reacts with electrogenerated HO radicals and originates products that may also react with these radicals;

2. The starting compound and its reaction products may be electroactive;

3. The rate of all reactions (including the heterogeneous charge transfer) is slow relative to diffusion, so that concentration polarization can be neglected.

Condition 3. is confirmed by means of a cyclic voltammetric study and potentiostatic electrolyses which results and discussion are presented in sections 4.1 and 4.2 and by the fact that values of k_{app} obtained for AOs are lower than the values of k_m (according to results in Table 1 and Table 2).

Under these conditions the consumption of an antioxidants can occur by reaction with electrogenerated HO radicals and by direct electron transfer:

$$AO + n_{AO}\, HO^{\bullet} \xrightarrow{\ k_{AO,HO}\ } P_{AO,i} \tag{8}$$

$$AO - ne_- \xrightarrow{\ k_{AO,e}\ } P_{AO,i} \tag{9}$$

Simultaneously, the species $P_{AO,i}$ can react with HO radicals:

$$P_{AO,i} + n_{P_{AO,i}} HO^{\bullet} \xrightarrow{\ k_{P_{AO,i},HO}\ } P_{AO,n} \tag{10}$$

where $P_{AO,i}$ (i = 1, 2, ..., n) corresponds to an intermediary or a product formed directly from AO or by subsequent reactions of $AO,$ either with HO radicals or by heterogeneous electron transfer. $k_{AO,HO}$ and $k_{P_{AO,i},HO}$ are the rate constants of the reactions of AO and of P_{AO_i} with HO and $k_{AO,e}$ is the rate constant of the oxidation of AO by direct electron transfer.

The steady state condition can be defined by Eq. (11), considering that HO radicals are consumed in reactions described in Eq. (2), Eq. (8) and Eq. (10).

$$v_{HO} = 2v_{O_2} + n_{AO}\, v_{AO,HO} + \sum n_{P_{AO,i}}\, v_{P_{AO,i},HO} \tag{11}$$

where v_{O_2}, the oxygen formation rate can be defined as follows:

$$v_{O_2} = k_{O_2} \Gamma \theta \tag{12}$$

$\Gamma\theta$ corresponds to the surface concentration of HO radical at the anode; θ is the surface coverage degree and Γ the saturation concentration of this species (mol m^{-2}).

The rate of reaction between HO radical and the *AO* is defined by:

$$v_{AO,HO} = k_{AO,HO}[AO]\Gamma\theta \tag{13}$$

An identical equation can be written regarding between HO radical and $P_{AO,i}$:

$$v_{P_{AOi},HO} = k_{P_{AOi},HO}[P_{AOi}]\Gamma\theta \tag{14}$$

Considering Eq. (3), Eq. (12), Eq. (13) and Eq. (14), Eq. (11) can be rewritten as follows:

$$\frac{j}{zF} = 2k_{O_2}\Gamma\theta + n_{AO}k_{AO,HO}[AO]\Gamma\theta + \sum n_{P_{AO,i}}k_{P_{AO,i},HO}[P_{AO,i}]\Gamma\theta \tag{15}$$

or in an equivalent form:

$$\Gamma\theta = \frac{j}{zF}\frac{1}{2k_{O_2} + n_{AO}k_{AO,HO}[AO] + \sum n_{P_{AO,i}}k_{P_{AO,i},HO}[P_{AO,i}]} \tag{16}$$

Combining Eq. (16) and Eq. (13) it is possible to define the rate of reaction between AO with HO radical as:

$$v_{AO,HO} = \frac{j}{zF}\frac{k_{AO,HO}}{2k_{O_2} + n_{AO}k_{AO,HO}[AO] + \sum n_{P_{AO,i}}k_{P_{AO,i},HO}[P_{AO,i}]}[AO] \tag{17}$$

According to Eq. (17) the apparent rate constant of this reaction is:

$$k_{app,HO} = \frac{j}{zF}\frac{k_{AO,HO}}{2k_{O_2} + n_{AO}k_{AO,HO}[AO] + \sum n_{P_{AO,i}}k_{P_{AO,i},HO}[P_{AO,i}]} \tag{18}$$

A simplified expression equivalent to Eq. (18) can be written as:

$$k_{app,HO} = \frac{j}{zF}\frac{1}{(2k_{O_2} + v_{SC})/k_{AO,HO}} \tag{19}$$

where v_{SC} is defined as follows:

$$v_{SC} = n_{AO}k_{AO,HO}[AO] + \sum n_{P_{AO,i}}k_{P_{AO,i},HO}[P_{AO,i}] \tag{20}$$

As most antioxidants are electroactive, the AO consumption will also occur by direct electron transfer with the anode, and the apparent rate constant of the global process must also consider the contribution from this process:

$$k_{app} = k_{app,HO} + k_{AO,e} \tag{21}$$

Therefore, the observed apparent rate constant of the AO consumption is defined as:

$$k_{app} = \frac{j}{zF}\frac{1}{(2k_{O_2} + v_{SC})/k_{AO,HO}} + k_{AO,e} \tag{22}$$

At a given moment, the total concentration of HO radical scavengers is $[SC]_i$.

$$[SC]_i = [AO] + \sum[P_{AO,i}] \tag{23}$$

A weighted arithmetic mean of the product between the stoichiometric coefficients and the rate constants of reactions with HO radical (considering both species AO and $P_{AO,i}$) can be defined, combining Eq. (20) and Eq. (23), where the weigh is the concentration of each species:

$$\overline{n_{AO,P}k_{AO,P}} = \frac{v_{SC}}{[SC]_i} \tag{24}$$

The value of $[SC]_i$ can be related to the initial concentration of the AO, assuming that the total concentration of the species decay by an exponential law:

$$[SC]_i = C_{AO}^0 \, e^{-k_{C(AO,P)}t} \tag{25}$$

where $k_{C(AO,P)}$ is the rate constant that expresses the total concentration decay of HO radical scavengers. In conditions where the AO concentration decay follows a first order reaction, it implies that the value of k_{app} is constant during electrolysis. Thus, considering Eq. (22) and Eq. (24) it can be concluded that the value of v_{SC}, and therefore the value of $[SC]_i$ are not likely to vary significantly along an electrolysis. The values of $[SC]_i$ can only keep constant if the decrease of $[AO]$ is compensated by the increase of $\sum[P_{AO,i}]$ (according to Eq. (23)) . In this case the following approach can be considered:

$$[SC]_i = C_{AO}^0 \tag{26}$$

where C_{AO}^0 is the initial concentration of the AO. The apparent rate constant can therefore be rewritten as:

$$k_{app} = \frac{j}{zF} \frac{1}{(2k_{O_2}/k_{AO,HO} + \overline{n_{AO,P}k_{AO,P}}/k_{AO,HO} \, C_{AO}^0)} + k_{AO,e} \tag{27}$$

The values of $\overline{n_{AO,P} \, k_{AO,P}}/k_{S,HO}$ ($= \overline{n_{AO,P} \, k_{AO,P}}/k_{AO,HO}$) corresponds to the product of the average stoichiometric coefficients by the average rate constants, regarding the AO and its products, $P_{AO,i}$, divided by the rate constant of the AO consumption.

The average value $\overline{k_{AO,P}}$ can be considered approximately equal to $k_{AO,HO}$. This assumption is based on the following considerations. As $\overline{k_{AO,P}}$ is calculated by a weighted arithmetic mean, regarding the concentrations of each species, for short times, i.e. low conversion levels of AO, it cannot differ significantly from $k_{AO,HO}$, as the AO is the main species present. Regardless the extent of the reaction, a constant k_{app} could not be observed if $\overline{k_{AO,P}}$ was significantly different from $k_{AO,HO}$. Therefore

whenever an exponential decay is observed $\overline{k_{AO,P}} \approx k_{AO,HO}$ can be considered valid. As a result, Eq. (27) can be rewritten as:

$$k_{app} = \frac{j}{zF} \frac{1}{(2k_{O_2} / k_{AO,HO} + \overline{n_{AO,P}}\, C_{AO}^0)} + k_{AO,e} \tag{28}$$

Similarly,

$$k_{app} - k_{AO,e} = k_{app,HO} = \frac{j}{zF} \frac{1}{(2k_{O_2} / k_{AO,HO} + \overline{n_{AO,P}}\, C_{AO}^0)} \tag{29}$$

or,

$$\frac{1}{k_{app,HO}} = \frac{zF}{j} \left(\frac{2k_{O_2}}{k_{AO,HO}} + \overline{n_{AO,P}} C_{AO}^0 \right) \tag{30}$$

To characterize the *AO* activity, relative values of the rate constant of the reaction between AO and HO radical, $k_{AO,HO} / k_{O_2}$, and the average number of HO radicals scavenged, $\overline{n_{AO,P}}$, can be estimated from the representation of $(k_{app,HO})^{-1}$ as a function of C_{AO}^0.

For antioxidant samples of unknown concentration, the assessment is performed in solutions prepared by dilution of the original sample. By means of the representation of $(k_{app,HO})^{-1}$ as a function of the dilution factor, *Df*, values of $k_{AO,HO} / k_{O_2}$ and $\overline{n_{AO,P}}\, C_{AO}^{sample}$ are estimated, according to Eq. (31).

$$\frac{1}{k_{app,HO}} = \frac{zF}{j} \left(\frac{2k_{O_2}}{k_{AO,HO}} + \overline{n_{AO,P}}\, C_{AO}^{sample} Df \right) \tag{31}$$

Where C_{AO}^{sample} is the antioxidant concentration of the original sample and $Df = C_{AO}^{sample} / C_{AO}^0$.

4. Results and discussion

4.1 Cyclic voltammetry

Cyclic voltammetry is a very convenient technique for the screening of antioxidant activity based on measurement of the oxidation peak potentials [18]. Besides results are generally in agreement with classical electron transfer based methods like DPPH [18,19].

The voltammetric response of T, CA, GA and AA in phosphate buffer pH 3.5 at a GC electrode are displayed in Figure 2. Although two electrons are commonly assigned to oxidation of T, CA, GA and AA by cyclic voltammetry [20–24], three electrons have been determinate for GA by electrolysis [16] and by chronoamperometry [25]. While the voltammograms of T and CA display a reverse peak

(electrochemical irreversible), those from GA and AA do not show a reverse process (due to the irreversible nature of the coupled chemical reactions). From the position of the voltammetric peaks of this set of antioxidants, it can be suggested a relative order for their antioxidant activity as follows: T > AA> CA > GA.
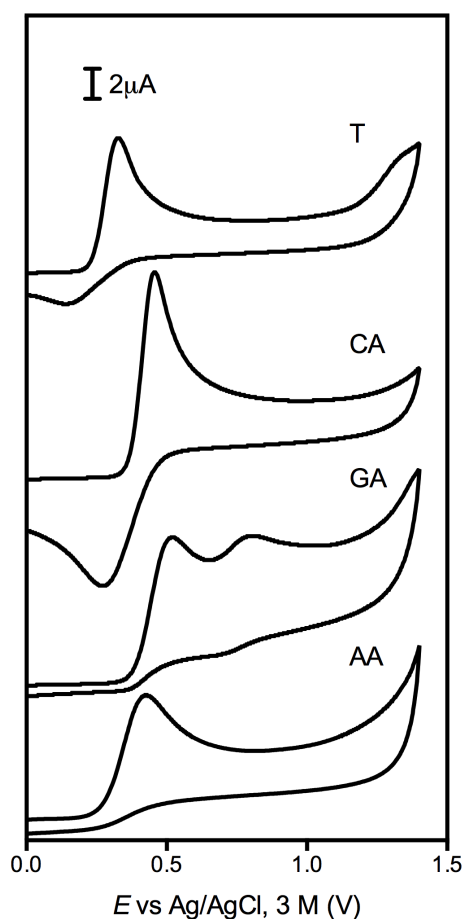

Figure 2: Cyclic voltammograms of 0.50 mM of T, CA, GA and AA in 0.15 M phosphate buffer solution pH 3.5, recorded at 100 mV s^{-1} at a GC electrode.

Voltammetry of T, CA, GA, and AA was also performed at a Pt electrode as the electrolysis assays are carried out using this anode material. As during electrolysis the anode is polarized at very positive potentials (O_2 evolution region) the Pt surface is extensively oxidized and a Pt oxide layer is likely to be formed. In order to check the effect of this oxide layer on electron transfer rate, a voltammetric study was carried out after submitting the electrode to two different electrochemical pre-treatments, procedure P1and procedure P2, as described in the experimental section. While in procedure P1 the electrode potential is cycled between -0.4 V to 1.2 V, in procedure P2 the electrode was strongly oxidized at the O_2 evolution region.

Figure 3A shows the voltammograms of T and of $Fe(CN)_6^{4-}$ at a Pt electrode submitted to procedure P1. Voltammogram of $Fe(CN)_6^{4-}$ displays its standard response with a peak separation, ΔE_p, of about 90 mV (a bit higher than the typically 59 mV). The voltammogram of T obtained at the Pt anode is not as well defined as that obtained at GC, nevertheless both direct and reverse processes are observed, with a peak separation of about 400 mV (higher than the 185 mV obtained at the GC electrode).
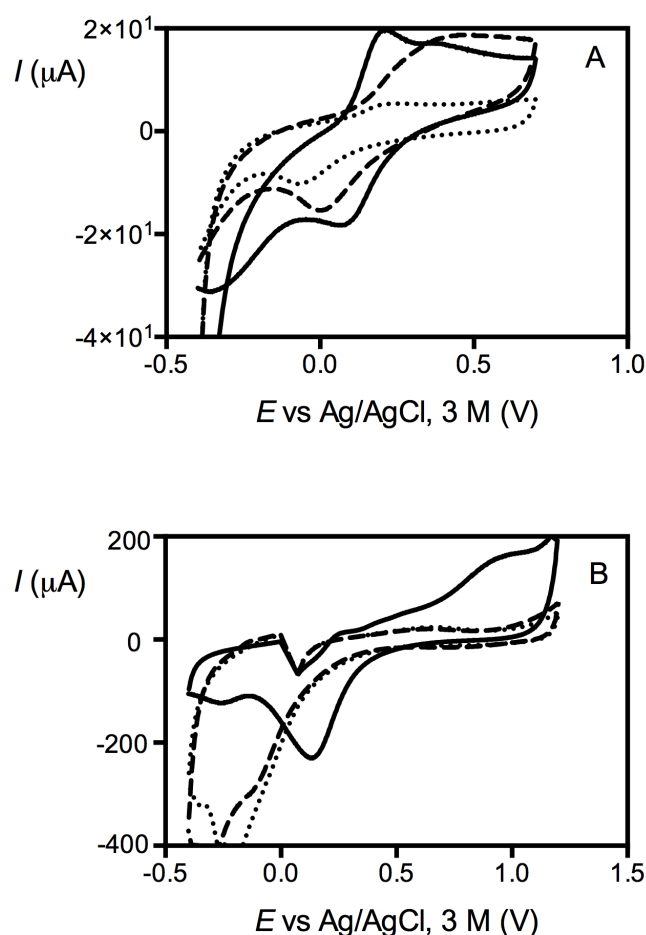

Figure 3: Cyclic voltammograms of the blank solution (...) and of 0.50 mM solutions of T (– –) and $Fe(CN)_6^{4-}$(——), in 0.15 M phosphate buffer solution pH 3.5, recorded at 100 mV s^{-1} using a Pt electrode electrochemically treated: (A) by potential cycling from -0.4 V to 1.2 V and (B) by anodic polarization $i = 0.02$ A.

The voltammograms of these two compounds recorded at oxidized Pt (following procedure P2) are displayed in Figure 3B. It must be remarked that the current scale of Figure 3B differ by one order of magnitude from Figure 3A, indicating that the Pt active surface area has increased by the electrochemical pre-treatment. Besides, the voltammogram of $Fe(CN)_6^{4-}$ exhibits a lower reversibility degree (ΔE_p = 813 mV), while voltammogram of T cannot be distinguished from the blank at the anodic scan, despite a small difference in the reverse scan. These results suggests slower electron transfer rates for both compounds at oxidized Pt, nevertheless diffusion control seems to be attained

for $Fe(CN)_6^{4-}$ at about 1 V (considering the peak shape of the voltammogram). Voltammograms of AA, GA and CA are similar to that of T, in the sense that they are similar to the blank (results not shown), demonstrating that the electron transfer rates at oxidized Pt are very slow.

4.2 Kinetic study of the antioxidant consumption by potentiostatic electrolysis

Potentiostatic electrolyses 1.2 V of AA, CA, GA and T (0.50 mM) in 0.15 M phosphate buffer pH 3.5 were conducted at using a Pt anode. Antioxidants consumption was evaluated by means of current decrease and the kinetic characterization was performed considering Eq. (6). Values of k^0_{app} of each compound were calculated. These values are presented in Table 1 together with the k_m values calculated by Eq. (7) (using D values also displayed in Table 1 and $\delta = 2.53 \times 10^{-3}$ cm estimated in section 2.4). As values of k^0_{app} are significantly lower than k_m, it can be concluded that the oxidation reactions are not limited by mass transport. This result is in agreement with the conclusions of the voltammetric study regarding the oxidized Pt electrode (after cleaning procedure P2) where the formation of an oxidation peak is not visible in the direct scan for all the AOs.

Table 1: Apparent rate constants from potentiostatic electrolysis (k^0_{app}), mass transport coefficient values (k_m) calculated using $\delta = 2.53 \times 10^{-5}$ m (according to section 2.4.) and diffusion coefficients (D) of the species: ascorbic acid (AA), caffeic acid (CA), gallic acid (GA) and trolox (T).

	k^0_{app} (10^{-6} m s^{-1})	D (10^{-9} m^2 s^{-1})	k_m (10^{-6} m s^{-1})
AA	30 ± 3	2.45 [21]	97
CA	37 ± 9	2.30 [20]	91
GA	30 ± 8	3.70 [16]	146
T	34 ± 7	-	-

4.3 Kinetic study of the antioxidant consumption by galvanostatic electrolysis

Galvanostatic electrolyses of AA, CA, GA and T (0.50 mM) in 0.15 M phosphate buffer pH 3.5 using a Pt anode were conducted at current densities of 50, 268, 625 and 1250 A m^{-2} with simultaneous oxygen evolution. Concentration decrease, expressed by means of concentrations ratio $[AO]/C^0_{AO}$, was

quantified by HPLC and is plotted against electrolysis time (Figure 4). Two relevant features must be remarked concerning the concentration decrease of the different species along time and its dependency on current density. First, the concentration variation along each electrolysis follows a first order reaction and second, the rate of AO consumption increases with the current density. Curves displayed are fitted to experimental data considering Eq. (32) that is characteristic of a 1st order kinetics:

$$\ln\frac{[AO]}{C_{AO}^0} = -\frac{k_{app}A}{V}t \qquad (32)$$

where *[AO]* is the concentration at a given time, C_{AO}^0 is its initial concentration, *A* is the anode area, *V* is the volume of solution and k_{app} is the apparent rate constant. Values of k_{app} from the consumption of all AOs at different current densities are reported in Table 2.
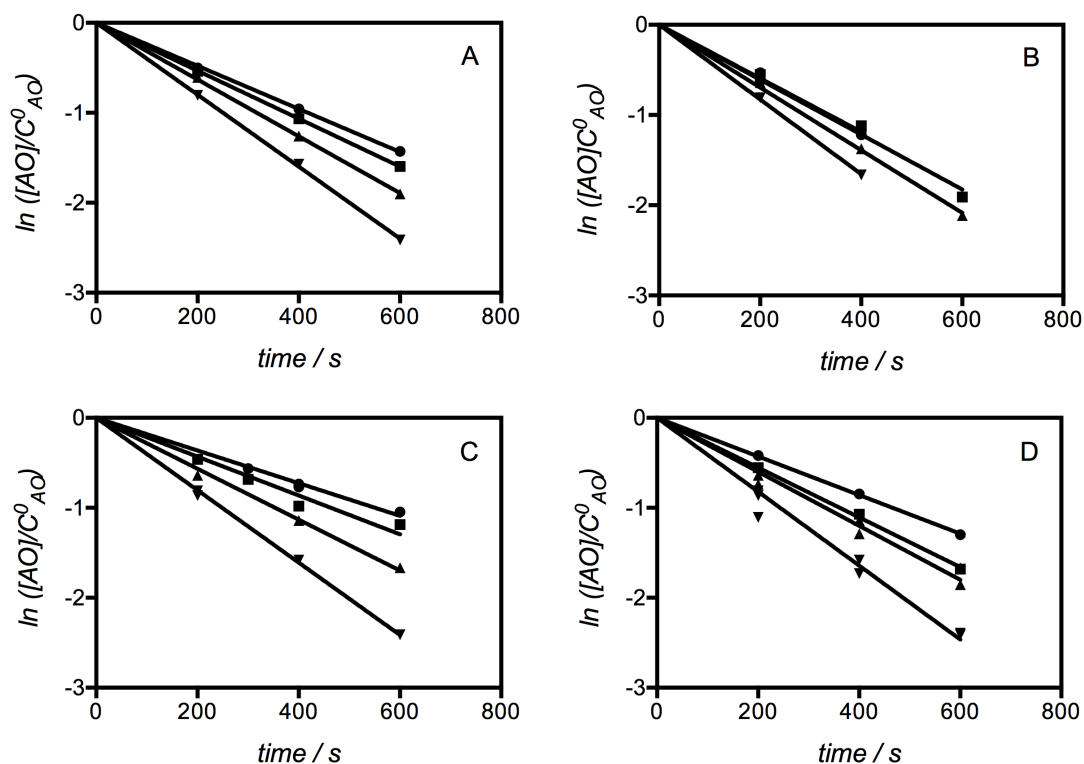

Figure 4: Concentration decrease during galvanostatic electrolyses of 0.50 mM solutions of: (A) ascorbic acid, (B) caffeic acid, (C) gallic acid and (D) trolox, using a Pt anode at (●) 50, (■) 268 ,(▲) 625 and (▼) 1250 A m^{-2}.

The apparent rate constants of antioxidants consumption from electrolysis with simultaneous O$_2$ evolution (k_{app}) (Table 2) are higher than those obtained by potentiostatic electrolysis in absence of O$_2$ evolution (k^0_{app}) (Table 1). This result was already reported by us in a previous study regarding the oxidation of a set of hydroxybenzoic acid derivative [15]. The increase of the effectiveness of the

species consumption can be attributed to their oxidation by electrogenerated HO radicals in addition to direct electron transfer. Furthermore, values of k_{app} increase with current density. It can also be observed that the values of k_{app} (Table 2) are lower than the values of k_m (Table 1) indicating that the oxidation rate is not limited by mass transport.

Table 2: Apparent rate constants from galvanostatic electrolysis (k_{app}) at different current densities of the species: ascorbic acid (AA), caffeic acid (CA), gallic acid (GA) and trolox (T). Values of $(k_{app})_{j=0}$ correspond to the intercept of the straight lines in Figure 5.

	$(k_{app})_{j=0}$	50 (A m^{-2})	268 (A m^{-2})	625 (A m^{-2})	1250 (A m^{-2})
	$(10^{-6}$ m s$^{-1})$	k_{app} $(10^{-6}$ m s$^{-1})$			
AA	37.1 ± 0.2	38 ± 3	43 ± 4	51 ± 4	64 ± 6
CA	39.9 ± 0.9	48 ± 2	49 ± 3	56 ± 4	67 ± 7
GA	30 ± 2	32 ± 2	39 ± 3	45 ± 4	66 ± 6
T	35 ± 2	35 ± 2	45 ± 3	51 ± 5	68 ± 8

The representation of k_{app} (open symbols), as a function of the electrolysis current density, is shown in Figure 5. Values of k^0_{app} are also represented in Figure 5 (as solid symbols) and are placed at $j=0$. According to Eq. (22) the intercept of the straight line corresponds to $k_{AO,e}$. The match between the intercept values, $(k_{app})_{j=0}$, and the values of k^0_{app} corroborates the meaning of the intercept as defined by Eq. (22). Besides, the linear increase of k_{app} with j indicates that $(k_{O_2} + v_{SC})/k_{AO,HO}$ is constant. This result is very important regarding the validity of Eq. (28) with respect of the assumptions of a constant value of v_{SC} and of $\overline{k_{AO,P}} \approx k_{AO,HO}$.
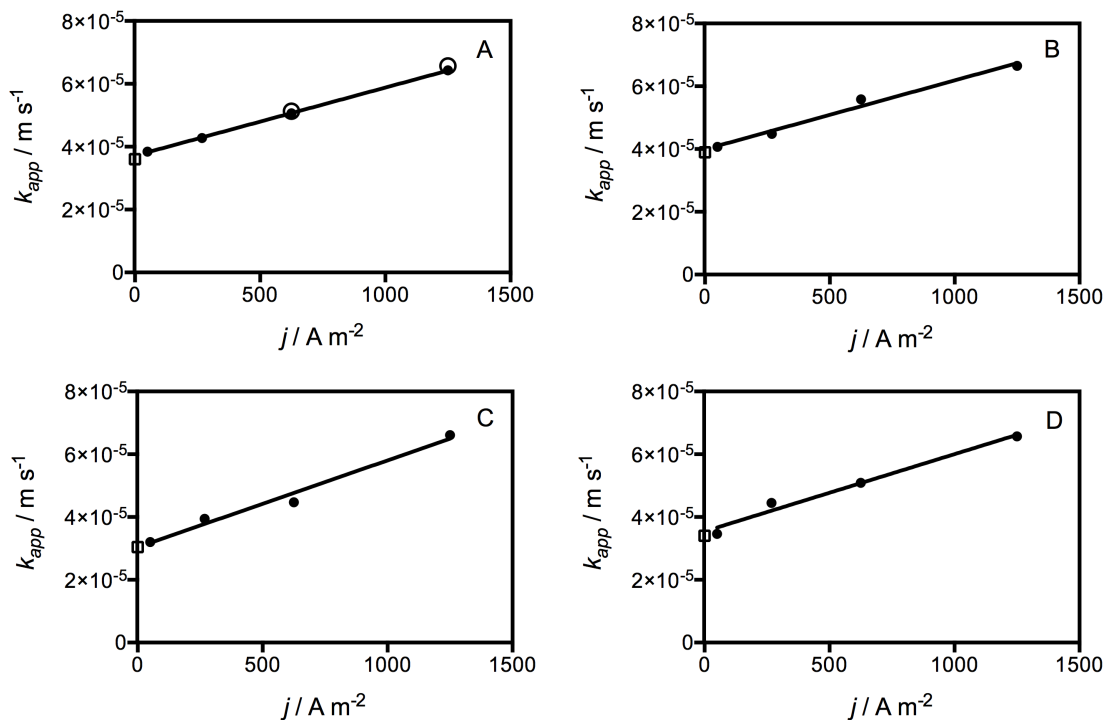
Figure 5: Effect of current density on the apparent rate constant of consumption of: (A) ascorbic acid, (B) caffeic acid, (C) gallic acid and (D) trolox. Solid symbols (k_{app}) correspond to data from galvanostatic electrolyses with simultaneous oxygen evolution, whereas open symbols (k^0_{app}) correspond to data from potentiostatic electrolyses carried out at E = 1.2 V (vs. Ag / AgCl, 3 M). The open circles in graphic (A) correspond to k_{app} obtained from a sample of green tea-based beverage.

4.4 Characterization of HO radical scavenging activity of antioxidants

Galvanostatic electrolyses of AA, CA, GA and T in 0.15 M phosphate buffer pH 3.5 using a Pt anode at 1250 A m^{-2} were conducted using of different starting concentrations. The values of k_{app} were estimated for all electrolysis considering the concentration decay along time, as described in the previous section. In order to characterize the scavenging properties of each AO, values of $k_{app,HO}$ were calculated according to Eq. (21).

In Figure 6 are represented the values of 1 / $k_{app,HO}$ as a function of the initial concentration of each AO, C^0_{AO}, according to Eq. (30). From the linear correlations defined for all the *AOs* values of $k_{AO,HO}$ / k_{O_2}, and of $\overline{n_{AO,P}}$ were estimated (Table 4).

Values of $k_{AO,HO}/k_{O_2}$ are a kinetic measure of the reactivity of the species towards the electrogenerated HO radicals and therefore can be used to characterize the HO radicals scavenging activity. By means of these results *AOs* can be ordered by their scavenging activity as follows: GA>T>AA>CA.

In order to validate our results correlations were attempted between the values of $k_{AO,HO}/k_{O_2}$ with results reported in literature for the same *AOs*. Regarding the three AOs that are common between our

work and reference [26], T, AA and GA, good correlations were obtained between our kinetic data and the activity results reported regarding peroxyl radicals generated either by an enzymatic assay (using a conjugate diene of linoleic acid as optical probe) ($R^2 = 0.96$) or by the oxidation of oxygenated methyl esters by Fe(II) (by EPR using PBN (α-phenyl-N-tert-butyl-nitrone) as a spin-trap) ($R^2 = 0.97$).
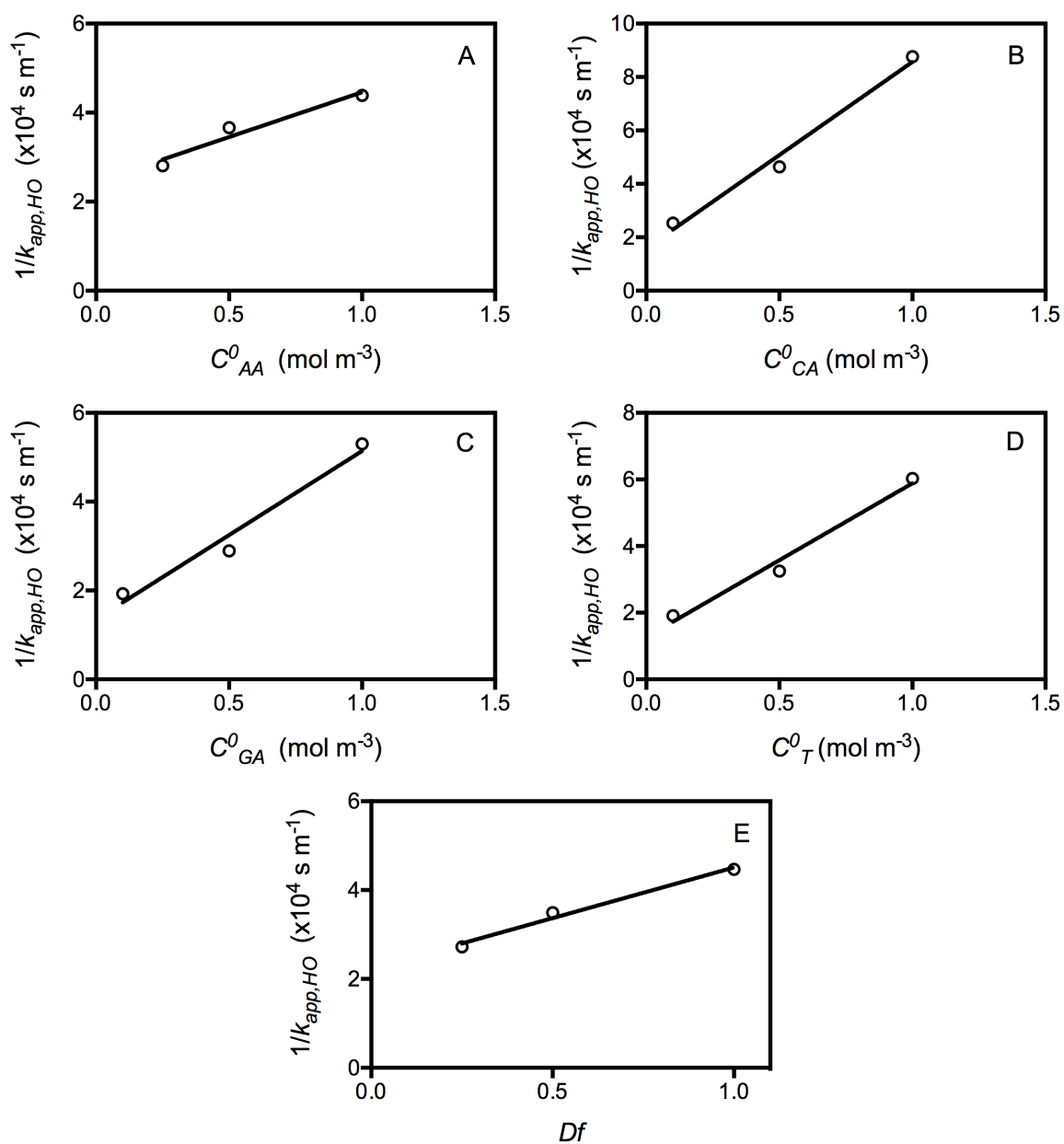

Figure 6: Representation of the reciprocal of k_{app} *vs* the initial concentration for: (A) AA, (B) CA, (C) GA, (D) T. In (E) the reciprocal of k_{app} of AA consumption in a sample of green tea-based beverage as a function of the dilution factor.

The estimated average number of HO radicals scavenged per molecule of AO (or $P_{AO,i}$), $\overline{n_{AO,P}}$, range from 260 (AA) to 500 (GA). The high values obtained for $\overline{n_{AO,P}}$ are in accordance with the fact that AOs can be quite effective in scavenging radicals even if they are present in very low concentrations.

Table 3: Apparent rate constants from galvanostatic electrolysis (k_{app}) for different *AO* concentrations. Values of $k_{AO,HO}/k_{O_2}$ and $\overline{n_{AO,P}}$ of were calculated from the intercept and slop of $k_{app,HO}^{-1}$ vs C_{AO}^0, respectively (Eq. (30)).

	k_{app} (10^{-6} m s^{-1})				$k_{AO,HO}/k_{O_2}$ (10^{-3} m^3 mol^{-1})	$\overline{n_{AO,P}}$ (10^2)
	0.1 mM	0.25 mM	0.5 mM	1 mM		
AA	–	73 ± 7	64 ± 6	60 ± 7	6.3 ± 0.9	2.6 ± 0.6
CA	85 ± 3	–	67 ± 7	56 ± 5	5.9 ± 0.3	2.8 ± 0.3
GA	82 ± 7	–	66 ± 6	49 ± 5	12 ± 2	5 ± 1
T	87 ± 9	–	68 ± 8	52 ± 5	9.8 ± 0.2	4.54 ± 0.08

4.5 Characterization of HO radical scavenging activity of a commercial tea-based beverage

The possibility of applying the electrochemical generation of HO radicals in assays with natural samples is examined as interferences from the matrix cannot be discarded *a priori*.

The sample analysed in this study, a commercial green tea-based beverage enriched with lemon juice, was used without any prior treatment. Sample was diluted with phosphate buffer pH 3.5. Galvanostatic electrolyses were performed at two current densities, 625 and 1250 A m^{-2}, with simultaneous oxygen evolution. Oxidation of the sample during galvanostatic electrolysis was monitored following the consumption of AA by HPLC. Concentration decrease of AA in tea sample follows a 1st order kinetics (results not shown). Values of k_{app} estimated using Eq. (32) are plotted in Fig. 5A as open circles. As it can be observed, k_{app} values obtained from the tea sample are identical to those from AA solutions. Galvanostatic electrolyses performed in diluted solutions of the sample allow to determine $\overline{n_{AO,P}}\, C_{AO}^{sample} = (3.0 \pm 0.4) \times 10^2$ mol m^{-3} and $k_{AO,HO}/k_{O_2} = (6.9 \pm 0.6) \times 10^{-3}$ mol^{-1} m^3 from the slope and from the intercept of the straight line in Figure 6E, according to Eq. (31). By comparison of the value of $\overline{n_{AO,P}}\, C_{AO}^{sample}$ obtained from the sample containing AA with the value of $\overline{n_{AO,P}}$ from AA

solutions, it can be concluded that $C_{AO}^{sample} \approx 1$ mol m^{-3} (corresponds to 1 mM). This value is identical to the AA concentration of the sample quantified by HPLC (section 2.5). With respect to the $k_{AO,HO}/k_{O_2}$ similar values are obtained from the natural sample and from the AA solutions. These results demonstrate that both $\overline{n_{AO,P}}$ and $k_{app,HO}$ values of AA were not affected by matrix composition.

5. Conclusion

The kinetic characterization of antioxidants consumption in galvanostatic assays with simultaneous oxygen evolution was performed. All antioxidants exhibit a concentration decay typical of a first order law. The apparent rate constants obtained for the four different AOs displayed a linear increase with current density. The intercept of k_{app} vs j was identified as the direct electron transfer constant rate. Form the dependency between $k_{app,HO}$, estimated by k_{app} - $k_{AO,e}$, on the initial concentration of the AO, values of $k_{AO,HO}/k_{O_2}$ and of $\overline{n_{AO,P}}$ are estimated. From the kinetic parameter $k_{AO,HO}/k_{O_2}$, it is proposed the following order in terms of the scavenging activity of the antioxidants: GA>T>AA>CA. Results are in agreement with the reactivity order pointed out for T, GA and CA from assays using peroxyl radical generated either by enzymatic assay or by oxygenated methyl esters. Experiments performed using a commercial green tea-based beverage demonstrates that the generation conditions of HO radicals as well as the reactivity of AA were not apparently modified by the presence of the tea constituents. The proposed method provides an interesting way for testing antioxidant activity that allow to estimate simultaneously a kinetic parameter and a stoichiometric constant of the reaction between the AO and HO radicals.

Acknowledgments

References

[1] J.F. Turrens, Superoxide production by the mitochondrial respiratory chain., Biosci. Rep. 17 (1997) 3–8.

[2] K. Jomova, D. Vondrakova, M. Lawson, M. Valko, Metals, oxidative stress and neurodegenerative disorders, Mol. Cell. Biochem. 345 (2010) 91–104.

[3] B. Lipinski, Hydroxyl radical and its scavengers in health and disease., Oxid. Med. Cell. Longev. 2011 (2011) 1–9.

[4] J.M.J. de Vos-Houben, N.R. Ottenheim, A. Kafatos, B. Buijsse, G.J. Hageman, D. Kromhout, et al., Telomere length, oxidative stress, and antioxidant status in elderly men in Zutphen and Crete, Mech. Ageing Dev. 133 (2012) 373–377.

[5] O. Hirayama, M. Yida, Evaluation of hydroxyl radical-scavenging ability by chemiluminescence, Anal. Biochem. 251 (1997) 297–299.

[6] C.-A. Calliste, P. Trouillas, D.-P. Allais, A. Simon, J.-L. Duroux, Free radical scavenging activities measured by electron spin resonance spectroscopy and B16 cell antiproliferative behaviors of seven plants, J. Agric. Food Chem. 49 (2001) 3321–3327.

[7] Z. Cheng, Y. Li, W. Chang, Kinetic deoxyribose degradation assay and its application in assessing the antioxidant activities of phenolic compounds in a Fenton-type reaction system, Anal. Chim. Acta. 478 (2003) 129–137.

[8] J. Ueda, N. Saito, Y. Shimazu, T. Ozawa, A Comparison of Scavenging Abilities of Antioxidants against Hydroxyl Radicals, Arch. Biochem. Biophys. 333 (1996) 377–384.

[9] N. Masomboon, C. Ratanatamskul, M.-C. Lu, Chemical oxidation of 2,6-dimethylaniline by electrochemically generated Fenton's reagent, J. Hazard. Mater. 176 (2010) 92–98.

[10] A. Özcan, Y. Şahin, M.A. Oturan, Complete removal of the insecticide azinphos-methyl from water by the electro-Fenton method – A kinetic and mechanistic study, Water Res. 47 (2013) 1470–1479.

[11] B.-Z. Zhu, N. Kitrossky, M. Chevion, Evidence for production of hydroxyl radicals by pentachlorophenol metabolites and hydrogen peroxide: A metal-independent organic Fenton reaction, Biochem. Biophys. Res. Commun. 270 (2000) 942–946.

[12] M. Panizza, G. Cerisola, Direct And Mediated Anodic Oxidation of Organic Pollutants, Chem. Rev. 109 (2009) 6541–6569.

[13] M. Panizza, G. Cerisola, Application of diamond electrodes to electrochemical processes, Electrochim. Acta. 51 (2005) 191–199.

[14] R. Oliveira, F. Bento, D. Geraldo, Aromatic hydroxylation reactions by electrogenerated HO radicals: A kinetic study, J. Electroanal. Chem. 682 (2012) 7–13.

[15] R. Oliveira, N. Pereira, D. Geraldo, F. Bento, Reactivity of hydroxy-containing aromatic compounds towards electrogenerated hydroxyl radicals, Electrochim. Acta. 105 (2013) 371–377.

[16] R. Oliveira, J. Marques, F. Bento, D. Geraldo, P. Bettencourt, Reducing Antioxidant Capacity Evaluated by Means of Controlled Potential Electrolysis, Electroanalysis. 23 (2011) 692–700.

[17] P.A. Kilmartin, H. Zou, A.L. Waterhouse, A Cyclic Voltammetry Method Suitable for Characterizing Antioxidant Properties of Wine and Wine Phenolics, J. Agric. Food Chem. 49 (2001) 1957–1965.

[18] A.J. Blasco, A. González Crevillén, M.C. González, A. Escarpa, Direct Electrochemical Sensing and Detection of Natural Antioxidants and Antioxidant Capacity in Vitro Systems, Electroanalysis. 19 (2007) 2275–2286.

[19] D. Zhang, L. Chu, Y. Liu, A. Wang, B. Ji, W. Wu, et al., Analysis of the Antioxidant Capacities of Flavonoids under Different Spectrophotometric Assays Using Cyclic Voltammetry and Density Functional Theory, J. Agric. Food Chem. 59 (2011) 10277–10285.

[20] C. Giacomelli, K. Ckless, D. Galato, F.S. Miranda, A. Spinelli, Electrochemistry of Caffeic Acid Aqueous Solutions with pH 2.0 to 8.5, J. Braz. Chem. Soc. 13 (2002) 332–338.

[21] Z. Taleat, M.M. Ardakani, H. Naeimi, H. Beitollahi, M. Nejati, H.R. Zare, Electrochemical Behavior of Ascorbic Acid at a 2,2′-[3,6-Dioxa-1,8-octanediylbis(nitriloethylidyne)]-bis-hydroquinone Carbon Paste Electrode, Anal. Sci. 24 (2008) 1039–1044.

[22] H. Masuhara, S. Kawata, F. Tokunaga, Preface, in: H. Masuhara, S. Kawata, F. Tokunaga (Eds.), Nano Biophotonics Sci. Technol. Proc. 3rd Int. Nanophotonics Symp. Handai, Elsevier, 2007.

[23] F. Sen, A.A. Boghossian, S. Sen, Z.W. Ulissi, J. Zhang, M.S. Strano, Observation of Oscillatory Surface Reactions of Riboflavin, Trolox, and Singlet Oxygen Using Single Carbon Nanotube Fluorescence Spectroscopy, ACS Nano. 6 (2012) 10632–10645.

[24] R. Abdel-Hamid, E.F. Newair, Electrochemical behavior of antioxidants: I. Mechanistic study on electrochemical oxidation of gallic acid in aqueous solutions at glassy-carbon electrode, J. Electroanal. Chem. 657 (2011) 107–112.

[25] R. Oliveira, F. Bento, C. Sella, L. Thouin, C. Amatore, Direct Electroanalytical Method for Alternative Assessment of Global Antioxidant Capacity Using Microchannel Electrodes, Anal. Chem. 85 (2013) 9057–9063.

[26] R. Lo Scalzo, A. Todaro, P. Rapisarda, Methods used to evaluate the peroxyl (ROO center dot) radical scavenging capacities of four common antioxidants, Eur. Food Res. Technol. 235 (2012) 1141–1148.

Conclusion

An electrochemical-based method was developed for the direct evaluation of total antioxidant capacity by means of controlled potential electrolysis. This method, denominated RACE (Reducing Antioxidant Capacity Evaluated by Means of Controlled Potential Electrolysis), characterizes antioxidants capacity by means of the amount of charge that antioxidants can transfer regarding a fixed electrode potential that simulates the reactivity of a specific reactive oxidant species (ROS). This method was applied to the characterization of isolated antioxidants and mixtures.

Using microchannel electrodes operating in a thin layer regime, a novel method for evaluating total antioxidant capacity of samples was developed. This method combines the advantages of electrochemistry and microfluidics. From one side, the selection of the operating potentials, which determine the analytical selectivity of the method, can easily simulate the oxidation power of many ROS like $O_2^{\bullet-}$ and H_2O_2. On the other side, the use of a microchannel electrodes provide all the benefits of confined environments such as the handling of low solution volumes and the set-up of fast electrochemical measurements. The antioxidant capacity of AOs mixtures or samples may be analyzed without making any prior assumptions about their composition. This method was validated by performing measurements with synthetic mixtures of AOs having dissimilar diffusion coefficients and involving different number of electron stoichiometries during their oxidation.

Concerning the studies on the electrogeneration of HO radicals by galvanostatic electrolysis, the consumption of hydroxybenzoic acid derivatives (HBA) was monitored and the hydroxylated products were identified. The consumption rate of HBA was analyzed by means of a kinetic model that accounts for the dependency of the HO radical concentration at the anode on the scavenger activity of the species. Following this analysis, the reactivity of the scavengers was characterized by means of a kinetic parameter $k_{S,HO} / k_{O_2}$ (ratio between the rate constant of reaction of the scavenger S with HO radicals and the rate constant of O_2 formation). The average stoichiometric coefficients regarding species S and their products and intermediaries, P, formed by reaction with HO radical, $\overline{n_{S,P}}$, is also assessed. The high values estimated for $\overline{n_{S,P}}$, for all the analysed compounds, indicate that elimination or dehydration reactions can play an important role in stabilizing reaction intermediaries in

conditions where the availability of HO radicals with sufficient energy to react (as a result of their strong adsorption strength at Pt) is quite low.